Precipitation-Runoff Processes in the Feather River Basin, Northeastern California, with Prospects for Streamflow Predictability, Water Years 1971–97

By Kathryn M. Koczot, Anne E. Jeton, Bruce J. McGurk, and Michael D. Dettinger

In cooperation with the California Department of Water Resources

Scientific Investigations Report 2004-5202

U.S. Department of the Interior
U.S. Geological Survey

U.S. Department of the Interior
Gale A. Norton, Secretary

U.S. Geological Survey
Charles G. Groat, Director

U.S. Geological Survey, Reston, Virginia: 2005
For sale by U.S. Geological Survey, Information Services
Box 25286, Denver Federal Center
Denver, CO 80225-0286

For more information about the USGS and its products:
Telephone: 1-888-ASK-USGS
World Wide Web: http://www.usgs.gov/

Suggested citation:
Koczot, K.M., Jeton, A.E., McGurk, B.J., and Dettinger., M.D., 2005, Precipitation-runoff processes in the Feather River Basin, northeastern California, with prospects for streamflow predictability, water years 1971–97: U.S. Geological Survey Scientific Investigations Report 2004–5202, 82 p.

Contents

Figures

Tables

Appendixes

Conversion Factors, Datum, Abbreviations, and Acronyms

CONVERSION FACTORS

Multiply	By	To obtain
acre	4,047	square meter
acre-feet (acre-ft)	1,233	cubic meter
cubic foot per second (ft^3/s)	0.02832	cubic meter per second
foot (ft)	0.3048	meter
inch (in.)	2.54	centimeter
inch per year (in/yr)	2.54	centimeter per year
mile (mi)	1.609	kilometer
square mile (mi^2)	12.590	square kilometer

Temperature in degrees Fahrenheit (ºF) may be converted to degrees Celsius (ºC) as follows:

ºC=(ºF-32)/1.8.

DATUM

Vertical coordinate information is referenced to National Geodetic Vertical Datum of 1929 (NGVD 29). Horizontal coordinate information is referenced to the North American Datum of 1927 (NAD 27).

Altitude, as used in this report, refers to distance above the vertical datum.

Water Year constitutes a 12-month period from October 1 through September 30, and is designated by the year in which the period ends (for example, water year 1995 began October 1, 1994, and ended September 30, 1995).

ABBREVIATIONS

asl	above sea level

ACRONYMS

ESP	Ensemble Streamflow Prediction
FTO	Feather River at Oroville
GIS	geographic information system
HRU	hydrologic response unit
MMS	Modular Modeling System
NWSRFS	National Weather Service River Forecasting System
PDO	Pacific Decadal Oscillation
PRISM	Parameter-Elevation Regressions on Independent Slopes Model
PRMS	Precipitation-Runoff Modeling System

RMSE	root-mean-square error
SCCT	Snow Cover Comparison Tool

Organizations

CCSS	California Cooperative Snow Surveys Program
CDEC	California Data Exchange Center
CNRFC	National Oceanic and Atmospheric Administration's California-Nevada River Forecasting Center
DWR	California Department of Water Resources
HEC	U.S. Army Corps of Engineers Hydrologic Engineering Center
NASA	National Aeronautics and Space Administration
NOAA	National Oceanic and Atmospheric Administration
NOHRSC	National Operational Hydrologic Remote Sensing Center
PG&E	Pacific Gas & Electric Company
SWP	California State Water Project
USDA	U.S. Department of Agriculture
USFS	U.S. Forest Service
USGS	U.S. Geological Survey

Precipitation-Runoff Processes in the Feather River Basin, Northeastern California, and Streamflow Predictability, Water Years 1971–97

By Kathryn M. Koczot[1], Anne E. Jeton[1], Bruce J. McGurk[2], and Michael D. Dettinger[1]

Abstract

Precipitation-runoff processes in the Feather River Basin of northern California determine short- and long-term streamflow variations that are of considerable local, State, and Federal concern. The river is an important source of water and power for the region. The basin forms the headwaters of the California State Water Project. Lake Oroville, at the outlet of the basin, plays an important role in flood management, water quality, and the health of fisheries as far downstream as the Sacramento-San Joaquin Delta. Existing models of the river simulate streamflow in hourly, daily, weekly, and seasonal time steps, but cannot adequately describe responses to climate and land-use variations in the basin. New spatially detailed precipitation-runoff models of the basin have been developed to simulate responses to climate and land-use variations at a higher spatial resolution than was available previously. This report characterizes daily rainfall, snowpack evolution, runoff, water and energy balances, and streamflow variations from, and within, the basin above Lake Oroville. The new model's ability to predict streamflow is assessed.

The Feather River Basin sits astride geologic, topographic, and climatic divides that establish a hydrologic character that is relatively unusual among the basins of the Sierra Nevada. It straddles a north-south geologic transition in the Sierra Nevada between the granitic bedrock that underlies and forms most of the central and southern Sierra Nevada and volcanic bedrock that underlies the northernmost parts of the range (and basin). Because volcanic bedrock generally is more permeable than granitic, the northern, volcanic parts of the basin contribute larger fractions of ground-water flow to streams than do the southern, granitic parts of the basin. The Sierra Nevada topographic divide forms a high altitude ridgeline running northwest to southeast through the middle of the basin. The topography east of this ridgeline is more like the rain-shadowed basins of the northeastern Sierra Nevada than the uplands of most western Sierra Nevada river basins. The climate is mediterranean, with most of the annual precipitation occurring in winter. Because the basin includes large areas that are near the average snowline, rainfall and rain-snow mixtures are common during winter storms. Consequently, the overall timing and rates of runoff from the basin are highly sensitive to winter temperature fluctuations.

The models were developed to simulate runoff-generating processes in eight drainages of the Feather River Basin. Together, these models simulate streamflow from 98 percent of the basin above Lake Oroville. The models simulate daily water and heat balances, snowpack evolution and snowmelt, evaporation and transpiration, subsurface water storage and outflows, and streamflow to key streamflow gage sites. The drainages are modeled as 324 hydrologic-response units, each of which is assumed homogeneous in physical characteristics and response to precipitation and runoff. The models were calibrated with emphasis on reproducing monthly streamflow rates, and model simulations were compared to the total natural inflows into Lake Oroville as reconstructed by the California Department of Water Resources for April–July snowmelt seasons from 1971 to 1997. The models are most sensitive to input values and patterns of precipitation and soil characteristics. The input precipitation values were allowed to vary on a daily basis to reflect available observations by making daily transformations to an existing map of long-term mean monthly precipitation rates that account for altitude and rain-shadow effects.

[1]U.S. Geological Survey

[2]Pacific Gas & Electric Company

The models effectively simulate streamflow into Lake Oroville during water years (October through September) 1971–97, which is demonstrated in hydrographs and statistical results presented in this report. The Butt Creek model yields the most accurate historical April–July simulations, whereas the West Branch model yields the least accurate simulations. Accuracy may reflect the quality of the streamflow measurements (or reconstructions) used in the calibration process. The overall simulated inflows to Lake Oroville reproduce reconstructed inflows with relative errors of –9 and –4 percent on monthly and annual time scales, respectively. The root-mean-squared errors of the simulated Lake Oroville inflows are 134,000 and 465,000 acre-feet for monthly and annual time scales, respectively. The accuracy of simulations appears to deteriorate for the period 1998–2000. Signatures of North Pacific decadal climate variations were observed in the Feather River Basin as a shift in the month of maximum streamflow (from April during the cooler Pacific decadal phase to March during the warmer decadal phase). The calibration period was dominated by the warmer (1977–98) phase. Since 1998, the simulations represent years in the newly re-established cool decadal phase. The response of the models to this subtle climatic fluctuation requires more evaluation.

Streamflow predictions for the April–July snowmelt season were made with the Feather River model using a standard "ensemble streamflow prediction" (ESP) methodology. In the ESP methodology, April–July weather records from past years were used to drive the model through its plausible range of April–July streamflow totals for the current year, yielding a probabilistic forecast. Retrospective "predictions" using the ESP method were compared to the actual flows for each year from 1971 to 2000 to evaluate the reliability of the ESP results. These comparisons indicate that ESP-estimated flow probabilities are more accurate for the largest and smallest flows and tend to underestimate the likelihood of intermediate flow rates. Presumably, these comparisons can provide a guide for adjusting the confidence levels for any given ESP forecast in the future.

Introduction

Background

The Feather River Basin, in Plumas, Butte, Lassen, Shasta, and Sierra Counties, California (fig. 1), is a valuable hydrologic resource for California. The basin is a major contributor to the California State Water Project (SWP), and the reservoir at the outlet of the basin, Lake Oroville, represents 8 percent of California's reservoir capacity [California Department of Water Resources (DWR), 1998, 2000]. Lake Oroville plays an important role in flood management, water quality, and the health of fisheries, affecting areas downstream at least as far south as the Sacramento/San Joaquin River Delta. Two of the basin's major tributaries have been developed for hydropower with the capacity of generating 3.7 percent of California's peak daily electrical power demands (Gary Freeman, Pacific Gas & Electric Company, unpub. data, 2000). Improved understanding of how and why the Feather River discharge varies, and how the river responds to changing climatic conditions and land-management actions, will help water managers safeguard this resource.

Precipitation in California occurs principally from November through March, and in that period, water resources managers are responsible for forecasting streamflow, planning and managing reservoirs for winter floods, and measuring snowpack accumulation in basins such as the Feather. DWR managers, in particular, must plan for, and forecast, warm-season water availability. The primary source of warm-season streamflow is melting snow. DWR defines this snowmelt season as April 1–July 31, and assumes April 1 snowpack accumulations represent annual accumulations (California Department of Water Resources, 2000). During the snowmelt season, when flood-generating storms are rare, Lake Oroville receives about 40 percent of the annual total inflow (California Department of Water Resources, 2000).

DWR publishes summaries of warm-season water availability in California each month from February through May (http://cdec.water.ca.gov/snow/bulletin120/, accessed March 12, 2002; California Department of Water Resources, 2000). These summaries include streamflow forecasts for the April through July snowmelt season. Forecasts for the Feather River Basin are based on statistical relations between seasonal (and monthly) inflows to Lake Oroville and observed antecedent and expected streamflow, precipitation, and snowpack conditions. DWR and other water managers use these forecasts to plan summer water deliveries and to schedule releases from reservoirs.

In addition to seasonal forecasts, there is a growing need to improve medium-range (one week to one month) streamflow forecasts. Currently, in the Feather River Basin, DWR is making medium-range forecasts of total streamflow into Lake Oroville, and hydroelectric power operators are using their own suite of statistical models to manage power generation within the basin. Additionally, agricultural, fishery, logging, and local user groups may benefit from improved medium-range forecasts.

Figure 1. Feather River Basin, California, modeled areas, major tributaries and reservoirs, larger towns, county lines, selected peaks and valleys, and stations where streamflow or climate variables used in the models are measured or reconstructed.

In cooperation with DWR and with assistance from Pacific Gas & Electric Company (PG&E, the major hydropower operator in the basin, which provided calibration data and general information on climate and streamflow), physically based models of the Feather River Basin have been constructed and calibrated. The models were developed to simulate responses to climate and land-use variations at a higher spatial resolution than existing statistical or lumped models. Furthermore, by incorporating more information about the basin physical characteristics than is possible in statistical models, the physically based models may improve forecasts and increase understanding of the basin hydrology. The models are designed to simulate streamflow responses to variations of temperature, precipitation, and land cover, and are currently focused on simulating April–July streamflow totals.

Purpose and Scope

This report documents the distributed-parameter, physically based, Precipitation-Runoff Modeling System (PRMS; Leavesley and others, 1983) constructed for the Feather River Basin. The Feather River PRMS is composed of eight models representing eight drainages of the basin. Together, these models simulate streamflow from 98 percent of the basin above Lake Oroville. This report characterizes the Feather River watershed precipitation, temperature, snowpack evolution, and water and energy balances that determine streamflow rates from, and within, the basin above Lake Oroville. It further documents the new models developed to assess the (physically based) predictability of seasonal inflows to Lake Oroville.

Previous Studies

Lake Oroville storage and releases are a key part of the hydropower and water-supply facilities of the Oroville Complex (figs. 1 and 2; Sabet and Creel, 1991), which is a cornerstone and major source of flexibility of the SWP. The Oroville Complex is used to balance energy and resource demands so that SWP power contracts are satisfied with strategically timed power sales, reserve power capacity is maintained, and SWP water deliveries are met. Other uses of the Oroville Complex include flood control, irrigation, recreation, fish and wildlife enhancements, and reservoir releases to maintain downstream Feather River, Sacramento River, and Sacramento–San Joaquin Delta water-quality standards.

Many different methods have been developed and are used to forecast inflows to Lake Oroville. To put the modeling effort described herein into perspective, it is necessary to briefly review previous hydrologic modeling studies of the Feather River and other applications of the Precipitation-Runoff Modeling System (PRMS; Leavesley and others, 1983) modeling code used here.

Several statistical (regression) models are used by PG&E to simulate streamflow in the North Fork, South Fork, and West Branch of the Feather River Basin (fig. 1) for various timeframes. A monthly model (run from about January through August) is used to predict annual runoff based on antecedent runoff and on wetness-dependent scenarios of future runoff (based on historical analogs) to complete the year. The predicted annual totals are then disaggregated into monthly natural runoff amounts on the basis of historical flow patterns. PG&E also uses a daily statistical runoff model that combines recent estimates of daily (natural) flows with 10 days of weather forecasts followed by historical median precipitation rates to predict daily runoff. The model is calibrated to the existing record by a least-squares fitting technique.

The National Oceanic and Atmospheric Administration (NOAA) California-Nevada River Forecasting Center (CNRFC; http://www.wrh.noaa.gov/cnrfc/, accessed on Jan. 6, 2000) employs the National Weather Service River Forecasting System (NWSRFS) for flood and water-supply forecasting for the Feather River Basin. This system includes the Sacramento Soil Moisture Accounting Model (Burnash and others, 1973) and a snow accumulation and ablation component (Anderson, 1973). The physically based model spatially lumps basin characteristics and processes into two altitude bands within which snow is expected to accumulate and not accumulate, respectively. The model is calibrated for discharges at the Lake Oroville Dam (Miller and others, 2001). Daily, weekly, and seasonal streamflow forecasts are made using the Ensemble Streamflow Prediction (ESP) method (Day, 1985). ESP develops an ensemble of forecast scenarios by combining current model conditions (observed initial conditions) with temperature and precipitation observations from previous years. This procedure yields a probabilistic distribution of possible outcomes that can be analyzed by the forecaster.

DWR uses statistical models to forecast April through July and water-year volumes of estimated natural inflow to Lake Oroville. These forecasts generally are updated weekly from February through June. Forecasts are issued for probability levels ranging from 99 percent exceedence to 10 percent exceedence based on historical distributions of precipitation, snowpack accumulation, and model error subsequent to the forecast date. Snow-water content from 22 snow courses, 10 snow sensors, 8 precipitation gages, and prior runoff from the Feather River Basin have been regressed against historical runoff volumes to develop the DWR prediction model. Specifically, data from each station are divided by its historical mean (50-year average), then weighted (in the case of precipitation) by month, averaged for a group of stations for each basin, and raised to a power (if needed) to account for a nonlinear relation with runoff. The resulting basin indices of precipitation, snowpack, and prior runoff are used as predictors of runoff in a linear equation developed as a multiple linear regression (J. Pierre Stephens, DWR Resources Hydrology Branch, unpub. data, 2002). This same technique is used for about 30 other basins within California.

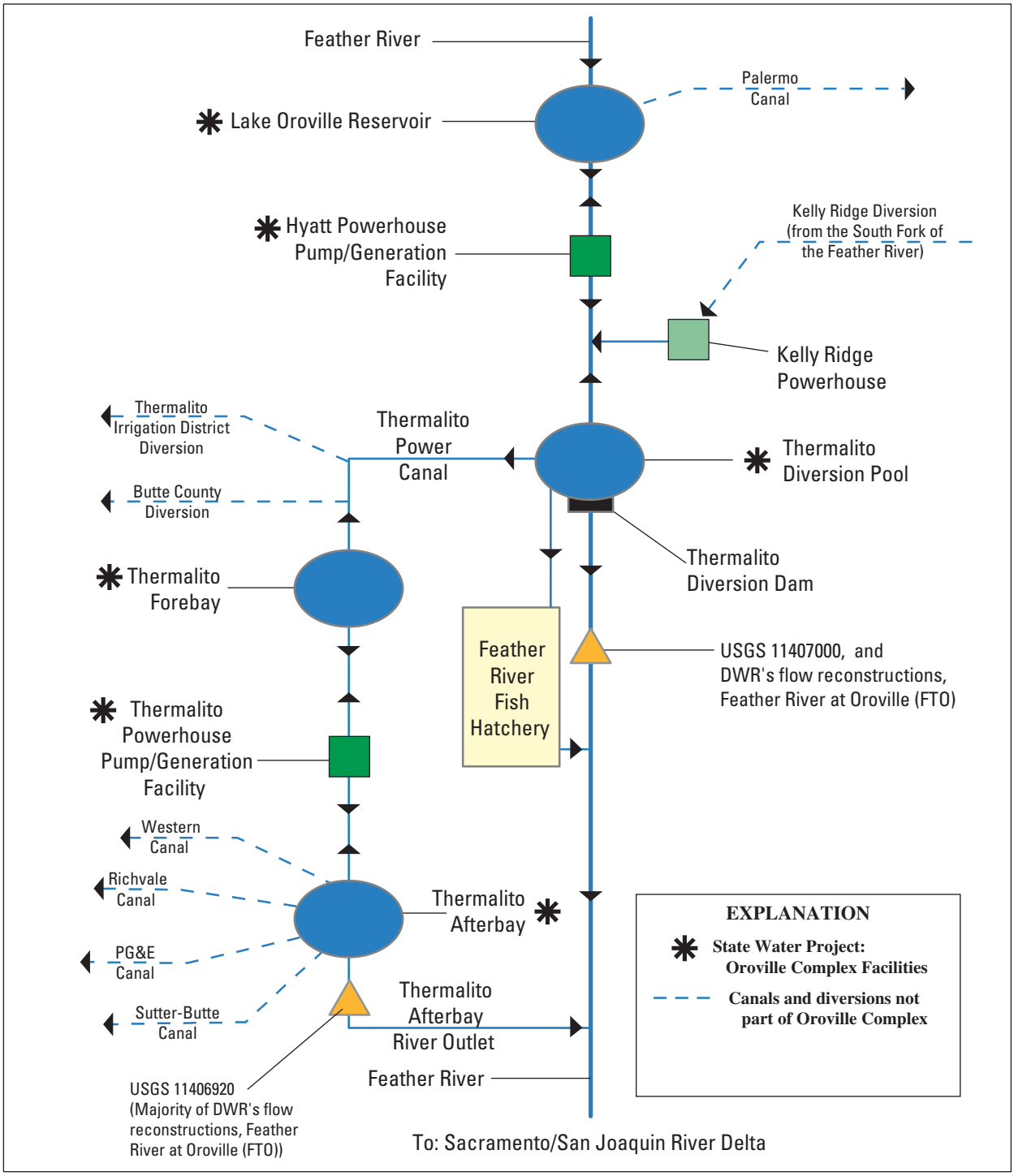

Modified from Sabet and Creel, 1991, and Rockwell and others, 1997.

Figure 2. Oroville Complex water-supply and hydropower facilities (including Lake Oroville), other improvements downstream from Lake Oroville including diversions for irrigation, and the locations of the U.S. Geological Survey streamflow stations from which monthly estimates of inflow to Lake Oroville are derived. The irrigation diversions and canals are NOT part of the Oroville Complex. Only the labels with an asterisk are part of the Oroville Complex. See Appendix A for components of reconstructed streamflow at the Feather River at Oroville (FTO).

The DWR forecasts streamflow for 1 to 20 days with physically based models that use observed and predicted precipitation and temperatures. The physically based models track snow and ground water in the basin. The models include HED71, which was developed by DWR (Buer, 1988) and the NWSRFS. During the spring snowmelt season, this latter model is operated in ESP mode for forecast leads of 20 or more days by blending 7 days of weather forecasts with historical weather traces. Previously, flood forecasting was done with other models, including U.S. Army Corps of Engineers Hydrologic Engineering Center (HEC) models and predecessors of the NWSRFS (J. Pierre Stephens, DWR Resources Hydrology Branch, unpub. data., 2002). Network flow modeling also has been used to simulate hydraulic operation and hydropower generation in the Oroville Complex on weekly and daily time scales (Sabet and Creel, 1991).

To run these various models, climate and hydrologic data are collected by DWR, PG&E, and others. Precipitation, air temperature, streamflow, and snow accumulations are routinely monitored in the basin. Some of these data are accumulated through the California Cooperative Snow Surveys Program (CCSS) and are made available to the public through the California Data Exchange Center (CDEC) web page (http://cdec.water.ca.gov).

Application of PRMS to the Feather River Basin was started in October 1996 by Bruce McGurk, under a grant from the DWR CCSS to the U.S. Department of Agriculture (USDA) Forest Service, Pacific Southwest Experiment Station. The goal was to develop a model of the five major forks of the Feather River to make historical and up-to-date predictions of daily inflows to Lake Oroville. Model areas were delineated and essential model parameters were estimated. In April 1997, an incomplete model was transferred to PG&E, and the goal was modified to include real-time updating of model inputs from telemetered data available to PG&E in all drainages except the Middle Fork of the Feather River. Natural streamflow records, which are not available publicly but required for calibration, were estimated by PG&E. Changes in management priorities and the approaching deregulation of the California energy market ended PG&E's efforts to develop this PRMS. In July 1999, PG&E provided data and parameter values to U.S. Geological Survey (USGS) staff, under a cooperative agreement with CCSS, for completing a model of the entire basin above Lake Oroville.

PRMS has been applied successfully in many settings, including basins in Colorado (Brendecke and Sweeten, 1985; Parker and Norris, 1989; Norris and Parker, 1985; Norris, 1986; Kuhn, 1989; Ryan, 1996), Kentucky (Bower, 1985), Montana (Cary, 1984), New Mexico (Hejl, 1989), North Dakota (Emerson, 1991), Oregon (Risley, 1994),West Virginia (Puente and Atkins, 1989), and Wyoming (Cary, 1991). PRMS models have been used to explore basin responses to climatic change (Hay and others, 1993; Ryan, 1996; Jeton and others, 1996; Wilby and Dettinger, 2000) and to land-cover changes (Puente and Atkins, 1989; Risley, 1994). PRMS has been used to model alpine basins of the Sierra Nevada that have physical characteristics similar to those of the Feather River Basin (Jeton and Smith, 1993; Jeton and others, 1996; Jeton, 1999a,b; Wilby and Dettinger, 2000). Knowledge gained in previous work, and especially in the construction and implementation of the other Sierra Nevada PRMS models (including parameter settings), was used to develop the Feather River PRMS models.

Acknowledgments

The authors gratefully acknowledge the diligent and patient assistance of Steven Markstrom and Roland Viger, USGS Denver, who provided modeling and geographic information system (GIS) computer programs and direction that made this modeling effort possible. Frank Gehrke, Chief of California Cooperative Snow Surveys at DWR, provided data, guidance, and motivation for this undertaking. Pierre Stephens of the DWR Resources Hydrology Branch provided vital information about DWR streamflow reconstructions, current streamflow forecasting methods, and the operation of the Oroville Complex. Pacific Gas & Electric Company, through Gary Freeman and co-author Bruce McGurk, provided climate data, reconstructed streamflows, and much guidance that made the study possible. The study was conducted by the USGS in cooperation with the California Department of Water Resources Cooperative Snow Surveys Program. Comparison of simulated and remotely sensed snow cover was funded through the National Aeronautics and Space Administration (NASA) Earth Science Information Partnership "Snow SIP" project at Scripps Institution of Oceanography.

Physical Characteristics of the Feather River Basin

Location and Land Cover

The Feather River above Lake Oroville drains about 3,600 mi^2 of the western slopes of the Sierra Nevada mountain range, between the Upper Sacramento and Yuba River Basins, north of Lake Tahoe and generally northeast of the city of Oroville, California (fig. 1). The Feather River Basin is bounded by Mt. Lassen to the northwest and the Diamond Mountains to the northeast. Altitudes range from about 843 ft at Oroville Dam to 9,525 ft near Mt. Lassen. Fifty-nine percent of the basin lies below the current average snowline altitude of 5,500 ft (fig. 3). The largest towns are Portola (population 2,227), Quincy (population 1,879), and Chester (population 2,316), according to the population census of 2000.

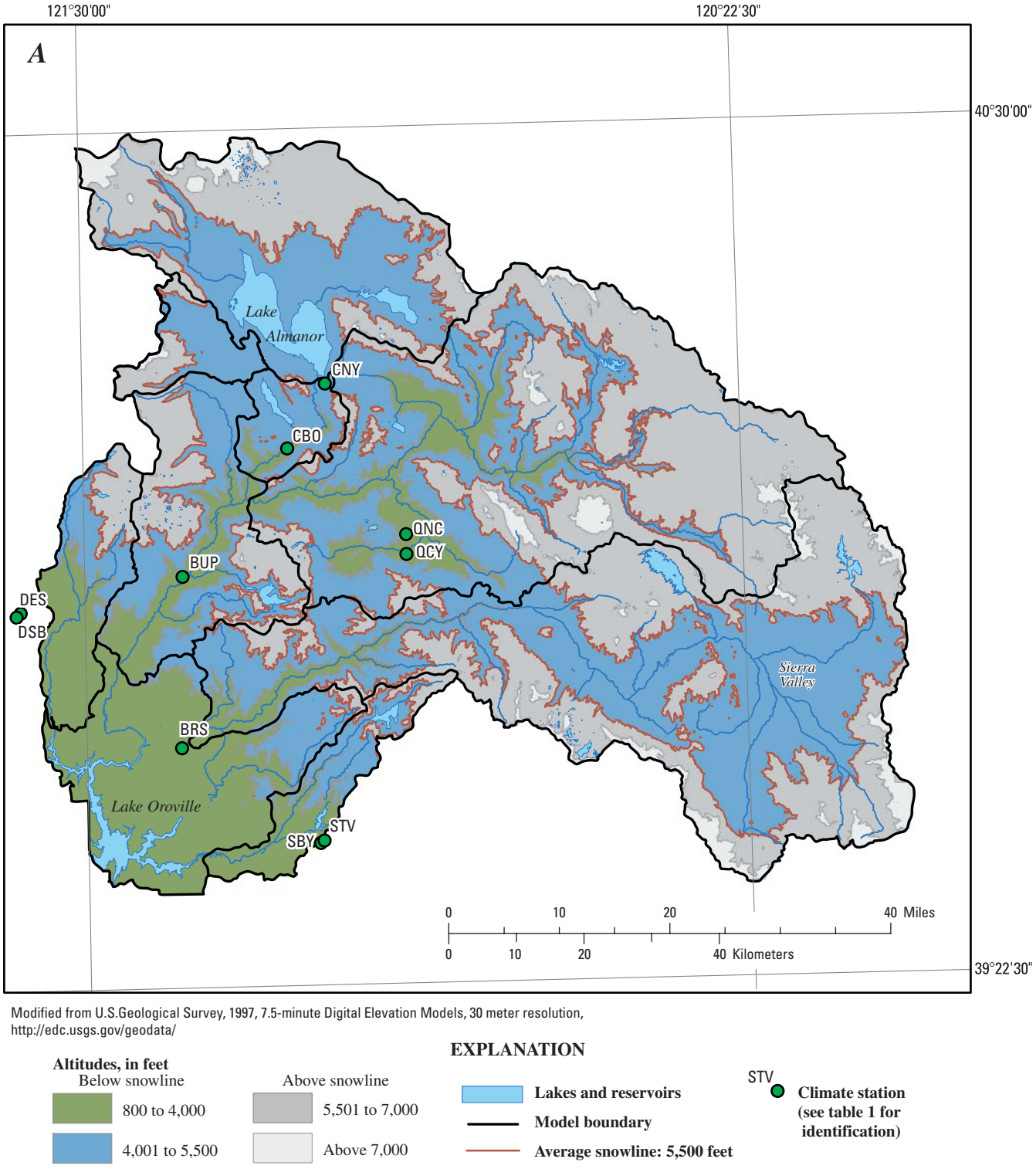

Figure 3. (*A*) Altitudes above and below the snow line (5,500 feet above sea level), and (*B*) area (square miles) at altitudes in the Feather River Basin, California.

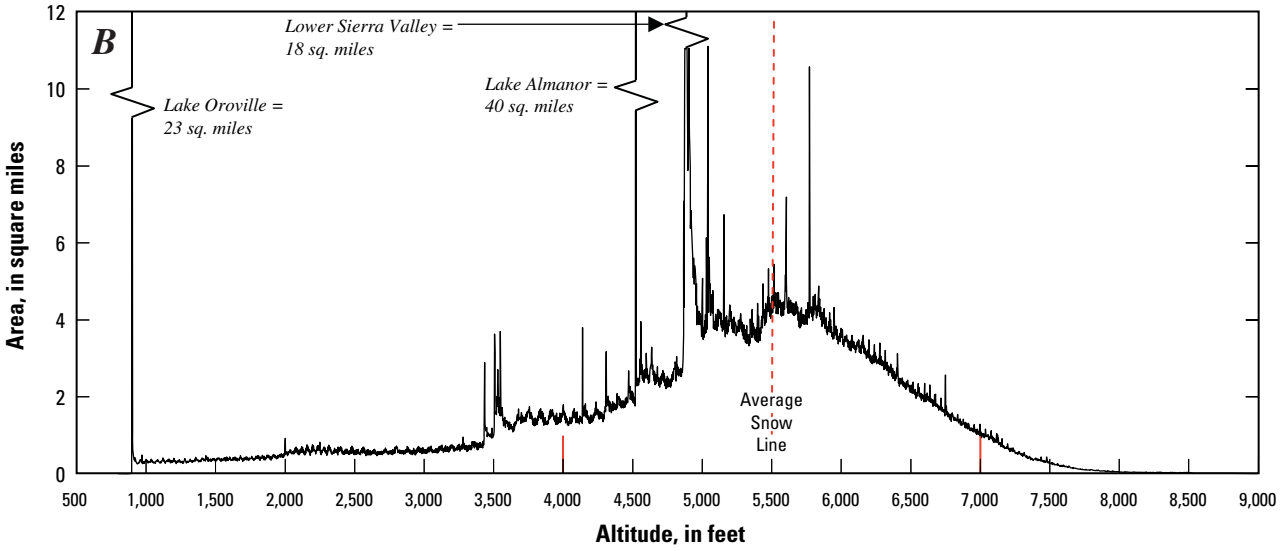

Figure 3.—Continued.

The Feather River Basin is drained by five major tributaries. Four of these—West Branch, North Fork, Middle Fork, and South Fork—flow directly into Lake Oroville. The fifth—the East Branch—is tributary to the North Fork, terminating near Belden (fig. 1). Where Lake Oroville now exists, the West Branch was once tributary to the North Fork, and therefore the designation for this western tributary remains "branch." The North and South Forks have been extensively engineered for hydropower generation, and numerous dams, reservoirs, penstocks, tunnels, and canals routinely move water from place to place (fig. 4). The largest reservoir is Lake Almanor (25,582 acres or 40 mi^2) on the North Fork.

Vegetation cover is predominantly coniferous trees, with some areas of shrubs and grasses mostly in the agricultural valleys (fig. 5). The basin contains parts of the Plumas, Lassen, and Tahoe National Forests, which include an active timber industry along the North Fork. There are two large irrigated agricultural areas in the basin (mapped in fig. 5 as shrubs and grasses)—Sierra Valley, east of Portola at the Middle Fork headwaters (149 mi^2), and Indian Valley in the East Branch drainage area (about 19 mi^2).

Geology and Soils

The Feather River Basin is located astride a north-south geologic transition in the Sierra Nevada—the transition between granitic bedrock that underlies and forms most of the central and southern Sierra Nevada and volcanic bedrock that underlies the northernmost parts of the Sierra Nevada and the Basin and Range Province (fig. 6*A*). In the Feather River Basin, volcanic rocks dominate in the north and west, and granitic and sedimentary rocks dominate in the south (Durrell, 1987; fig. 6*A*). The higher permeability of the volcanic rocks (Freeze and Cherry, 1979, table 2.2) allows more deep percolation of water and greater ground-water flow contributions to tributaries in the northern part of the basin. In PRMS, the ground-water flow is considered to be from the slower subsurface pathways beneath the local water table to the streams.

In this study, geology (Jennings and others, 1977; fig. 6*A*) is classified according to how it affects surface runoff, infiltration, and the transmission of water to streams. The classes are (1) volcanic formations (pyroclastic flows and volcanic mudflows); (2) sedimentary formations (shales, dolomites, Quaternary alluvium, playas, terraces, glacial till and moraines, marine and non marine sediments); and (3) intrusive igneous formations (granites and ultramafics). Volcanic formations are assumed to have the highest permeability (Freeze and Cherry, 1979, table 2.2) and contribute the highest amount of ground water to streams. Sedimentary formations, considered more permeable than igneous and less so than volcanic, are assumed to contribute water to streams from ground water, subsurface flow, and surface runoff. In PRMS, the subsurface flow is considered to be the pathways the soil-water excess takes in percolating through shallow unsaturated zones to stream channels, arriving at streams above the water table, and surface runoff is considered to be directly from snowmelt and rainfall. Intrusive igneous formations are considered to be the least permeable and assumed to produce the highest surface runoff rates to streams.

In this study, soil texture is categorized according to how it affects the transmission of water through the soil profile to streams, and how much storage of water it provides for evapotranspiration. Sand has a faster percolation rate than silt. In this study, the presence of vegetation cover (fig. 5) is assumed to indicate loam. Soil texture is presented in figure 6*B* (U.S. Department of Agriculture Forest Service, 1988, 1993, 1994; U.S. Environmental Protection Agency, 1998; http://www.essc.psu.edu/soil_info/index.cgi?soil_data&statsgo at 1:250,00 scale, accessed on Jan. 6, 2000).

Hydroclimatology

The Feather River Basin has a mediterranean climate, with warm, dry summers and cool, wet winters and springs. Precipitation occurs mostly during the cool season (winter and spring) and, in the higher altitudes, mostly as snow. Most of the basin lies at altitudes where winter temperatures can easily vary from below to above freezing. Therefore, streamflow fluctuations in the basin may be as dependent on temperatures as they are on precipitation rates, because snowmelt and the form of precipitation (rain, snow, or a mixture of both) are temperature dependent. Both precipitation and temperatures must be understood in order to characterize streamflow in this basin.

Data from 10 climate stations measuring temperature and/or precipitation and 2 stations measuring pan evaporation were used in this study (fig. 7; table 1). PRMS requires inputs of daily precipitation and daily maximum and minimum temperatures. Evaporation measurements, which are not required as input to PRMS, were used to gain an understanding of potential evaporation rates in the area. Station data may be retrieved from the California Data Exchange Center (CDEC) web page (http://cdec.water.ca.gov, accessed March 12, 2002) or from PG&E. CDEC is intended to provide access to data for immediate use, but most data are not reviewed. PG&E provides data for Bucks Creek Powerhouse (temperature and precipitation), Caribou Powerhouse (precipitation), and Canyon Dam (temperature).

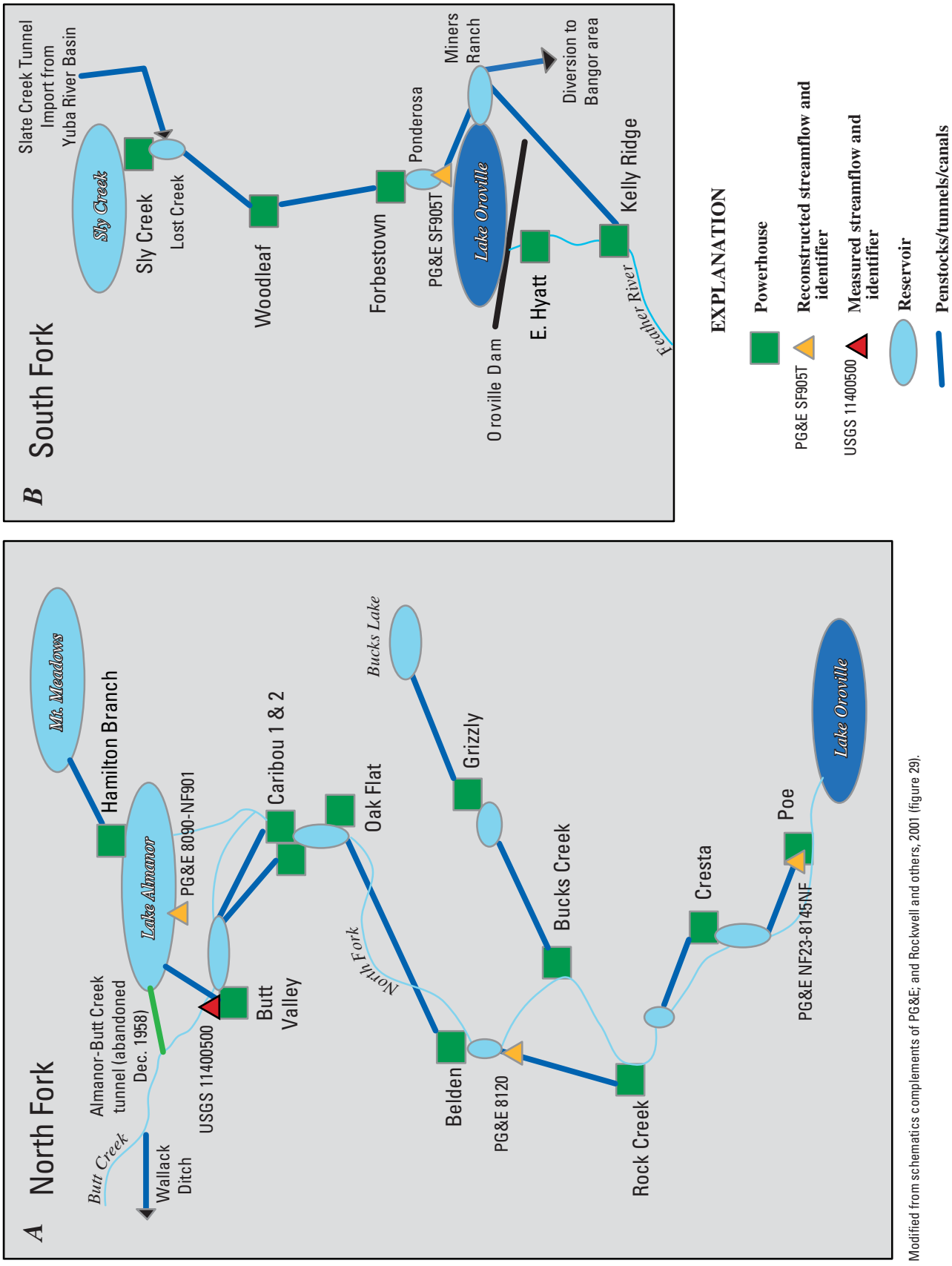

Modified from schematics complements of PG&E; and Rockwell and others, 2001 (figure 29).

Figure 4. North Fork and South Fork Feather River powerhouses and locations of reconstructed streamflow, Feather River Basin, California.

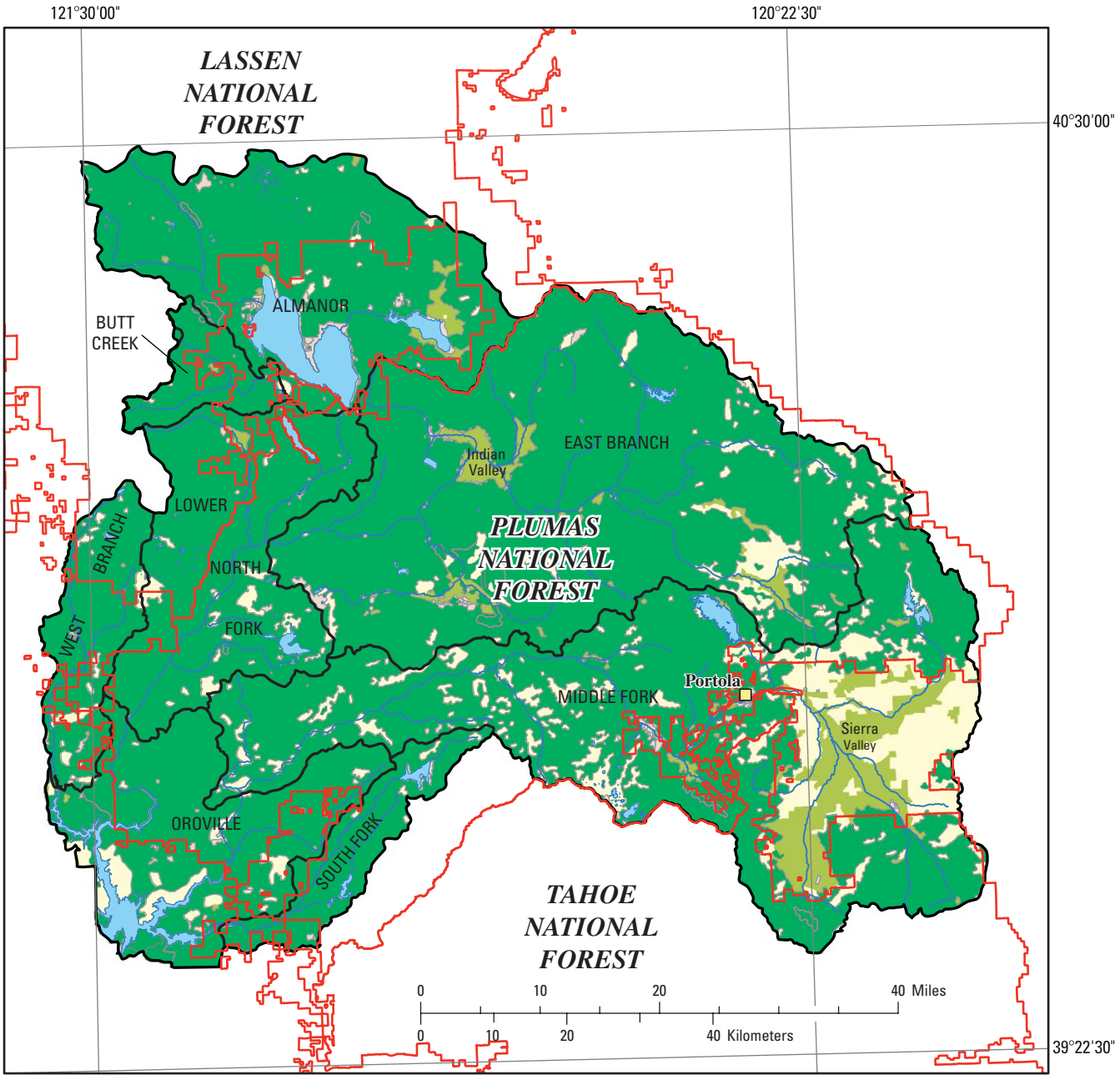

Modified from U.S. Geological Survey, EROS Data Center, Land Use Land Cover 1:250,000 (http://edc.usgs.gov/glis/hyper/guide/1_250_lulcfig/states.html, accessed on January 6, 2000), and Daniel Spring, U.S. Department of Agriculture Forest Service, written commun., 2002.

Figure 5. Vegetation cover types and National Forests in the Feather River Basin, California.

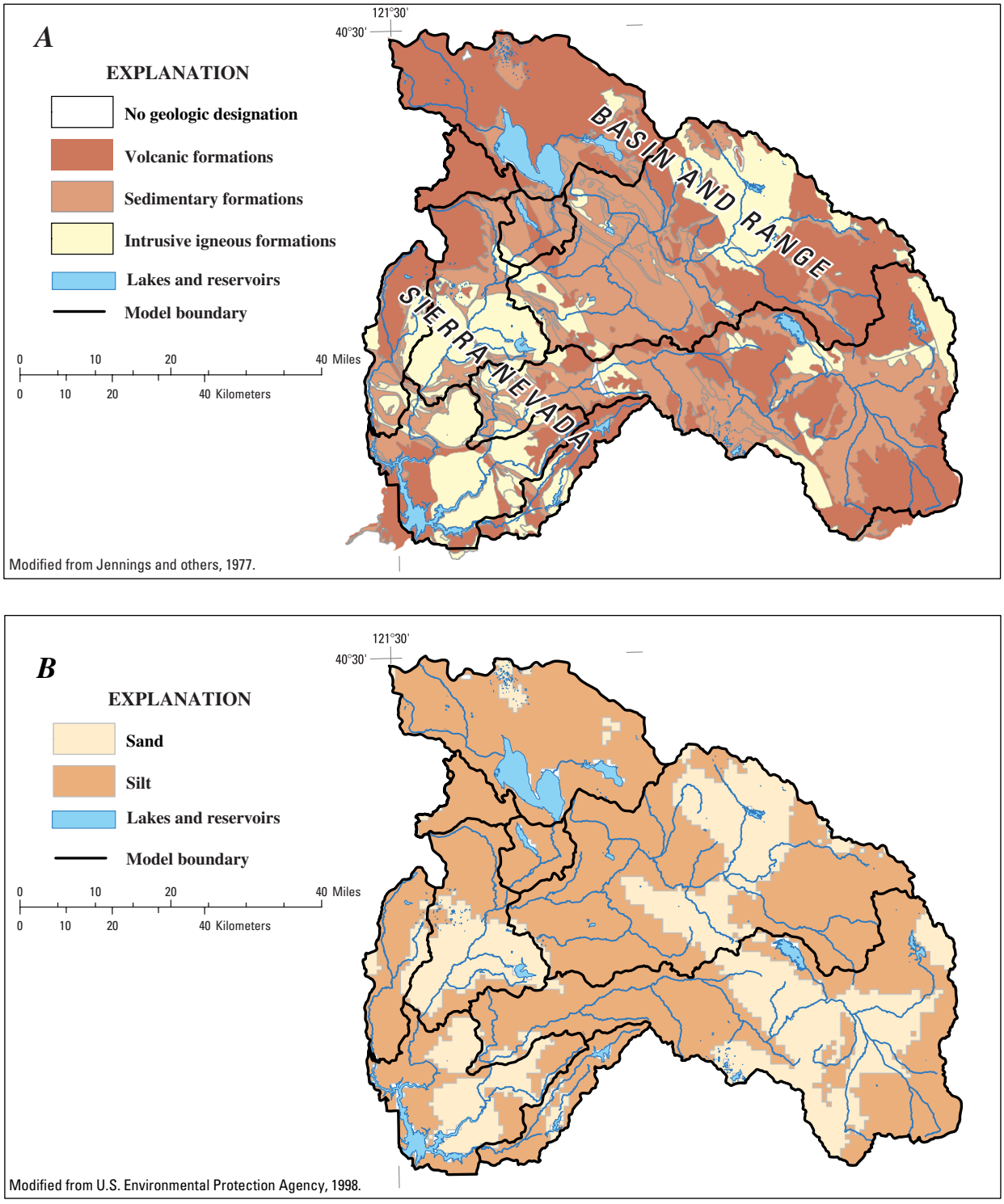

Figure 6. (*A*) Geology and (*B*) soil texture of the Feather River Basin, California.

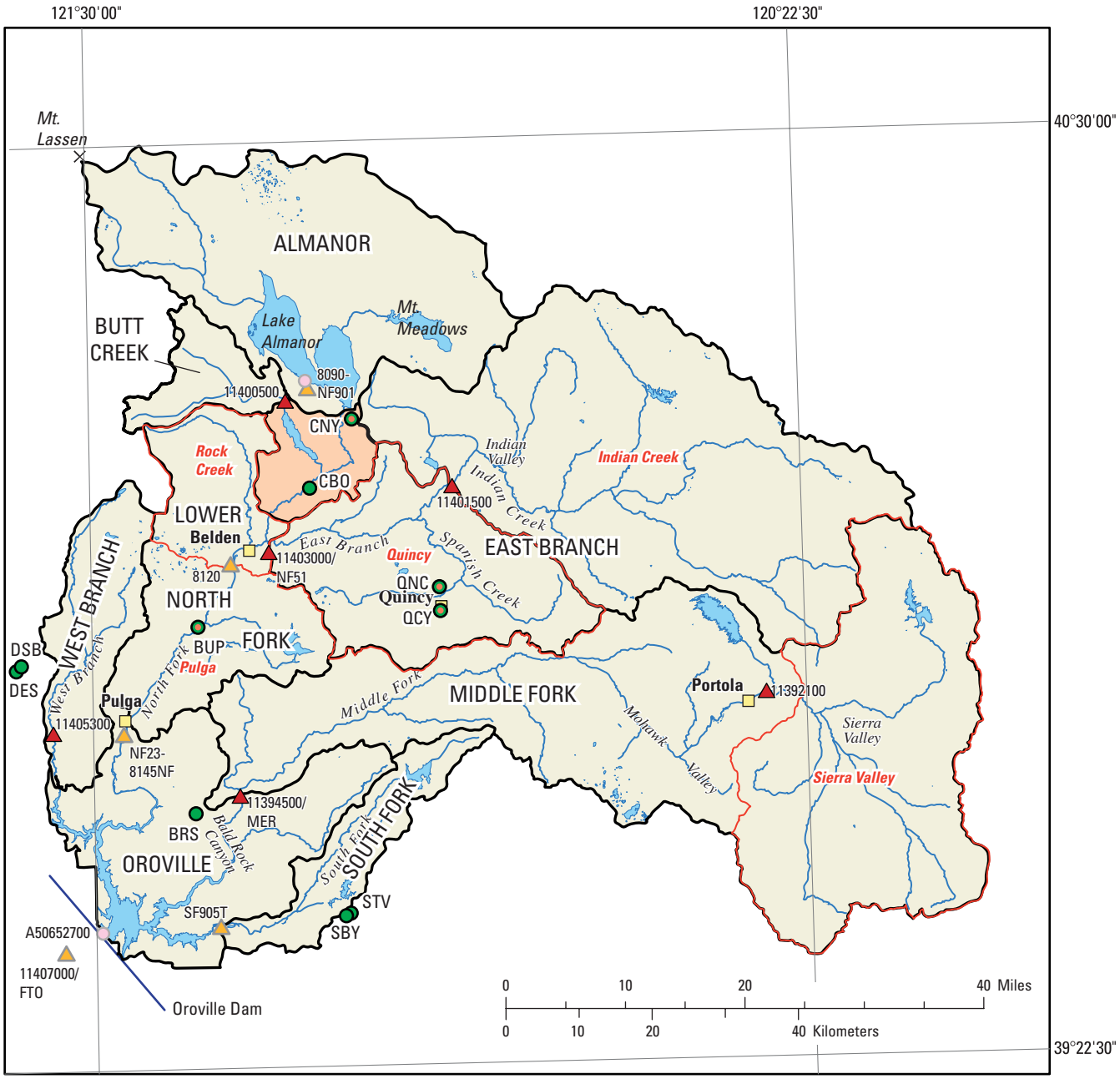

Modified from the California State Water Resources Control Board Basin Plain Maps, The California Watershed Map CALWATER version 2.0, 1:500,000, subbasins, catchments, and planning watershed area units.

EXPLANATION

- Belden — Cities and towns
- Model boundary
- Subdrainage model boundary
- Not modeled area
- Lakes and reservoirs

Streamflow station and number (see table 2 for identification)

- 11392100 — Measured data
- SF905T — Reconstructed data

Climate station (see table 1 for identification)

- BRS — Precipitation only
- QCY — Precipitation and temperature
- Pan evaporation only

Figure 7. Modeled areas and supporting catchments, and streamflow and climate stations, in/near the Feather River Basin, California.

Table 1. Climate stations used in Precipitation-Runoff Modeling System (PRMS) models for the Feather River Basin, California. Pan evaporation stations are not listed.

[See figs. 3 or 7 for locations of climate stations. CDEC, California Data Exchange Center; DWR, California Department of Water Resources; PG&E, Pacific Gas and Electric; RS, Ranger Station; USFS, U.S. Forest Service; NOAA, National Oceanic and Atmospheric Administration; ft asl, feet above sea level]

Model	Temperature			Precipitation[1]			
	Climate station name	Identifying designation	Source of data	Climate station name[2]	Identifying designation	Station altitude (ft asl)	Source of data
Almanor	Canyon Dam	CNY	PG&E				
Butt Creek	Canyon Dam	CNY	PG&E	Brush Creek (DWR)	BRS	3,560	CDEC website
				Bucks Creek Powerhouse	BUP	1,760	PG&E
East Branch	Quincy RS (USFS)/ Quincy (DWR)	QNC to 9/30/97 thereafter QCY	CDEC website	Canyon Dam	CNY	4,560	CDEC website
				Caribou	CBO	2,986	PG&E
				Desabla (PG&E)	DSB	2,710	CDEC website
Lower North Fork	Bucks Creek Powerhouse	BUP	PG&E	Desabla (DWR)	DES	2,710	CDEC website
				Quincy (DWR)	QCY	3,408	CDEC website
Middle Fork	Quincy RS (USFS)/ Quincy (DWR)	QNC to 9/30/97 thereafter QCY	CDEC website	Quincy RS (USFS)	QNC	3,420	CDEC website
				Strawberry-NOAA	STV	3,808	CDEC website
				Strawberry-DWR	SBY	3,810	CDEC website
South Fork	Bucks Creek Powerhouse	BUP	PG&E				
West Branch	Bucks Creek Powerhouse	BUP	PG&E				
Oroville	Bucks Creek Powerhouse	BUP	PG&E				

[1]All precipitation stations are used in the procedure to compute model input from PRISM surfaces.

[2]Many precipitation records are 'spliced.' Early manual gages were replaced by telemetered gage (BUP), or manual gage supplemented by telemetered gage (Brush Creek RS (BCR)/BRS, DSB/DES, QNC/QCY, STV/SBY). Monthly precipitation totals from these pairs commonly differ by 10 percent. For example, QCY is significantly wetter than QNC.

The streamflow simulations developed in this study were calibrated against data from daily measured or reconstructed-streamflow stations (fig. 7; table 2). These sites include data from five catchments. In this study, catchments are subdrainages with measured streamflow used to establish initial parameter settings in some of the models. These records were provided by USGS (http://waterdata.usgs.gov/nwis, accessed March 12, 2002), PG&E (proprietary), and DWR (http://cdec.water.ca.gov/, accessed March 12, 2002).

The USGS rates the accuracy of its streamflow records on the basis of (1) the stability of the stage-discharge relation, (2) the accuracy of measurements of stage and discharge, and (3) the interpretation of records (Bonner and others, 1998). Accuracy levels of "good" indicate that about 95 percent of the daily discharges are within 10 percent of their true values. "Fair" indicates that 95 percent of the daily discharges are within 15 percent (Bostic and others, 1997).

Because PG&E has proprietary knowledge of the hydropower operations along the North and South Forks, PG&E reconstructed natural streamflows for some of the model areas. The proprietary reconstructed streamflows provided by PG&E for the Almanor, Lower North Fork, and South Fork drainages were computed using mass-balance calculations cross-referenced against nearby measured natural flows (for example, at Butt Creek). Daily flows from the Almanor drainage were estimated, from measured daily changes in lake storage and outflow, as apparent inflows to the lake. Reconstructed flows were accumulated in downstream directions and corrected for intervening diversions and impoundments to reconstruct natural flow at six gaging locations. PG&E estimates the accuracy of the reconstructed flows to be about 15 percent.

Total natural inflows to Lake Oroville were needed for comparison with the total simulated inflow, which is a summation of results from the eight models. Because natural daily inflow was not available, monthly reconstructions from DWR (Feather River at Oroville, FTO) were used (http://cdec.water.ca.gov). The FTO inflow station (http://cdec.water.ca.gov, accessed on March 12, 2002) is referenced to USGS gaging station 11407000 (fig. 2). The monthly FTO reconstructions were computed by DWR using measurements from USGS gaging stations 11407000, 11406920 (figs. 2 and 7, Appendix A) and many other gages. Monthly reconstructions include corrections for streamflow regulation above the gage (including exports, imports, and diversions for power and irrigation) and changes in storage and evaporation in the larger reservoirs. Imports from the Yuba and Little Truckee Rivers (fig.1 and 4) were explicitly taken into account. Prior to construction of the Oroville Dam and the Thermalito Complex downstream (in 1967, fig. 2), the 11407000 gage was located a few miles farther upstream with 17 mi^2 less contributing area (Markham and others, 1996). Although gaged streamflows in canals, releases from dams, and reservoir storage probably are accurate to within several percent most of the time, other aspects of the reconstructions, such as evaporation and assumed consumptive use, are much more uncertain. According to J. Pierre Stephens of CCSS, when streamflows exceed the Thermalito Powerhouse capacity (fig. 2), large flows are released at the Thermalito Diversion Dam. The net effect of moving the gage, and measurement accuracy, consumptive-use estimates, and regulation during high flows on reconstruction accuracy is uncertain. The USGS has not quantified the accuracy of the FTO reconstructions. However, DWR assumes that the calculated monthly reconstructed streamflow at FTO is within 5 to 10 percent of its true value most of the time (J. Pierre Stephens, DWR Resources Hydrology Branch, unpub. data, 2001).

Climate

The most significant limitation in the practice of snowmelt-runoff modeling is the scarcity of climate data and the need to extrapolate point measurements to areal values. Comparisons of snowmelt-runoff simulation models, which were made in 1986 (World Meteorological Organization, 1986), indicate that the distribution and temperature-dependent form of precipitation were the most important factors in producing accurate estimates of runoff volume. The orographic effect of increasing precipitation with increasing altitude can cause significant spatial variations of precipitation. Usually, these are accommodated by specifying long-term mean precipitation relations to altitude. However, the spatial variations in the relations may be large (Leavesley, 1989). Besides precipitation amount, snowpack modeling also requires that precipitation form be specified on a daily basis.

In PRMS, precipitation form (rain or snow) is dependent on daily temperatures and controlled by setting a snow-threshold temperature. Precipitation is assumed to be snow when the maximum daily temperature is below this threshold, and rain when the minimum temperature is above it. At intermediate temperatures, precipitation is computed in PRMS to be a mix of rain and snow. Temperature generally decreases with increasing altitude except where and when temperature inversions develop. In PRMS, temperature measurements are extrapolated over a basin by assuming a fixed lapse rate (the rate of temperature decrease upward through the atmosphere). In PRMS, constant monthly maximum and minimum temperature lapse rates are specified. However, these constants generally do not reflect the actual variability observed in daily lapse rates (Leavesley, 1989).

Table 2. Streamflow stations used in watershed modeling of the Feather River Basin, California.

[ID, identifying designation; mi^2, square miles. PG&E, Pacific Gas and Electric; USGS, U.S. Geological Survey; DWR, California Department of Water Resources]

Model	Sub-drainage model[1]	Model ID	Station name	ID[2]	Gaged area (mi^2)	Source of streamflow data	Collection method	Reconstructed-streamflow modification	Daily record used in study
Almanor		AC	Inflow above Almanor Canyon Dam	8090-NF901	488	PG&E	Reconstructed	At headwaters, no modification	10/1/69–9/30/97
Butt Creek		BC	Butt Creek below Almanor—Butt Creek Tunnel, near Prattville	11400500	69	USGS	Measured[3]		10/1/64–10/31/2001
East Branch		EB	East Branch of North Fork Feather River near Rich Bar, California/Flow at NF51 E. Branch NF Feather	11403000/NF51	1,025	USGS/PG&E	Measured		10/1/50–9/30/61 and 12/1/67–9/30/82, 10/1/82–10/31/2001
	Indian Creek	IC	Indian Creek near Crescent Mills	11401500	738	USGS	Measured		10/1/50–9/30/93
	Quincy	QC			287	USGS/PG&E	Reconstructed	QC flow = EB flow – IC flow	10/1/50–9/30/93
Lower North Fork		LO	Inflow above NF23-8145NF at Pulga	NF23-8145NF	290	PG&E	Reconstructed	LO flow = NF23-8145NF flow – EB flow –BC flow – AC flow	10/1/69–9/30/97
	Rock Creek	RC	Inflow above Rock Creek Diversion Dam	8120	112	PG&E	Reconstructed	RC flow = 8120 flow – EB flow –BC flow –AC flow	10/1/69–9/30/97
	Pulga	PC			178	PG&E	Reconstructed	PC flow = LO flow – RC flow	10/1/69–9/30/97
Middle Fork		MF	Middle Fork Feather River near Merrimac	11394500/MER	1,046	USGS/DWR	Measured		10/1/51–9/30/86, 10/1/86–10/31/2001
	Sierra Valley	SV	Middle Fork Feather River near Portola	11392100/no DWR ID	590	USGS/DWR	Measured		10/1/70–9/30/86
South Fork		SF	South Fork Outlet	SF905T	107	PG&E	Reconstructed	At headwaters, no modification	10/1/69–9/30/97
West Branch		WB	West Branch Feather River near Paradise	11405300	110	USGS	Measured		10/1/57–9/30/86

Table 2. Streamflow stations used in watershed modeling of the Feather River Basin, California—Continued.

[ID, identifying designation; mi^2, square miles. PG&E, Pacific Gas and Electric; USGS, U.S. Geological Survey; DWR, California Department of Water Resources]

Model	Sub-drainage model[1]	Model ID	Station name	ID[2]	Gaged area (mi^2)	Source of streamflow data	Collection method	Reconstructed-streamflow modification	Daily record used in study
Oroville		OR	No daily measured or reconstructed data	—	—	—	—		—
			Feather River at Oroville/Total inflow to Lake Oroville[4]	11407000/FTO	3,600	USGS/DWR	Reconstructed	Full basin, no modification	10/01/1901–11/2001 (monthly record)

[1]Used to develop parameter settings for the larger model, but not part of the final suite of models.

[2]See figure 7 for location.

[3]Measured at each gaging station as noted.

[4]Provided by DWR (computed using a water-budget approach), reconstructed from gage data measured below Thermalito Diversion Dam. These monthly values are compared with the combined simulated inflow from the PRMS models.

Spatial variation of temporal statistical means of precipitation and temperatures, and deviations of precipitation and temperature around their long-term means, must be specified when constructing watershed models. Spatial variations of the means are represented in PRMS through precipitation and temperature correction factors for each modeled area, which typically are specified as lapse rates to account for altitude differences. Deviations around the means are represented by imposing daily variations at each modeled area that are proportional (for precipitation), or additive (for temperatures), to the daily weather series from specified climate stations.

To allow for future real-time applications, data from climate stations that reported measurements on a daily basis were preferred for the Feather River PRMS models. Ten daily real-time climate stations were used for this study. All ten report real-time precipitation. Of these, one station manually reports daily precipitation measurements, and nine are telemetered. Three of the telemetered stations are also manually observed. Temperature is reported on a real-time basis at three of the ten climate stations. Temperature and precipitation data measured at these 10 climate stations were used in this study (fig. 7; table 1). The period of record began as early as October 1, 1937, but most records span 1969 to October 1, 2001.

The climate stations available for this study are concentrated on the western, wetter side of the basin, below Lake Almanor (figs. 7, 8). Therefore, some bias toward higher precipitation probably exists (fig. 8*A*). Also, the three temperature stations used in this study (fig. 7, table 1), are located in lower altitude, warmer areas so that biases in temperature may exist. Increasing the number and distribution of real-time data-collection stations could improve model accuracy and streamflow prediction performance.

Precipitation

The Feather River Basin receives about 45 in. of precipitation per year, as interpolated by the Parameter-Elevation Regressions on Independent Slopes Model (PRISM) of Daly and others (1994; 30-year mean-average, 1961–90). Annual precipitation varies from a low of 13 in. on the rain-shadow side of the Sierra Nevada in the Middle Fork headwaters, to a high of 125 in. near Mt. Lassen (in the upper reaches of the North Fork in the Almanor drainage; fig. 8*A*). The drier areas are in the southeastern third of the basin (fig. 8*A*). These include Lake Oroville and areas to the east, the eastern half of the East Branch, and most of the Middle Fork. The wettest areas, which can receive more than 85 in. per year, are near Mt. Lassen and in a band immediately above Lake Oroville. The wettest areas include the headwaters of West Branch, Bucks Lake, Table Mountain, and La Porte Bald Mountain, all of which are about 6,000 ft above sea level (asl) (figs. 3, 8*A*). An intermediate amount of precipitation falls in the middle of the basin and around the Lake Oroville drainage.

Monthly patterns of precipitation are generally similar to the annual pattern (selected months shown in figs. 8*B–E*; Daly and others, 1994). In October, precipitation averages 1 to 2 in. in the eastern drier areas and 2 to 6 in. in wetter areas. In November (fig. 8*B*) and December, the basin averages from 1.75 to 6 in. in drier areas and about 16 to 20 in. in wetter areas. January (fig. 8*C*), which historically is the wettest month, averages 23 in. of precipitation on Grizzly Mountain and Mt. Lassen but only about 3 in. of precipitation in Sierra Valley. Less precipitation falls in February through March but, nevertheless, averages as much as 14 in. over the wetter areas. By April, most of the basin averages between 2 and 6 in. of precipitation, except on the wetter peaks (6 to 8 in.) including Mt. Lassen (12 in.). By May (fig. 8*D*), the basin averages between 0.25 to 6 in. of precipitation. The months June through September (fig. 8*E*) are historically very dry, averaging less than 2 in. in most of the basin.

PRISM is designed to map climate in complex environmental regimes, including high mountainous terrain and rain shadows, such as found in the Feather River Basin (Daly and others, 1994). PRISM uses point measurements, digital elevation models, and other spatial data to generate gridded estimates of monthly and yearly precipitation. PRISM fits separate precipitation/altitude relations to neighboring stations with the same topographic aspect to generate interpolated values. This is a departure from simply applying a single altitude-dependent precipitation measurement to similar altitudes within the basin. Thus, PRISM is automated to adjust its frame of reference to accommodate local and regional climatic differences and rain shadows to create a pattern of precipitation (Daly and others, 1994). Because precipitation varies strongly with topography, and few long-term precipitation measurements are reported real-time in the Feather River Basin, PRISM simulations are well suited for use in this study. The mean-monthly PRISM simulations were generally found to be within 1 in. of the measurements at stations in the Feather River Basin (figs. 9*B, C*).

During the cool season, days with measurable precipitation are common in the basin. The number of days of precipitation in each month was computed from observations at the 10 precipitation stations used in this study (table 1). From November to April, precipitation fell about every 1 out of 2 days. In May, precipitation occurred 4 out of 10 days. During June-September, precipitation occurred 1 or 2 days out of 10, and in October, 3 out of 10 days.

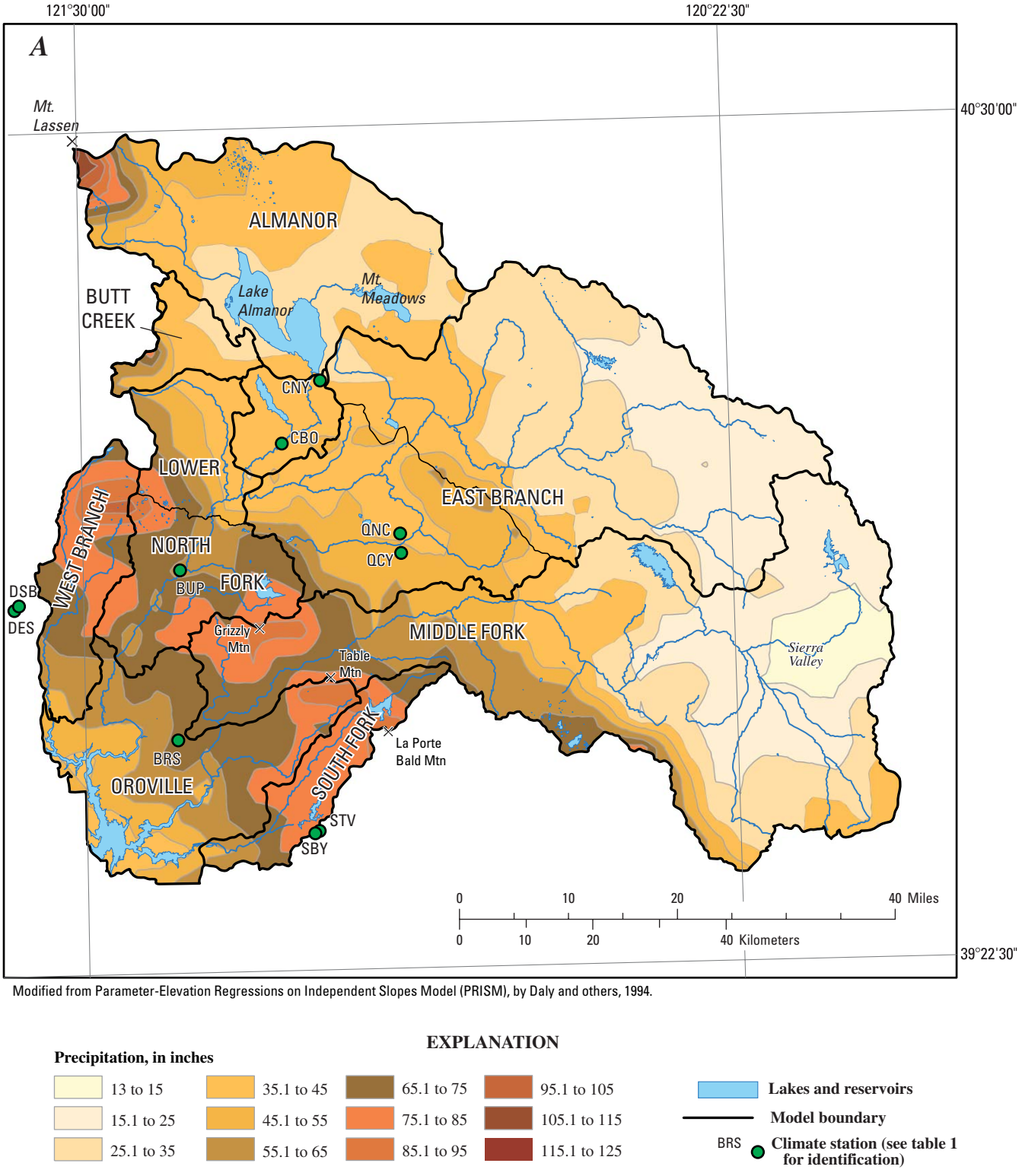

Figure 8. Distributions of precipitation over the Feather River Basin, California, including (*A*) 30-year mean-annual, and selected 30-year mean-monthly, (*B*) November, (*C*) January, (*D*) May, and (*E*) September patterns.

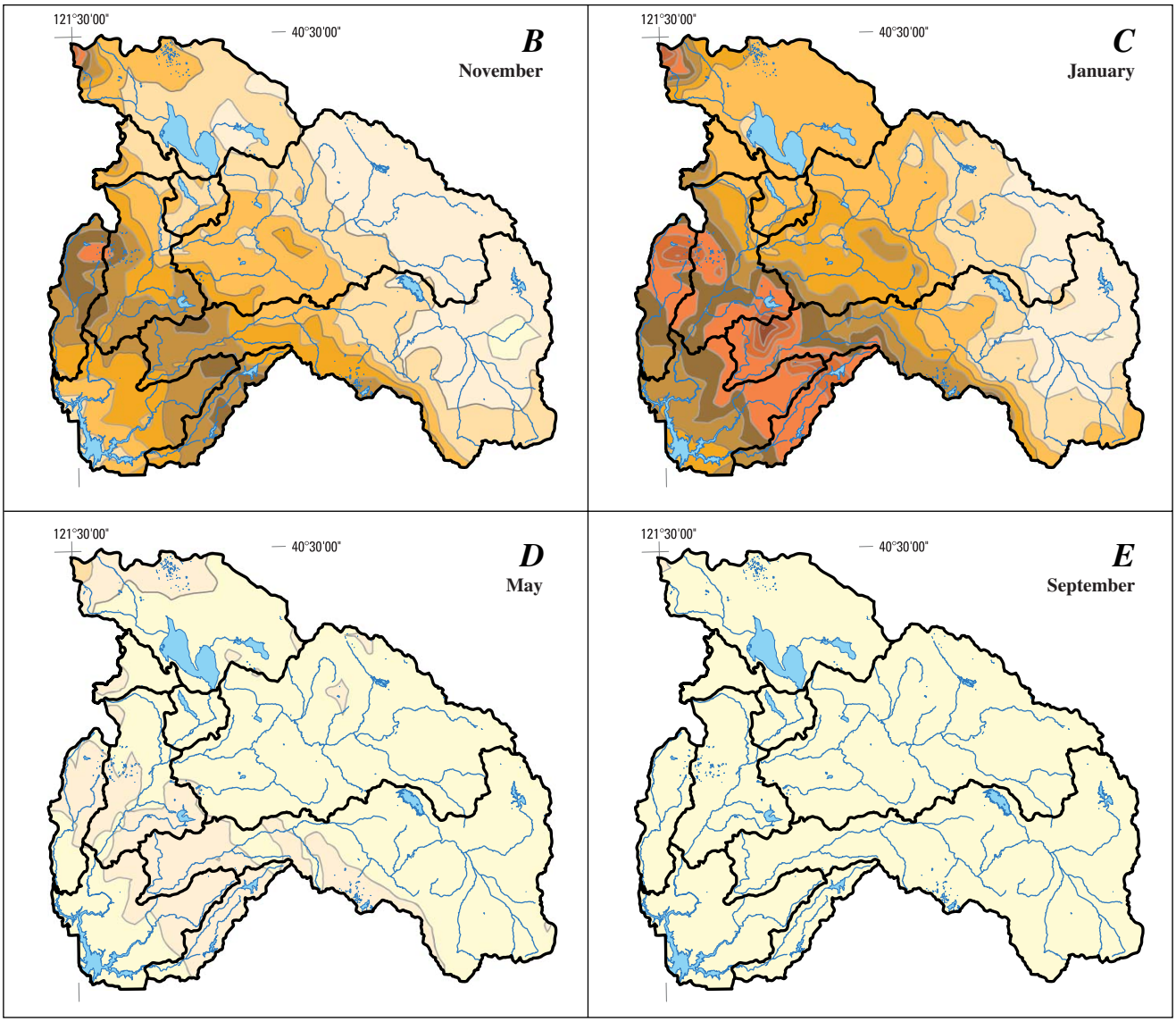

Figure 8.—Continued.

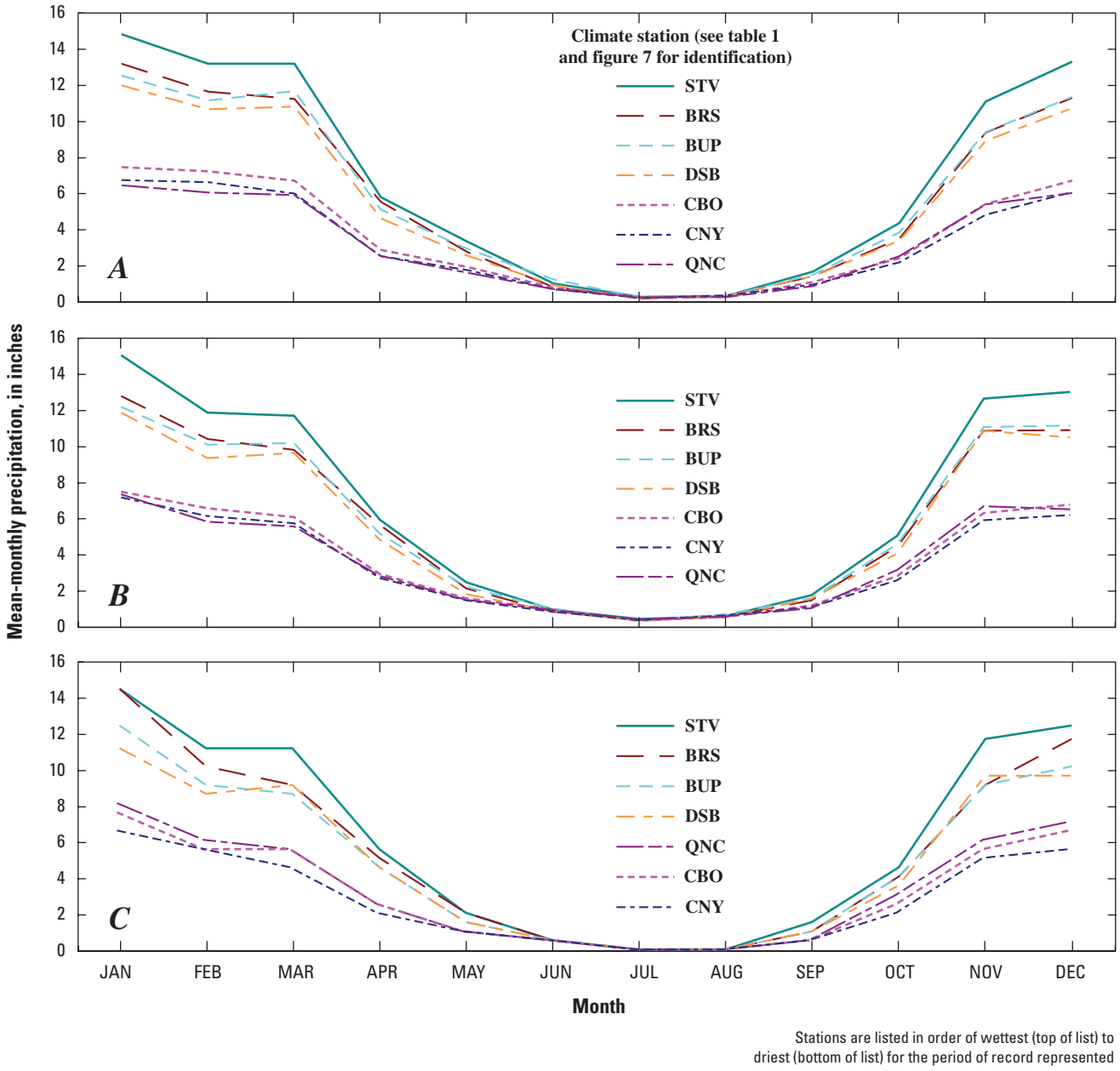

Figure 9. Mean-monthly precipitation (in inches) for the Feather River Basin measured at climate stations (*A*) during the modeling period 1971–97, (*B*) measured in the 1961–90 period, and (*C*) estimated from Precipitation-Elevation Regressions on Independent Slopes Model (PRISM, Daly and others, 1994) at locations of the precipitation stations for 1961–90. Stations are listed in order of wettest (top of list) to driest (bottom of list) measurements for the period of record presented.

PRISM simulations of orographic and rain-shadow patterns agree with the precipitation measurements in the basin. Historically, Canyon Dam (CNY), Caribou (CBO), and Quincy (QNC and QCY) receive the least precipitation (table 1; figs.8*A*, 9). Much more precipitation (as much as two to three times that of the driest stations) falls on Strawberry Valley (SBY and STV), Brush Creek (BRS), Buck Creek Powerhouse (BUP), and Desabla (DSB and DES). The Desabla stations are located outside the study area, on the windward side of the ridge bounding the western edge of the Feather River Basin (fig. 8*A*). On a daily basis, the Desabla stations measure a wider range of precipitation (wetter or drier) than other stations, and may be exposed to slightly different weather patterns.

Precipitation was analyzed using descriptive statistics and graphing to understand how precipitation compares between gage sites, and generally how storms may vary over the basin. There is considerable variation in daily precipitation between climate stations. However, monthly-mean values for water years 1971–97 were closely correlated ($r > 0.90$), especially from September through May. In summertime (June–August), the correlation decreased to about $r = 0.80$ (fig. 10) because summer rainfall is light and intermittent over the basin. Throughout the year, the poorest correlations (table 3) were typically between the drier Quincy stations (QCY, QNC) and the wettest stations, Desabla (DES), Brush Creek (BRS), and Strawberry (STV). As with the monthly comparisons, the precipitation stations were found to be closely correlated on a water-year-mean scale (generally above 0.90; table 3). Lower correlations between water-year means were observed between the Quincy (QCY, QNC) and wetter stations (DES, BRS, STV), but were still above 0.75. These results show that for a month or year, precipitation variations are generally similar and uniformly timed among the 10 measurement stations.

Temperature

It is important to understand the spatial and temporal distribution of temperatures when studying and predicting streamflow. Based on daily temperatures, PRMS computes heat balances, solar radiation, precipitation form, snowmelt and accumulation, sublimation, evapotranspiration, and other critical elements (Leavesley and others, 1983). Temperatures vary from one station to another due to local effects (wind, cloud cover, instrument shading, and aspect), and decrease with altitude. Also, temperature changes seasonally, and from year to year, and even from decade to decade.

In model operation, daily temperature measurements are extrapolated to each area using a specified monthly lapse rate. Temperature lapse rates were initially estimated to be 3.6 degrees Fahrenheit (^{o}F) per 1,000 ft of altitude change (Jeton, 1999b). Lapse-rate parameter settings were then adjusted at specific sites during model calibration.

Temperature records for the three stations used in this study date from at least the 1950s. The stations are centrally located and in the lower altitudes of the basin, below the snow line (figs. 3 and 7; table 1). The stations are Bucks Creek Powerhouse (BUP) at 1,760 ft, Quincy (QNC-QCY) at 3,408 ft, and Canyon Dam (CNY) at 4,560 ft above sea level. The average daily minimum and maximum temperatures at CNY, the highest of these stations, were 33 and 60 ^{o}F; respectively. At the lowest station, BUP, the corresponding averages were 46 and 71 ^{o}F. Temperatures at QNC-QCY are generally between the other two. Occasionally, however, temperature inversions cause QNC-QCY to register temperatures cooler than those at CNY.

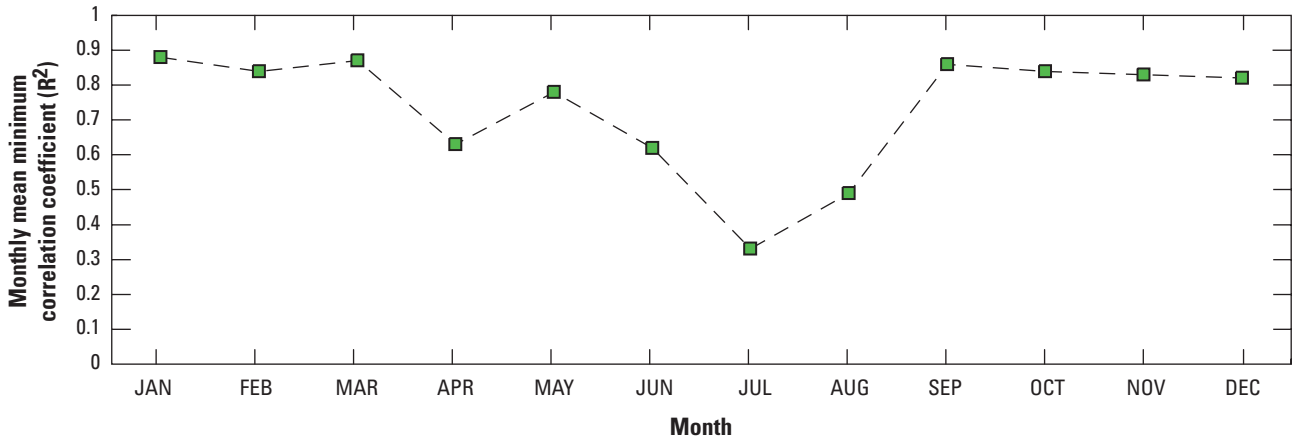

Figure 10. Minimum correlation of precipitation measurements (monthly means) between stations used in watershed modeling of the Feather River Basin, California, water years 1971–97. Trend lines were added to assist the reader in visualizing results and do not reflect actual data.

Table 3. Correlation of precipitation (water-year means) between stations used in watershed modeling of the Feather River Basin, California, water years 1971–97.

[Because of limited reported data, Strawberry-DWR (SBY) was not included in this analysis; see table 1 for climate station identifying designation; DWR, California Department of Water Resources]

Climate station	BRS	BUP	CBO	CNY	DES[1]	DSB	QCY[2]	QNC	STV
BRS	1.00	0.94	0.94	0.93	0.96	0.95	0.89	0.75	0.95
BUP		1.00	0.98	0.97	0.99	0.97	0.94	0.86	0.99
CBO			1.00	0.98	0.98	0.95	0.94	0.84	0.98
CNY				1.00	0.98	0.94	0.97	0.89	0.98
DES					1.00	1.00	0.93	0.87	0.99
DSB						1.00	0.90	0.80	0.97
QCY							1.00	0.97	0.97
QNC								1.00	0.89
STV									1.00

[1]Computations based on available data, water years 1989–97.
[2]Computations based on available data, water years 1988–97.

These temperature stations may not be entirely representative of conditions in model areas in which they were used as a surrogate for temperature, but the other stations that might replace them are not yet reporting on a real-time basis. There are local environmental conditions which may affect temperature at these stations. BUP (fig. 8; table 1) is located in a very narrow valley affected by winter storms that reportedly funnel up the canyon (Gary Freeman, Pacific Gas & Electric Company, unpub. data, 1999). CNY (below Lake Almanor Dam; fig. 7) is in one of the drier areas of the basin. Because the U.S. Forest Service stopped reporting temperatures for QNC mid-water year (October through September) 1998, QCY (operated by DWR) was used to continue its record. For the period October 1997–May 1998, QCY had average maximum daily temperatures 4 to 10 °F warmer than those of QNC and minimum temperatures of 3 °F warmer. The differences in temperature between the two gages may be due to location or to calibration. QCY is located in the town of Quincy, whereas QNC is located on the lee of a ridge, 3 mi north of town.

Double-mass analyses (Linsley and others, 1975) of the daily temperatures between climate stations located inside and outside the basin showed no unusual breaks in the slope of graphed results during the model calibration period, October 1, 1970, through September 30, 1997. This indicated that the instrumentation measured similar (parallel) temperature variations at all stations. Therefore, temperatures appear to have been measured in consistent ways throughout the calibration period. However, after the calibration period, a break was observed in the Quincy records in about November 1998, indicating an increase in minimum daily temperatures measured at the new station, QCY, as compared with the old station, QNC.

Temperature determines the form of precipitation (rain only, snow only, or rain-on-snow mixture). To get a sense of the variations in precipitation form, the percentage of days when temperatures were above and below freezing was compiled. The percentages of freezing days in all recorded data are shown in tables 4 (full year) and 5 (precipitation days only). Most notably, on days with precipitation, maximum daily temperatures in December–February at the CNY station were above freezing over 80 percent of the time, and minimum temperatures were below freezing over 80 percent of the time. Thus, on most winter days, temperatures fluctuated around and near freezing. Precipitation form must vary considerably in the middle altitude areas of the basin. Although snow may accumulate even when surface temperatures are a few degrees above freezing, precipitation on most occasions within the Feather River Basin probably takes the form of rain, or rain-on-snow, during the daytime and then snow at night. At higher altitudes (for example, CNY), there are more days with consistently freezing temperatures and, therefore, more snow. Monthly estimates of mean-maximum and mean-minimum temperatures are given in tables 6 and 7. In the Feather River Basin, January is the coldest month with a daily measured extreme of –24 °F, and July is the warmest with a daily measured extreme 115°F.

Evaporation

Pan evaporation is not required as input to PRMS because it is computed within the models. However, pan-evaporation records from various sites within the basin provide an indication of the potential for evapotranspiration and so aid in calibrating the models. Typically, less evaporation occurs at higher altitudes. In the Feather River Basin, pan-evaporation rates have been measured at Oroville Dam (station #A50652700; California Department of Water Resources, 1979; fig. 7) and Lake Almanor (Jim Trask, University of California at Davis, unpub. data, 2000; fig. 7). The mean-annual rate at Oroville Dam (900 ft asl), during water years 1960–76, is 67.5 in. The mean-annual rate at Lake Almanor (4,500 ft asl) is about 45 in.

Table 4. Period-of-record percentages of days with maximum (first number) and minimum (second number) temperatures less than or equal to freezing, at climate stations in the Feather River Basin, California.

[ID, identifying designation; ft asl, feet above sea level; CDEC, California Data Exchange Center; DWR, California Department of Water Resources; PG&E, Pacific Gas and Electric; RS, ranger station; USFS, U.S. Forest Service]

Temperature station	ID	Source	Altitude (ft asl)	Period of record	Oct.	Nov.	Dec.	Jan.	Feb.	Mar.	Apr.	May	June	July	Aug.	Sept.
Bucks Creek Powerhouse	BUP	PG&E	1,760	1/1/59–10/31/01	0, 0	0, 6	1, 25	0, 29	0, 19	0, 11	0, 4	0, 0	0, 0	0, 0	0, 0	0, 0
Quincy RS (USFS)/ Quincy (DWR)	QNC/ QCY	DWR, CDEC website	3,420/ 3,408	10/1/37–10/31/01	0, 58	0, 73	2, 82	2, 81	1, 78	0, 73	0, 59	0, 24	0, 6	0, 3	0, 10	0, 28
Canyon Dam	CNY	PG&E	4,560	10/1/37–10/31/01	0, 40	1, 79	11, 91	14, 94	6, 93	1, 90	0, 70	0, 28	0, 4	0, 0	0, 0	0, 6

Table 5. Period-of-record percentages of days with observed precipitation with maximum (first number) and minimum (second number) temperatures less than or equal to freezing, at climate stations in the Feather River Basin, California.

[ID, identifying designation; ft asl, feet above sea level; CDEC, California Data Exchange Center; DWR, California Department of Water Resources; PG&E, Pacific Gas and Electric; RS, ranger station; USFS, U.S. Forest Service]

Temperature station	ID	Source	Altitude (ft asl)	Period of record	Oct.	Nov.	Dec.	Jan.	Feb.	Mar.	Apr.	May	June	July	Aug.	Sept.
Bucks Creek Powerhouse	BUP	PG&E	1,760	1/1/59–10/31/01	0, 1	0, 8	1, 24	1, 26	0, 21	0, 15	0, 7	0, 1	0, 0	0, 0	0, 0	0, 0
Quincy RS (USFS)/ Quincy (DWR)	QNC/ QCY	DWR, CDEC website	3,420/ 3,408	10/1/37–10/31/01	0, 34	0, 53	2, 68	2, 67	2, 63	0, 60	0, 48	0, 21	0, 5	0, 1	0, 1	0, 10
Canyon Dam	CNY	PG&E	4,560	10/1/37–10/31/01	0, 34	2, 67	12, 85	14, 88	9, 88	2, 85	0, 69	0, 34	0, 8	0, 0	0, 0	0, 6

Table 6. Period-of-record mean-monthly maximum (first number) and minimum (second number) temperatures, at climate stations in the Feather River Basin, California.

[DWR, California Department of Water Resources; RS, Ranger Station; USFS, U.S. Forest Service]

Temperature station	Period of record	Oct.	Nov.	Dec.	Jan.	Feb.	Mar.	Apr.	May	June	July	Aug.	Sept.
Bucks Creek Powerhouse	1/1/59–10/31/01	74, 49	58, 41	49, 36	50, 36	56, 37	62, 39	69, 43	77, 49	86, 56	93, 61	92, 60	86, 56
Quincy RS (USFS)/ Quincy (DWR)	10/1/37–10/31/01	72, 32	56, 28	46, 25	47, 24	52, 26	58, 29	65, 32	74, 37	82, 42	90, 44	89, 41	83, 37
Canyon Dam	10/1/37–10/31/01	64, 34	48, 28	40, 24	39, 22	43, 23	49, 26	57, 30	67, 36	76, 42	85, 47	84, 45	77, 41

Table 7. Mean-monthly maximum (first number) and minimum (second number) temperatures, water years 1971–97, at climate stations in the Feather River Basin, California.

[DWR, California Department of Water Resources; RS, Ranger Station; USFS, U.S. Forest Service]

Temperature station	Oct.	Nov.	Dec.	Jan.	Feb.	Mar.	April	May	June	July	Aug.	Sept.
Bucks Creek Powerhouse	74, 49	58, 41	49, 36	50, 36	57, 38	63, 40	70, 44	78, 49	86, 55	93, 61	92, 60	86, 56
Quincy RS (USFS) / Quincy (DWR)	72, 31	56, 27	46, 24	47, 23	54, 26	59, 30	66, 32	75, 37	84, 42	91, 44	90, 43	84, 38
Canyon Dam	64, 35	48, 28	40, 24	40, 22	44, 24	49, 28	58, 31	68, 37	76, 43	84, 48	83, 46	76, 41

Streamflow

Hydrographs of tributary streamflow show a similar response to the climatic variations within the basin (fig. 11). The magnitudes differ, but all display a similar signature: higher winter flows with less dramatic springtime snowmelt peaks than are typically encountered in the higher altitude basins of the southern Sierra Nevada. Higher winter flows (January-March) are due to frequent warmer-than-freezing temperatures (tables 4, 5, 6, and 7), which result in sudden winter runoff from rain and melting snow. In the Feather River Basin, owing to winter melt and a portion of precipitation falling as rain, less snowpack remains by April, and thus the spring snowmelt produces lower peaks than seen in typical hydrographs of the southern Sierra Nevada. By July, most snow in the Feather River Basin has melted. Summer streamflow comes from subsurface and ground-water flows. By October, regardless of the part of the basin evaluated, streamflow rates are at their minimum.

Streamflow has been measured at the mouth of the Feather River Basin near the city of Oroville since 1901 (USGS 11407000), and at areas within the basin since the 1950s (table 2). During the 20th century, the river and all its reaches were increasingly developed for hydroelectric power production and irrigation. These uses impede or change streamflow, and thus measurements at gaging stations no longer reflect natural streamflow. Where hydropower has been developed in the basin, natural streamflows have been reconstructed by DWR (Appendix A) and PG&E (proprietary) using knowledge of impoundments, evaporation, and diversions. The USGS has not quantified the uncertainty of these reconstructions.

Lake Oroville has a capacity of 3,538,000 acre-ft of water and, in the average water year, DWR's reconstructed inflows to Lake Oroville (Feather River at Oroville (FTO), table 2; fig. 1) have been about 4,539,000 acre-ft (from water years 1906–2000, http//: cdec.water.ca.gov), with a standard deviation of 2,127,000 acre-ft. During the 95 water years evaluated here, the total annual inflow equaled or exceeded the maximum storage capacity of Lake Oroville 58 times. Historically, maximum monthly inflow to Lake Oroville has occurred as early as December and as late as May, but, most often, maximum monthly inflows occurred in March or April. Over the 95-year period of reconstructed data, 1906–2000, the maximum mean-monthly inflow to Lake Oroville (FTO) was in April. The minimum inflow typically occurred in September (table 8).

Table 8. Mean-monthly reconstructed inflow to Lake Oroville (FTO), California, water years 1906–2000

[FTO, California Department of Water Resources streamflow reconstruction site: Feather River at Oroville, California]

Month	Mean-monthly inflow, in acre-feet	Maximum monthly inflow, in acre-feet	Minimum monthly inflow, in acre-feet	Standard deviation, in acre-feet
Oct.	105,665	855,300	40,225	83,341
Nov.	188,073	1,240,390	57,400	187,820
Dec.	350,047	1,997,200	61,803	385,630
Jan.	517,128	2,539,490	69,429	521,346
Feb.	567,797	2,677,102	88,900	404,159
Mar.	692,632	2,282,679	91,640	441,250
April	733,687	1,830,000	99,940	372,853
May	673,486	1,700,000	101,000	391,825
June	354,865	1,121,710	63,900	240,286
July	161,558	391,800	62,700	75,080
Aug.	104,546	197,330	57,800	29,481
Sept.	89,580	157,899	52,500	22,322

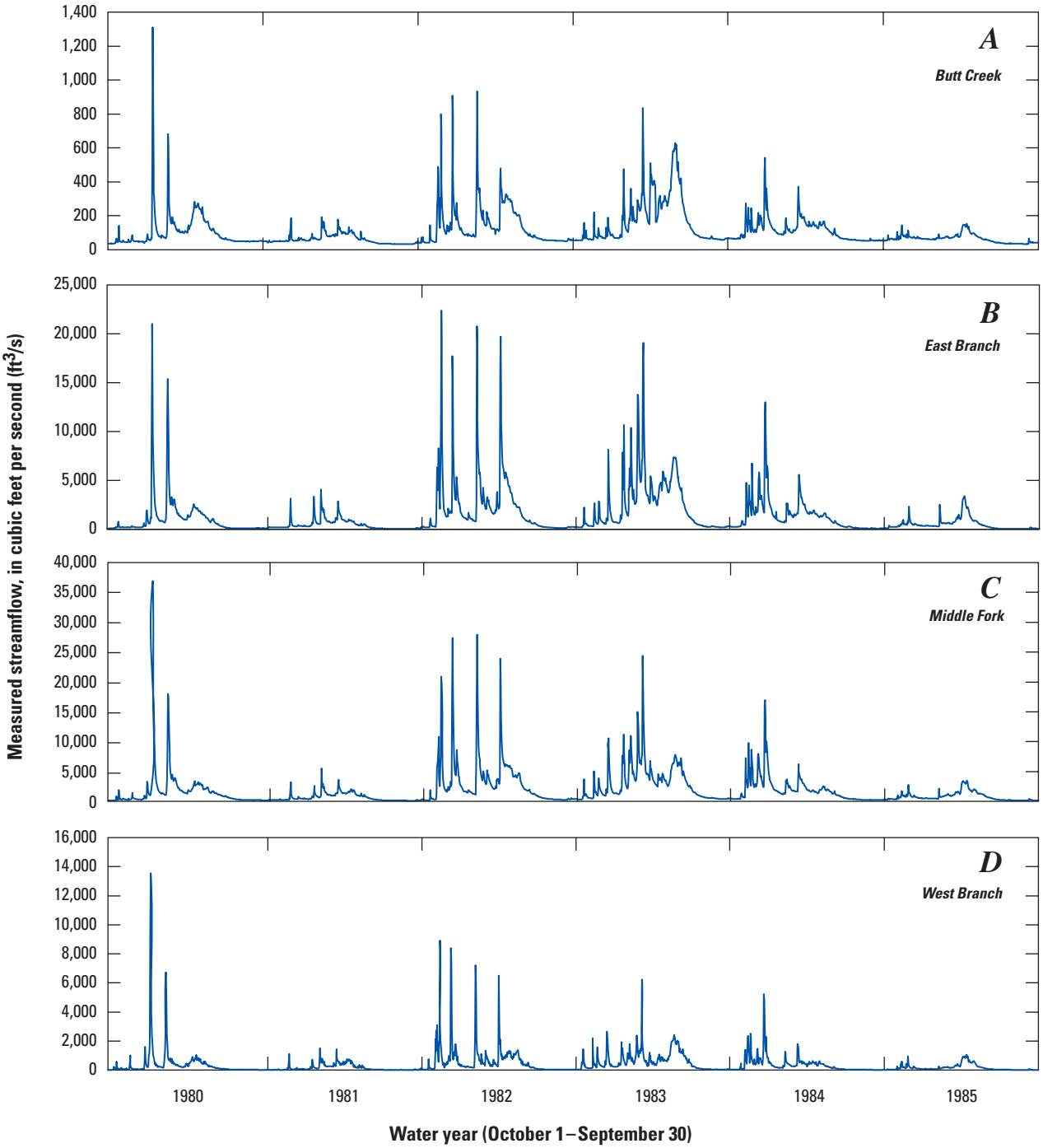

Figure 11. Daily measured streamflow, Feather River Basin, California, water years 1980–85, for (A) Butt Creek, (B) East Branch, (C) Middle Fork, and (D) West Branch. Y-axes vary.

Table 9. Mean-seasonal reconstructed inflow to Lake Oroville (FTO), California, water years 1906–2000

[FTO, California Department of Water Resources streamflow reconstruction site: Feather River at Oroville, California]

Streamflow season	Mean volume, in acre-feet	Minimum volume, in acre-feet	Maximum volume, in acre-feet	Standard deviation, in acre-feet	Percent of annual volume
October–December	643,785	168,060	2,713,700	520,062	14
January–March	1,777,556	275,660	4,684,328	1,049,563	39
April–July	1,923,596	391,850	4,676,000	1,009,089	43
August–September	194,126	110,300	343,310	48,577	4
Total	4,539,065				

Measured and reconstructed tributary streamflows during water years 1971–97 were compared with DWR's FTO reconstructions to get a sense of the contribution of water from different parts of the basin. The East Branch and Middle Fork drainages straddle the Sierra Nevada rain shadow. Their western sides received the most precipitation (fig. 8*A*), and were measured as contributing more to streamflow than their eastern sides. On average, the West Branch contributed 5 percent of FTO, the Middle Fork 22 percent, and the South Fork 5 percent. The average North Fork inflow was 53 percent of FTO. From subareas in the North Fork drainage, the East Branch was estimated to contribute 16 percent, the Lower North Fork 20 percent, Butt Creek 2 percent, and Almanor 15 percent of FTO. The Oroville modeled area (fig. 7) contributed about 15 percent of FTO. This contribution was calculated by assessing PRISM estimates of precipitation (fig. 8*A*), then subtracting inflows estimated by other models from DWR's FTO reconstructions. This was done because measured or reconstructed streamflow does not exist for the Oroville model area.

The Feather River Basin streamflow is analyzed in this report according to the seasons defined by DWR forecasts: (1) October–December, during which the primary source of streamflow is from rain and early snowmelt, (2) January–March, during which the basin receives the most precipitation, (3) April–July, during which the main source of streamflow is snowmelt, and (4) August–September, during which the main sources of streamflow are from subsurface and ground-water flows. During the 1906–2000 period, 43 percent of the reconstructed inflow to Lake Oroville (FTO) occurred during the April–July snowmelt period, 39 percent during January through March, 14 percent during October through December, and only about 4 percent during August through September (table 9).

The seasonality of streamflow in the Feather River has varied on interdecadal time scales. For example, the long-term (1906–97) mean of Lake Oroville inflow peaked in April (fig. 12), but during the 1971–97 modeling period the mean-monthly inflow to Lake Oroville peaked in March (fig. 12). This earlier, March peak during 1971–97 also was observed in streamflows from the East Branch, Middle Fork, South Fork, and West Branch tributaries (table 10). The peak of the North Fork tributary during 1971–97 lagged to April–May, although flow in these months was only slightly higher (1 to 1.5 percent) than in March (table 10).

The shift in the mean month of peak FTO streamflow reconstructions, as seen in figure 12, corresponds to warmer conditions in recent decades. This warming may correspond to an influence on the Feather River Basin climate by Pacific Decadal Oscillation (PDO). PDO is a long-term sea-surface temperature fluctuation of the North Pacific Ocean, which—along the west coast of North America—is seen to abruptly become warmer or cooler every 20 to 30 years (Mantua and others, 1997). Between 1949 and 1976, the North Pacific climate was characterized by a warm wedge of higher than normal sea-surface temperatures in the central-to-western North Pacific and a horseshoe pattern of lower-than-normal sea-surface temperatures along the west coast of North America (cool PDO). In contrast, between 1977 and 1998, the west Pacific Ocean was cool and the ocean along the west coast of North America was warm (warm PDO). These distributions of warm and cool water affect atmospheric temperature and reflect long-term changes in the paths of storms and winds across the United States. In 1999, the Pacific Ocean along the west coast of North America appears to have returned to the PDO phase that dominated the earlier (cool) 1970–76 period, which—if true—can be expected to influence the hydroclimatology of the Feather River Basin for years to come (Cayan and others, 2001; Dettinger and others, 2001; Schmidt and Webb, 2001; McCabe and Dettinger, 2002; http://topex-www.jpl.nasa.gov/science/pdo.html, accessed on Dec. 10, 2002).

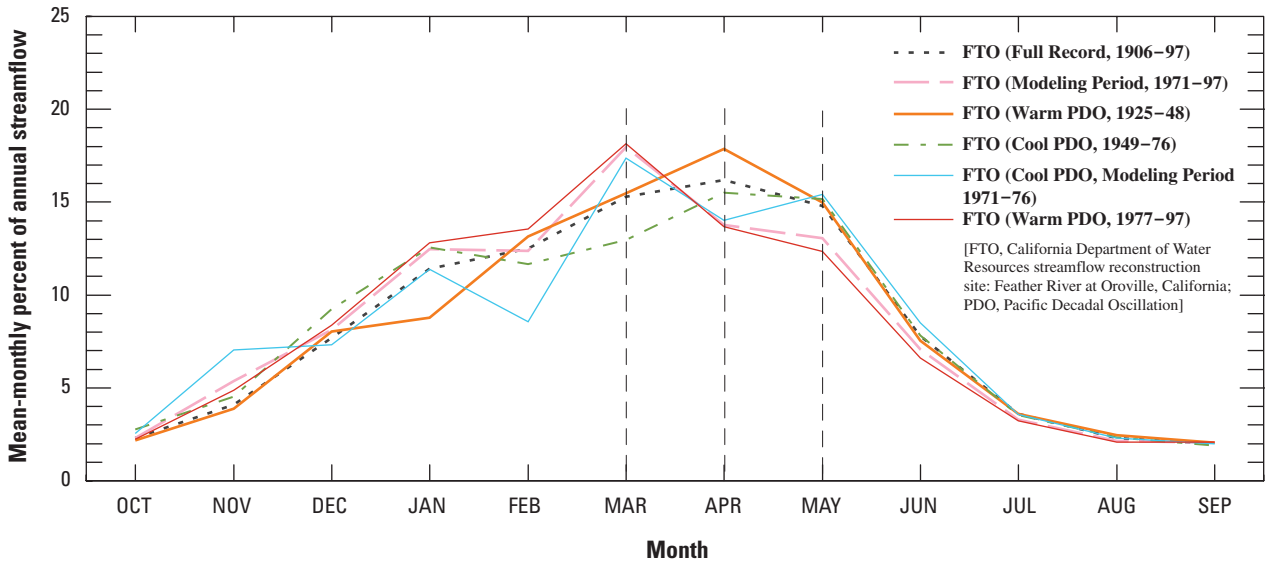

Figure 12. Historical mean-monthly peak variations in reconstructed inflow to Lake Oroville (FTO), California.

Table 10. Mean-monthly reconstructed (R) or measured (M) streamflow for areas modeled as percent of annual total, water years 1971–97, and Lake Oroville (FTO) 1906–2000; peak monthly streamflow listed in bold italics.

[FTO, California Department of Water Resources streamflow reconstruction site: Feather River at Oroville, California]

Month	North Fork of the Feather River				Middle Fork	South Fork	West Branch	Total Lake Oroville inflow (FTO 1971–97)	Total Lake Oroville inflow (FTO 1906–2000)
	Almanor	Butt Creek	East Branch	Lower North Fork					
	R	M	M	R	M	R	M	R	R
Oct.	4.9	4.3	1.5	2.8	1.7	0.9	0.5	2.3	2.3
Nov.	7.1	5.8	4.4	5.8	5.2	5.3	6.7	5.4	4.1
Dec.	7.8	6.9	7.1	7.4	8.0	8.3	9.7	8.1	7.7
Jan.	8.9	9.5	14.1	10.4	11.3	12.4	16.6	12.5	11.4
Feb.	10.0	9.9	14.2	11.7	13.8	13.2	17.6	12.4	12.5
Mar.	13.1	13.6	***20.8***	14.7	***18.4***	***18.2***	***18.1***	***18.0***	15.3
April	12.6	***14.7***	16.0	14.4	14.9	15.7	13.0	13.8	***16.2***
May	***14.5***	14.4	13.0	***16.5***	14.1	16.9	11.9	13.1	14.8
June	9.2	8.2	5.4	8.7	7.6	6.7	4.9	7.1	7.8
July	4.7	4.6	1.6	3.3	2.5	1.4	0.6	3.3	3.6
Aug.	3.4	4.2	0.9	2.2	1.4	0.5	0.1	2.1	2.3
Sept.	3.7	3.9	1.0	2.2	1.2	0.5	0.2	2.1	2

To determine whether the PDO affected Feather River Basin streamflow timing, the FTO record was evaluated for various PDO periods (fig. 12). The "warm" (1977–98) phase of PDO was expected to result in warmer conditions in the basin (Dettinger and others, 2004) and in an earlier peak monthly streamflow. Conversely, the "cooler" (1949–76) PDO would result in later peak streamflow, as the basin would be cooler and more precipitation would fall as snow, and snow would melt later in the year. The data plotted in figure 12 confirm these expectations, and also show that streamflow timing of the Feather River has come earlier in recent decades (1970s–90s), as has occurred in rivers throughout California and the western United States (Dettinger and Cayan, 1995; Cayan and others, 2001). Thus, simulations of seasonal cycles of Feather River Basin streamflow may be sensitive to the climate during the period of record utilized.

The model calibration period (1971–97) used here straddles these PDO phases, with most years from the recent warm (1977–98) PDO phase. The beginning years (1971–76) of the model calibration period, however, presumably were influenced by the earlier cool (1949–76) PDO. The mean FTO inflows during the 1971–76 period (fig. 12) display a seasonality that is less smooth because fewer years were averaged. Results, however, display a broad April peak similar to the cool PDO (1949–76) period. The modeling period was dominated by the warm (1977–98) PDO, which may bias study results towards warmer conditions in the basin.

Watershed Modeling

Conceptually, a watershed system, such as that found in the Feather River Basin, can be described in terms of a few key hydrologic processes that, working in combination, result in observed daily streamflow variations (Beven, 2001). These processes are represented mathematically in such models as PRMS (http://wwwbrr.cr.usgs.gov/mms/html/prms_page.html, accessed on Jan. 1, 1999; Leavesley and others, 1983, 2002; Leavesley and Stannard, 1995).

PRMS is a distributed-parameter, physically based watershed model that was developed to evaluate the effects of various combinations of climate and land use on watershed response (Leavesley and Stannard, 1995). Responses to climatic events and land-cover changes are simulated in terms of water and energy balances, streamflow regimes, flood peaks and volumes, soil-water relations, and ground-water recharge. A basic assumption in PRMS is that streamflow travel time, from the headwaters to the outlet of a defined model area, is less than or equal to the daily time step, and thus these daily streamflows need not be explicitly routed along river channels. Hydrologic components of the system, including streamflow, are computed on daily time steps.

The current PRMS is part of the Modular Modeling System (MMS) (http://wwwbrr.cr.usgs.gov/mms/; Leavesley and others, 1996). MMS combines a library of subroutine modules to simulate components of the hydrologic system including water, energy, and biogeochemical processes. PRMS is the combination of modules that was described by Leavesley and others (1983) and has been used for many modeling studies since.

Spatial Representation

In PRMS, spatially distributed hydrologic properties and responses are represented by partitioning the watershed into spatial subdivisions on the basis of land characteristics such as slope, aspect, altitude, vegetative cover (type and density), soil (type and depth), geology, and climate (daily temperature and precipitation distributions). Hydrologic processes within each subdivision, including streamflow generation, are assumed to vary uniformly in response to temperature and precipitation. In order to justify this simplification, the subdivisions, called hydrologic response units (HRUs), typically are delineated to encompass land properties that are as spatially homogeneous as is practical. HRUs may consist of noncontiguous or contiguous areas of similar land properties. Water and energy balances are computed each day for each HRU on the basis of the HRU physical and hydrologic characteristics and the weather on that day. These balances represent fluxes through the snowpack, vegetation canopies, land surface, and soil through the root zone of the HRU. In PRMS, percolation down through the bottom of the root zone enters two conceptual reservoirs, a "subsurface reservoir" and a shallow "ground-water reservoir," which affect the timing of the overall simulated streamflow (Leavesley and others, 1983)(fig. 13*A*). In the Feather River PRMS models, each HRU is contiguous and, with the exception of Butt Creek, has its own HRU-scale subsurface and ground-water reservoirs. In Butt Creek, as in other PRMS applications, the reservoirs have been assumed to underlie multiple HRUs (for example, Jeton and others, 1996). Thus, in the Feather River PRMS models, water balances are computed for each HRU, including all surface and subsurface components. The smallest spatial scales at which climatic variations or land-cover changes can be imposed in the model is the HRU scale. The sum of the individual responses of all HRUs, weighted on a unit-area basis, produces the daily watershed response and streamflow.

For flexibility, the Feather River Basin was modeled as eight separate drainages representing the major tributaries (fig. 7). The sum of the simulated daily flows from these eight separate models represents the total inflow to Lake Oroville.

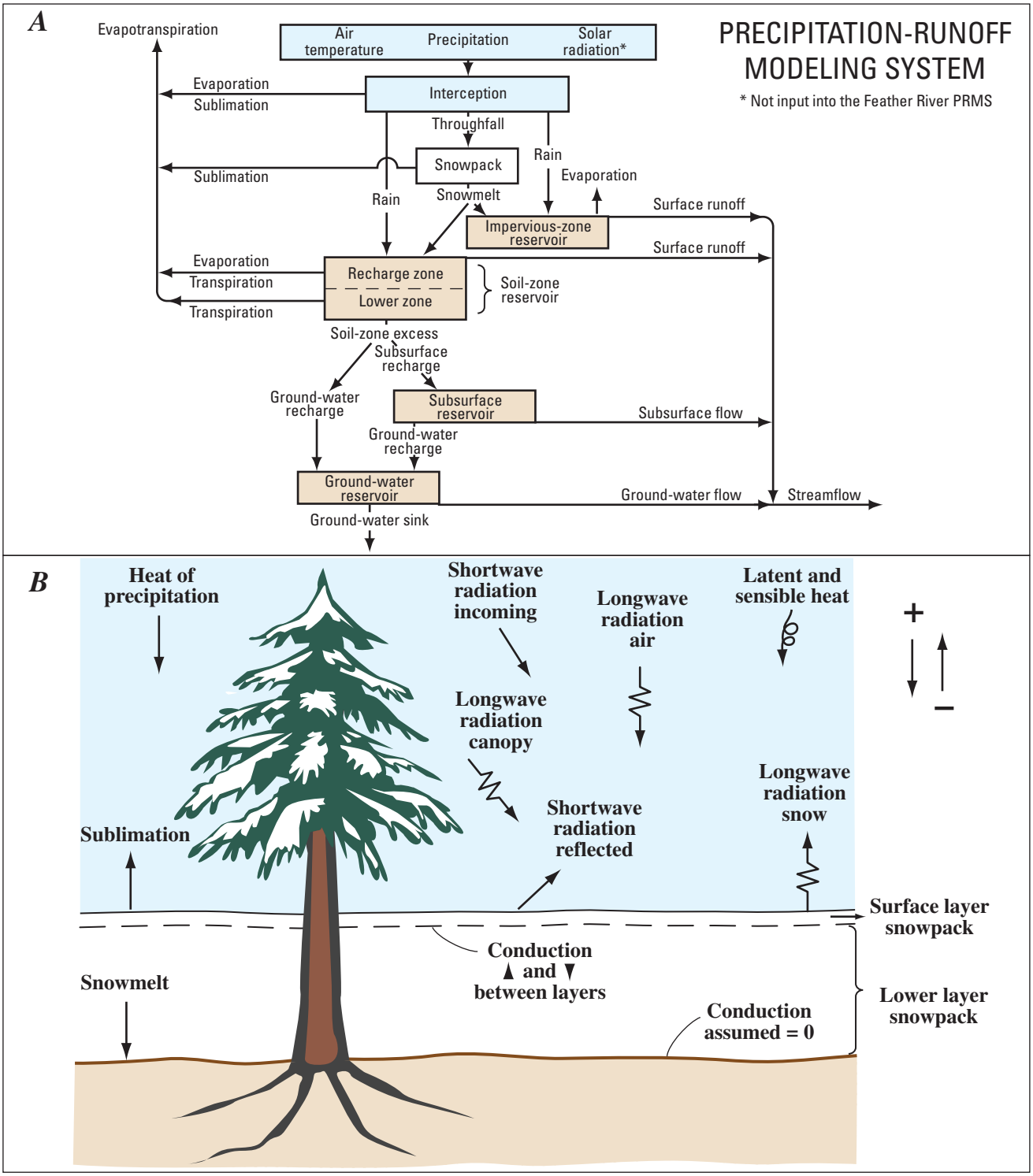

Modified from Leavesley and others, 1983 (figures 2 and 9).

Figure 13. Precipitation-Runoff Modeling System (PRMS) conceptually illustrated, including (*A*) schematic diagram of the conceptual water system and inputs, and (*B*) components of the snowpack energy-balance equations (Leavesley and others, 1983).

Watershed Processes

For PRMS modeling, the watershed system is conceptualized as a series of heat and water reservoirs whose outputs combine to produce the total system response and, therefore, daily streamflow (fig. 13*A*; Leavesley and others, 1983). System inputs are daily precipitation, minimum and maximum daily air temperature, and (if available) solar radiation. Precipitation falls, is reduced by interception in the plant canopy, and becomes a net precipitation rate delivered to the watershed surface. Temperature drives the processes of evaporation, transpiration, sublimation, and snowmelt, and determines the form of any precipitation (snow, rain, or a mix). A rain/snow mixture is computed using maximum and minimum daily temperatures, and temperature thresholds bracketing precipitation type (all rain or all snow). If precipitation is considered a mixture, rain is assumed to occur first and the portion occurring as rain is computed using a user-specified monthly adjustment factor.

In the Feather River Basin, long-term observations of daily solar radiation are not available. Therefore, as in many previous applications, solar radiation is estimated in PRMS each day on the basis of air temperatures and the presence or absence of precipitation. The estimation method used was developed for the Rocky Mountain region, and it is most applicable in regions where predominantly clear skies prevail on days without precipitation (Frank and Lee, 1966; Swift, 1976). On days with precipitation, a temperature threshold is used to distinguish between days when precipitation is from convective storms and days when precipitation is from frontal storms. Convective storms are typically of short duration and have more solar radiation than do days with frontal storms (Leavesley and others, 1983). PRMS distributes solar radiation to each HRU on the basis of latitude, slope, and aspect.

Snowpack components of PRMS simulate the initiation, accumulation, and depletion of snow on each HRU (fig. 13*B*). The snowpack is simulated both in terms of its water storage and as a dynamic-heat reservoir (Leavesley and others, 1983; Obled and Rosse, 1977; Anderson, 1968, 1973). A snowpack water balance is computed within each HRU each day, and a snowpack energy balance is computed each day and night. The snowpack is simulated as a two-layered system, with a 1-to 2-in. (3-to 5-cm) surface layer that interacts directly with the atmosphere, and a lower layer that is the underlying snowpack. In nonmelt conditions, when the surface layer is less than 32 ^{o}F, the surface layer temperature is computed using air temperature. When the temperature of the surface layer reaches 32 ^{o}F, an energy balance is computed between the snow interface and the atmosphere. The energy balance includes radiation, condensation, and the heat content of the precipitation falling on the snowpack. In nonmelt conditions, heat is transferred between the surface layer and the lower layer by conduction. When the surface layer temperature increases to greater than or equal to 32 ^{o}F, snowmelt occurs. Heat moves from the surface layer to the lower layer by the mass-transfer of heat stored in rain and melt water. The water is refrozen in the lower layer until the temperature of the lower layer is increased to 32 ^{o}F. Once the temperatures of the upper and lower layers increase to 32 ^{o}F, the entire snowpack is in a melt state and melt water from both the upper and lower layers moves out of the bottom of the snowpack. Conduction of heat across the soil-snow interface is assumed negligible in comparison with the energy exchange at the air-snow interface and is set to zero. The conceptual snowpack system and the components of the snowpack energy-balance equations are shown in figure 13*B*.

In PRMS, areas with impermeable surfaces that permit no infiltration into soil or ground water are represented by impervious-zone reservoirs (fig. 13*A*). These reservoirs have specified maximum retention-storage capacities that must be satisfied before surface runoff will be simulated. Snow and rain can accumulate on these surfaces. The retention storage is depleted by evaporation when the area is snow free.

In PRMS, the soil-zone reservoir (fig. 13*A*) represents that part of the soil mantle that can lose water to the atmosphere through evaporation and transpiration. The average rooting depth of the predominant vegetation covering the soil surface defines the depth of this zone. Water storage in the soil-zone reservoir is increased by infiltration of rainfall and snowmelt and depleted by evapotranspiration. Maximum retention storage occurs at field capacity; minimum storage is assumed to be zero and occurs at wilting point. The maximum available water-holding capacity (the difference between field capacity and wilting point) of the soil-zone reservoir is specified by the user. The soil-zone reservoir is treated as a two-layered system. The upper layer is termed the recharge zone and has user-specified depth and water-storage characteristics. Losses from the recharge zone are assumed to occur from evaporation and transpiration; losses from the lower zone occur only through transpiration (Zahner, 1967). In PRMS the maximum available water-holding capacity of the lower zone is the difference between the soil-zone reservoir and the maximum available water-holding capacity of the recharge zone. In PRMS both the recharge and lower zones are filled at equal rates until the water-holding capacity is met. When the soil-zone reservoir reaches the maximum available water-holding capacity, all additional infiltration is routed to the subsurface and ground-water reservoirs (Leavesley and others, 1983).

In PRMS, infiltration into the soil-zone reservoir depends on the daily snowmelt or net rainfall rates, soil field capacities, specified maximum infiltration rates (for snow), and antecedent soil-moisture conditions. Surface runoff occurs where net applications of liquid water to the soil surface exceed defined infiltration thresholds. Infiltration thresholds are defined depending on whether the water is derived from rain (by PRMS) or snowmelt (by the user; Leavesley and others, 1983).

In PRMS, the subsurface reservoir (fig. 13*A*) represents the pathways that the soil-water excess takes in percolating through shallow unsaturated zones to stream channels, arriving at the streams above the water table (Leavesley and others, 1983). Inflow to a subsurface reservoir occurs when the maximum available water-holding capacity of the soil-zone reservoir is exceeded, and this excess is greater than the recharge rate to the ground-water reservoir. Subsurface flow into the river varies relatively rapidly, in response to infiltration changes, but not as rapidly as the occasional surface-runoff events. Thus, the subsurface reservoir contributes to the gradual recessions of flow lasting a few days following a storm or snowmelt episode.

In PRMS, the ground-water reservoir (fig. 13*A*) represents the slower subsurface pathways beneath the local water table to the streams. Recharge to the ground-water reservoir can occur from both the soil-zone and subsurface reservoirs (fig. 13*A*). Recharge from the soil-zone reservoir has a daily user-specified upper limit and occurs only when the maximum available water-holding capacity of the soil-zone reservoir is exceeded. Recharge from the subsurface reservoir to the ground-water reservoir is computed as a function of the volume of water stored in the subsurface reservoir each day. The model representation of the ground-water reservoir is designed to respond more slowly to hydrologic fluctuations than the surface runoff or the subsurface reservoirs. The ground-water reservoir typically provides most of the seasonal flow recessions each year.

Movement of water through the ground-water system to points beyond the modeled basin can be represented in PRMS by a ground-water sink that removes water from the ground-water reservoir at a rate that is a function of storage there. In most of the Feather River PRMS models, this sink is set to zero; the sink is nonzero in the Sierra Valley of the Middle Fork model.

Model Areas

The Feather River Basin was modeled as eight separate drainages. The results of these models sum to simulate total inflow to Lake Oroville (fig. 7, table 11). Several of the models used parameter settings developed in calibrations of smaller subdrainages, referred to herein as "subdrainage models." These subdrainage models were preliminary and used solely to arrive at a better understanding of a particular part of a drainage model. The current models assume a constant land-surface and plant canopy throughout the simulation.

Streamflow data are available to calibrate and verify the models, except for the area below Lake Almanor ("Not Modeled" in fig. 7; table 11) and the area surrounding Lake Oroville ("Oroville Model" in fig. 7; tables 2, 11). Further, the "Not Modeled" area was excluded from this study because it did not significantly contribute to Lake Oroville inflow. The "Not Modeled" area is similar in size to the Butt Creek drainage, which generates 2 percent of the annual inflow to Lake Oroville. However, the "Not Modeled" area likely produces less streamflow because it receives less precipitation (fig. 8*A*) and is at warmer, lower altitudes (fig. 3). In contrast, the area around Lake Oroville was modeled. Although this area lacks measured or reconstructed streamflow for calibration, it receives a significant amount of precipitation (fig. 8*A*). The area around Lake Oroville was estimated to generate about 15 percent of annual inflow to Lake Oroville. The estimation was made by subtracting model simulations from FTO reconstructions.

North Fork Tributary of the Feather River

The North Fork drainage (1,947 mi^2, including lakes) was modeled in four sections: Almanor and Butt Creek in the north, the East Branch in the east, and the Lower North Fork in the south (fig. 7, table 11). Each has different topography, land cover, and climatic conditions and is similar enough in its physical characteristics to stand alone. Each has a long record of streamflow data available for calibration. Simulations from these models are summed to estimate the total inflow from the North Fork tributary to Lake Oroville.

Butt Creek and Almanor

The headwaters of the North Fork originate above Lake Almanor, as a series of tributaries that drain meadows and surrounding mountains, including the highest point in the basin, Mt. Lassen (fig. 7). Altitudes decline from about 9,500 ft near Mt. Lassen to about 4,300 ft asl just below Lake Almanor (fig. 3). Precipitation is greatest near Mt. Lassen (about 95 to 125 in. per year; fig. 8*A*), which is the wettest part of the Feather River Basin. The driest part of the entire North Fork drainage is adjacent to this wet area. It receives as little as 25 in. of precipitation a year (fig. 8*A*).

The Butt Creek and Almanor drainages are underlain by permeable and porous volcanic formations (fig. 6*A*). In late summer, when precipitation and snowmelt is minimal or nonexistent, base flow into these streams is relatively large, which results in a smoother hydrograph and a greater amount of streamflow, as compared to the other drainages (fig. 11*A*). In PRMS, base flow is considered to be the movement of shallow ground water to a stream channel.

Streamflow records used in calibrating the Almanor PRMS model have been reconstructed by PG&E at Lake Almanor (PG&E 8090-NF901; table 2; fig. 7). The Almanor drainage contains Lake Almanor and the Mt. Meadows Reservoir (fig. 7). At Lake Almanor and Mt. Meadows Reservoir, estimates of precipitation gain and evaporation loss were roughly the same, and the net contribution of these lakes to streamflow was negligible. Consequently, the two reservoirs were not included in the model.

Table 11. Feather River Basin models, modeling period, altitude range, and drainage area; area of the basin not modeled listed in italics.

[ft asl, feet above sea level; —. not applicable]

Model	Modeling period	Altitude range (ft asl)	Drainage area	
			Square miles	Acres
[North Fork modeled as four drainages]				
Almanor	10/1/70–9/30/97	4,523–9,525	[1]442	283,389
Butt Creek	10/1/70–9/30/97	4,316–7,698	69	44,205
East Branch	10/1/70–9/30/97	2,381–8,357	1,025	656,503
Lower North Fork	10/1/70–9/30/97	1,345–7,190	290	186,191
Area not modeled, excluding lakes	—	*2,460–6,353*	*73*	*46,442*
[Other modeled drainages]				
Middle Fork	10/1/70–9/30/97	1,580–8,735	1,046	669,595
South Fork	10/1/70–9/30/97	971–7,449	107	68,906
West Branch	10/1/70–9/30/97	899–7,016	142	90,823
Oroville	10/1/70–9/30/97	843–6,137	[2]314	201,336
TOTAL AREA MODELED			3,435	2,200,948

[1]Excluding Lake Almanor and Mountain Meadows Reservoir, which are about 48 square miles of the North Fork drainage.
[2]Excluding Lake Oroville, which is about 25 square miles of the Oroville drainage.

Streamflow records from Butt Creek (USGS 11400500; table 2) were used in calibrating the Butt Creek PRMS model. The accuracy of these streamflow data was reported as "good" in the early part of its record, but uncertain after 1969, when data collection was turned over to PG&E. The PG&E records since 1970 have been reviewed by the USGS. The Butt Creek streamflow record was not corrected for improvements above and below the gage that affect natural streamflow. The Lake Almanor-to-Butt Valley powerhouse conduit, which is opened for short periods several times a year, releases water just below the station, causing sharp flow surges at the gage (Markham and others, 1996). The Wallack ditch above 11400500 (fig. 4) diverts several cubic feet per second during the irrigation season into the Lower North Fork model area. The abandoned Lake Almanor-Butt Creek tunnel (fig. 4) leaks, adding to natural flow at a rate of 4,700 to 8,200 acre-ft per year, amounting to a 6 to 17 percent increase (USGS gaging station 11400500 Butt Creek below Almanor-Butt Creek Tunnel, near Prattville, California; U. S. Geological Survey Water-Data Reports, 1965–2001). Appropriate data were not available to make measurement corrections. Because Butt Creek only produces about 2 percent of annual inflow to Lake Oroville, the 11400500 data were considered an acceptable approximation of natural flow and were used for calibration.

East Branch

The East Branch is east-west trending and flows into the North Fork near Belden (fig. 7; table 11). The eastern headwaters are in the foothills at the eastern side of the Sierra Nevada (6,000 ft), although still west of the Pacific Crest. The headwater tributaries combine to form Indian Creek, which flows between canyon walls into Indian Valley (about 3,600 ft asl), and then through steep forested canyon walls of the Plumas National Forest (fig. 5). In the western third of the drainage, Indian Creek joins Spanish Creek to form East Branch, and then flows into the North Fork (fig. 7). The eastern side of the East Branch drainage is in a rain shadow (15 to 35 in. of precipitation per year). In contrast, the western side receives as much as 85 in. per year (fig. 8*A*).

The East Branch drainage is modeled as a single PRMS model and is calibrated against measured streamflows (USGS 11403000; table 2). To manage the varying precipitation patterns, parameters were determined initially from the Quincy (to the west) and Indian Creek (to the east) subdrainages (fig. 7, table 2). Streamflow at station 11403000 was measured by PG&E and reviewed by the USGS. The accuracy is uncertain. Records used for the Indian Creek subdrainage (11401500) are considered "good" (1969–93). However, natural streamflow in the Indian Creek subdrainage was obstructed by Round Valley and Antelope Valley reservoirs (fig. 1). Also, water is diverted upstream from 11401500 for irrigation of about 11,800 acres, of which 9,700 acres are in and around Indian Valley (fig. 7; Mullen and others, 1987). The measured streamflow data were not corrected to remove these influences.

Lower North Fork

In the southern half of the North Fork drainage, the North Fork tributary flows south from Lake Almanor (4,500 ft asl) through steep, forested canyon walls of the Plumas National Forest (fig. 5), past the East Branch confluence near Belden, and down into Lake Oroville (900 ft asl). Precipitation on the Lower North Fork drainage is high (55 to 105 in. per year; fig. 8*A*). Generally each year, numerous winter storms funnel up the canyon and are concentrated over this area (Gary Freeman, Pacific Gas & Electric Company, unpub. data, 1999; fig. 8*A*).

The Lower North Fork PRMS model was calibrated to reconstructed streamflow records (NF23-8145NF; table 2). Reconstructed streamflow was corrected to remove any inflow from upstream drainages of Butt Creek, Almanor, and East Branch. Further, water year 1994 was removed because reconstructed flows in that year were suspect. Therefore, the model is calibrated to simulate streamflow solely from the Lower North Fork model area (fig. 7). Accounting for hydropower structures (fig. 4), PG&E has reconstructed natural flows at Poe Powerhouse (NF23-8145NF; fig. 4) and Rock Creek Powerhouse (8120; fig. 4), and has computed flows for the entire Lower North Fork PRMS model (NF23-8145NF; table 2; fig. 7). The Lower North Fork model uses parameters determined in models of subdrainages (Rock Creek and Pulga, fig. 7, table 2) made possible by the existence of an intermediate reconstruction site (PG&E 8120). Parameter estimations from the subdrainage models provided added control in the calibration process of the Lower North Fork model.

Middle Fork

The Middle Fork tributary is east-west trending and, like the East Branch, straddles the Sierra Nevada (fig. 7, table 11). The headwaters of the Middle Fork are in the eastern mountains surrounding Sierra Valley. Sierra Valley is a broad alluvium-filled agricultural plain (149 mi^2) with surrounding mountains that reach about 8,700 ft asl. Due to irrigation, infiltration into the alluvium, and low precipitation, very little streamflow escapes this valley (USGS 11392100; fig. 7). From Sierra Valley, the river flows westward, through a ridge to Portola, meanders through Mohawk Valley (about 4,375 ft asl; fig. 7), through the steep forested canyon walls of the Plumas National Forest (fig. 5) and Bald Rock Canyon (fig. 1), and finally into Lake Oroville. The Middle Fork drainage receives an uneven pattern of precipitation. The western side receives the most precipitation. The Sierra Valley is in a rain shadow and is the driest part of the Feather River Basin, receiving only about 15 in. of precipitation per year (fig. 8*A*).

The Middle Fork drainage is represented by a single PRMS model and is calibrated against measured streamflow (USGS 11394500; table 2, fig. 7). Parameters from a model of the Sierra Valley subdrainage (calibrated to USGS 11392100 data) were used in the final Middle Fork PRMS model (figs. 7 and 8). This subdrainage model was constructed to better simulate the physical characteristics of the Sierra Valley. In the Middle Fork model, the Sierra Valley and surrounding mountains were simulated as one HRU. To simulate infiltration losses from streamflow into the deep alluvium, the Sierra Valley HRU was modeled with a ground-water sink.

The USGS 11394500 records used to calibrate the Middle Fork PRMS model are considered "good" for 1969-86 (fig. 7; table 2). This gage was operated by the USGS prior to 1986 and by DWR since then. No estimate of record accuracy after 1986 is available. No record of accuracy is available for streamflow used to calibrate the Sierra Valley subdrainage model (USGS 11392100; table 2, fig. 7). Streamflow records were not corrected for upstream obstructions to natural flow. Streamflow has been partly regulated by Lake Davis and Frenchman Lake (fig. 1). Irrigation diversions of about 1,000 acres exist between 11392100 and 11394500 (Mullen and others, 1987). Diversions exist in the Sierra Valley for irrigation, and about 6.6 acre-ft per year of irrigation water is imported to Sierra Valley from rivers south of the study area (J. Pierre Stephens, DWR Resources Hydrology Branch, unpub. data, 2001).

South Fork

The South Fork drainage consists of steep forested terrain of the Plumas National Forest (fig. 5) and is northeast-southwest trending. It flows directly into Lake Oroville. Although smallest in size (107 mi^2), this drainage receives some of the highest precipitation in the Feather River Basin (fig. 8*A*). Altitude ranges from 971 to 7,449 ft asl (fig. 3; table 11).

The South Fork drainage is represented by a single PRMS model and has been calibrated against reconstructed streamflow (PG&E SF905T; fig. 7; table 2). The reconstructed streamflow was corrected for hydropower obstructions to natural flow (fig. 4) and for reservoirs at Little Grass Valley, Sly Creek, and Lost Creek (fig. 1).

West Branch

The West Branch is represented by a single PRMS model and is calibrated against measured streamflow (USGS 11405300; table 2, fig. 7). The gage is located a few miles upstream from Lake Oroville. The drainage is north-south trending and is heavily forested with evergreen trees and (in the south) some shrubs (fig. 5). This is one of the wettest areas in the Feather River Basin (fig. 8*A*). Streamflow records from 1969–86 for 11405300 are considered "good" (fig. 7, table 2). Since 1986, only low flows have been measured by DWR and record accuracy is uncertain. Owing to scant streamflow data, the calibration/verification period of this model is water years 1971–86.

Measured streamflow recedes in late summer to very low rates (fig. 11*D*) and is not sustained by base flow to the extent that other Feather River tributaries are. Flow is regulated upstream from11405300 by Snag Lake (also known by PG&E as "Round Valley Reservoir") and Philbrook Reservoir (fig. 1). Canals divert water from the headwaters of West Branch (above 11405300) into the Butte Creek Basin (west of the study area) for PG&E powerhouse use (Mullen and others, 1987). Streamflow is diverted for summertime irrigation. Because streamflow has not been corrected to account for upstream developments, values for simulated streamflow for the summer and (especially) fall are expected to exceed the measured flow values.

Oroville

The Oroville drainage is driest near Lake Oroville and wettest adjacent to other models (figs. 7, 8*A*, table 11). However, overall, the modeled area receives a significant amount of precipitation. No measured or reconstructed streamflow exists for the calibration of Oroville model, but the area contributes a significant amount of streamflow to Lake Oroville.

The Oroville model surrounds Lake Oroville (fig. 7, table 11). PRMS is not well suited to simulate streamflow from large lake surfaces. Evaporation from Lake Oroville equals or slightly exceeds precipitation, and thus the lake does not effect a net change in streamflow. Therefore, the lake area is not included in the Oroville model. Parameters were estimated from similar HRU characteristics in the seven calibrated models.

Parameters

The long-term climate and land-surface characteristics of the eight PRMS models are quantified by a large number of model parameters. Spatial variations of these characteristics are represented by HRU-specific and reservoir-specific (fig. 13*A*) parameters. Other properties that are homogeneous over the whole model area are quantified by nondistributed parameters (table 12). Parameters are specified as constants or monthly values. All parameters are independent of daily fluctuations of the temperature and precipitation inputs.

Sources of key model parameters are presented in table 12. The designation "calibrated" means that the initial estimates of the parameter values were adjusted during iterative model runs to minimize differences between simulated and measured or reconstructed streamflows. "Computed" values were first derived from the literature (Black, 1996) and then revised prior to calibration to reflect conditions specific to the Feather River Basin. "GIS derived" parameters are computed directly from spatial data.

Table 12. Source of parameter values for selected Hydrologic Response Unit [HRU] (distributed) and whole-model (nondistributed) Precipitation-Runoff Modeling System (PRMS) parameters for the Feather River Basin, California (modified from Jeton, 1999b).

[GIS, Geographic Information System; MF, Middle Fork; SF, South Fork]

Model parameter	Description of parameter	Range of values (or cover type)	Source of parameter value				
			GIS derived[1]	Com-puted[2]	Litera-ture[3]	Default value[4]	Cali-brated[5]
	HRU (distributed) parameters						
CAREA_MAX	Maximum area contributing to surface runoff (decimal percent)	0.0001–0.01					X
COV_TYPE	Vegetation cover type (bare soil, grasses, shrubs, trees)	Grasses, shrubs, trees	X				
COVDEN-SUM	Vegetation cover density (decimal percent) for summer	0.23–0.78	X				
COVDEN-WIN	Vegetation cover density (decimal percent) for winter	0–0.76	X				
GWFLOW_COEF	Ground-water routing coefficient to obtain the ground-water flow contribution to streamflow	0.001–0.5					X
GWSINK_COEF	Ground-water sink coefficient to compute the seepage from each reservoir to a ground-water sink	0–.05					X
GWSTOR_INIT	Storage in each ground-water reservoir at the beginning of the simulation (in inches)	0.001–20					X
HRU_AREA	HRU area (in acres)	382–14,774 (excluding Sierra Valley 325,118 acres)	X				
HRU_DEPLCRV	Index number for snowpack depletion curve	1		X			
HRU_ELEV	Mean HRU altitude (in feet)	1,067–7,257	X				
HRU_GWRES	Index number for ground-water reservoir	1–111		X			
HRU-PERCENT_IMPERV	HRU impervious area as a decimal percent of the total HRU area	0– 0.10 percent	X				
HRU_PSTA	Index number of the precipitation station time series to compute rain and snow on HRU	1–111		X			
HRU_RADPL	Index number of the solar radiation plane	1–111		X			
HRU_SLOPE	HRU slope in decimal percent (vertical feet/horizontal feet)	0.02–0.66	X				
HRU_SSRES	Index number of the subsurface reservoir receiving excess water from the HRU soil zone	1–111		X			
HRU_TSTA	Index number of the temperature station used to compute HRU temperatures	1–3		X			
IMPERV_STOR_MAX	Maximum impervious retention storage for the HRU (in inches)	0.02 (SF only), 0.20 (all others)				X	
JH_COEF-HRU	Air temperature coefficient used in the Jensen-Haise (1963) potential-evapotranspiration computations for each HRU	13–17		X			
RAD_TRNCF	Transmission coefficient for short-wave radiation through the winter canopy (decimal percent)	0.12– 0.99		X			
SMIDX-COEF	Coefficient in the nonlinear contributing area algorithm (computing surface runoff)	0.01–0.03				X	
SMIDX_EXP	Exponent in nonlinear contributing area algorithm (computing surface runoff)	0.10–0.30				X	

Table 12. Source of parameter values for selected Hydrologic Response Unit [HRU] (distributed) and whole-model (nondistributed) Precipitation-Runoff Modeling System (PRMS) parameters for the Feather River Basin, California (modified from Jeton, 1999b)—Continued.

[GIS, Geographic Information System; MF, Middle Fork; SF, South Fork]

Model parameter	Description of parameter	Range of values (or cover type)	Source of parameter value				
			GIS derived[1]	Computed[2]	Literature[3]	Default value[4]	Calibrated[5]
SNAREA_THRESH	Maximum snow water equivalent below which the snow-covered area depletion curve is applied	5–25		X			
SNOW_INTCP	Snow interception storage capacity for the major vegetation type on an HRU (in inches)	0–0.35			X		
SNOWINFIL_MAX	Maximum infiltration rate for snowmelt (in inches per day)	3–8					X
SOIL2GW_MAX	Amount of soil water excess for an HRU that is routed directly to the associated ground-water reservoir each day (in inches)	0.05–0.25					X
SOIL_MOIST_INIT	Initial value of available water in soil profile (in inches)	0.09–5.54		X			
SOIL_MOIST_MAX	Maximum available water-holding capacity of soil profile (in inches)	1.00–11.08		X			
SOIL_RECHR_INIT	Initial value for available water in the soil recharge zone, (in inches) (upper soil zone)	0.06–3.32		X			
SOIL_RECHR_MAX	Maximum value for available water in the soil recharge zone (in inches)	0.17–5.54		X			
SOIL_TYPE	HRU soil type (sand, loam, or clay)	Sand or loam	X				
SRAIN_INTCP	Summer interception storage capacity for the major vegetation type on an HRU (in inches)	0.05–0.35			X		
SS2GW_RATE	Coefficient to route water from the subsurface to ground-water reservoir	0.01–0.1					X
SSRCOEF_LIN	Linear subsurface routing coefficient to route subsurface storage to streamflow	0.01–0.04					X
SSRCOEF_SQ	Nonlinear subsurface routing coefficient to route subsurface storage to streamflow	0.01–0.03					X
TMAX_ADJ	HRU maximum temperature adjustment in Fahrenheit (°F) to HRU temperature, based on slope and aspect of HRU	–3 (MF only), 0 (all others)				X	
TMIN_ADJ	HRU minimum temperature adjustment in Fahrenheit (°F) to HRU temperature, based on slope and aspect of HRU	–3 (MF only), 0 (all others)				X	
TRANSP_BEG	Month to begin summing maximum temperature for each HRU; when sum is greater than or equal to TRANSP_TMAX transpiration begins	February – April			X		
TRANSP_END	Last month for transpiration computations	July–November			X		
TRANSP_TMAX	Temperature index to determine the specific date of the start of the transpiration period	500				X	
WRAIN_INTCP	Winter rain interception storage capacity for the major vegetation type on an HRU (in inches)	0–0.35			X		

Table 12. Source of parameter values for selected Hydrologic Response Unit [HRU] (distributed) and whole-model (nondistributed) Precipitation-Runoff Modeling System (PRMS) parameters for the Feather River Basin, California (modified from Jeton, 1999b)—Continued.

[GIS, Geographic Information System; MF, Middle Fork; SF, South Fork]

Model parameter	Description of parameter	Range of values (or cover type)	Source of parameter value				
			GIS derived[1]	Computed[2]	Literature[3]	Default value[4]	Calibrated[5]
	Selected non-distributed parameters						
ADJMIX_RAIN	Monthly factor to adjust rain proportion in a mixed rain/snow event (decimal percent)	0.50–1					X
JH_COEF	Monthly air temperature coefficient used in the Jensen-Haise (1963) potential evapotranspiration computations	0.011–0.014					X
RAIN_ADJ	Monthly factor to adjust precipitation (rain) to each HRU (decimal percent)	0.70–1.20					X
SNOW_ADJ	Monthly factor to adjust precipitation (snow) to each HRU (decimal percent)	0.70–1.25					X
TMAX_ALLSNOW	Maximum temperature (°F) below which all precipitation is simulated as snow	31–35					X
TMAX_ALLRAIN	Maximum temperature (°F) above which all precipitation is simulated as rain	38–43					X
MELT_LOOK	Julian date to start looking for spring snowmelt	60–61					X
MELT_FORCE	Julian date to force snowpack to spring snowmelt	60–120					X
TMAX_LAPSE	Monthly maximum temperature lapse rate (°F) representing the change in maximum temperature per 1,000 feet of altitude change for each month	3.3–4.75					X
TMIN_LAPSE	Monthly minimum temperature lapse rate (°F) representing the change in minimum temperature per 1,000 feet of altitude change for each month	3.3–4.75					X

[1]Computed in geographic information system (GIS) from digital coverages.
[2]Computed from climatological data or other measured data.
[3]Obtained from the literature as estimated or empirical estimates (Black, 1996, table 4-1, p. 93).
[4]Parameters that are considered constant, as provided by Leavesley and others (1983).
[5]Parameters that (a) cannot be estimated from available data and are adjusted during calibration or (b) have initial estimates from measured or published data that were adjusted during calibration.

Model Development

The ARC/INFO (Environmental Systems Research Institute, 1992) geographic information system (GIS) was used to manage spatial data and to characterize model drainages and HRUs in terms of slopes, aspects, altitudes, vegetation cover densities and types, soil types and depths, geology, and the distribution of precipitation. These analyses provided estimates of many spatially varying HRU-specific model parameters. The methods used to develop parameter estimates were similar to methods used by Battaglin and others (1993), Frankoski (1994), Jeton and Smith (1993), Jeton and others (1996), Jeton (1999a,b), Ryan (1996), and Viger and others (1996, 1998).

Model-Area Delineations

The eight PRMS models (table 11), and the HRUs within the models (fig. 14), were first delineated by Bruce McGurk for the USDA Forest Service. PRMS models and HRUs were based on the CALWATER State Water Resources Control Board standardized watershed boundaries (http://www.watershed.org/news/spr_94/calwater_gis.html, accessed on Dec.18, 2001). These were modified with the GIS WEASEL tool (Viger and others, 1996, 1998; http://wwwbrr.cr.usgs.gov/projects/SW_precip_runoff/weasel/, accessed on Jan. 6, 2000) to better reflect the basic hydrologic concepts used in PRMS and the locations of streamflow gages. The Butt Creek catchment was delineated from the drainage for USGS 11400500 gage (U.S. Geological Survey, 1965; digitized from USGS topographic quadrangles). Other minor revisions were made as model development proceeded.

HRUs were delineated as approximately homogeneous polygons within the model areas, with more emphasis on drainage divides and hydrography than on other physical characteristics. Measurements of the physical characteristics of altitude, slope, aspect, vegetation, and soils were averaged to estimate HRU-scale parameters. This is in contrast to the earlier studies by Jeton (1999a,b) and Jeton and others (1996) in other study areas in which HRUs were delineated as noncontiguous cell clusters. HRU land areas ranged from 382 to 14,774 acres (not including the Sierra Valley HRU, which encompassed 325,118 acres; table 13).

Table 13. Model Hydrologic Response Unit (HRU) counts and ranges within each model of specified-HRU areas, mean altitudes, mean slopes, and mean aspects.

[ft asl, feet above sea level]

Model	Total number of HRUs	HRU ranges			
		Area (acres)	Altitude (ft asl)	Slope (decimal percent)	Aspect (degrees)
Almanor	45	901–14,774	4,555–7,257	0.02–0.25	21–310
Butt Creek	6	6,063–12,081	4,722–5,985	0.07–0.30	25–358
East Branch	111	1,100–13,539	3,586–6,554	0.09–0.55	0-–358
Lower North Fork	37	1,506–10,458	3,083–6,319	0.16–0.66	14–359
Middle Fork	58	1,793–14,311 (Sierra Valley: 325,118)	3,083–6,437	0.13–0.57	21–358
South Fork	15	2,524–8,149	2,067–5,943	0.19–0.42	139–354
West Branch	11	7,960–8,310	1,883–5,941	0.20–0.40	168–267
Oroville	41	382–10,122	1,067–5,130	0.18–0.57	4–354

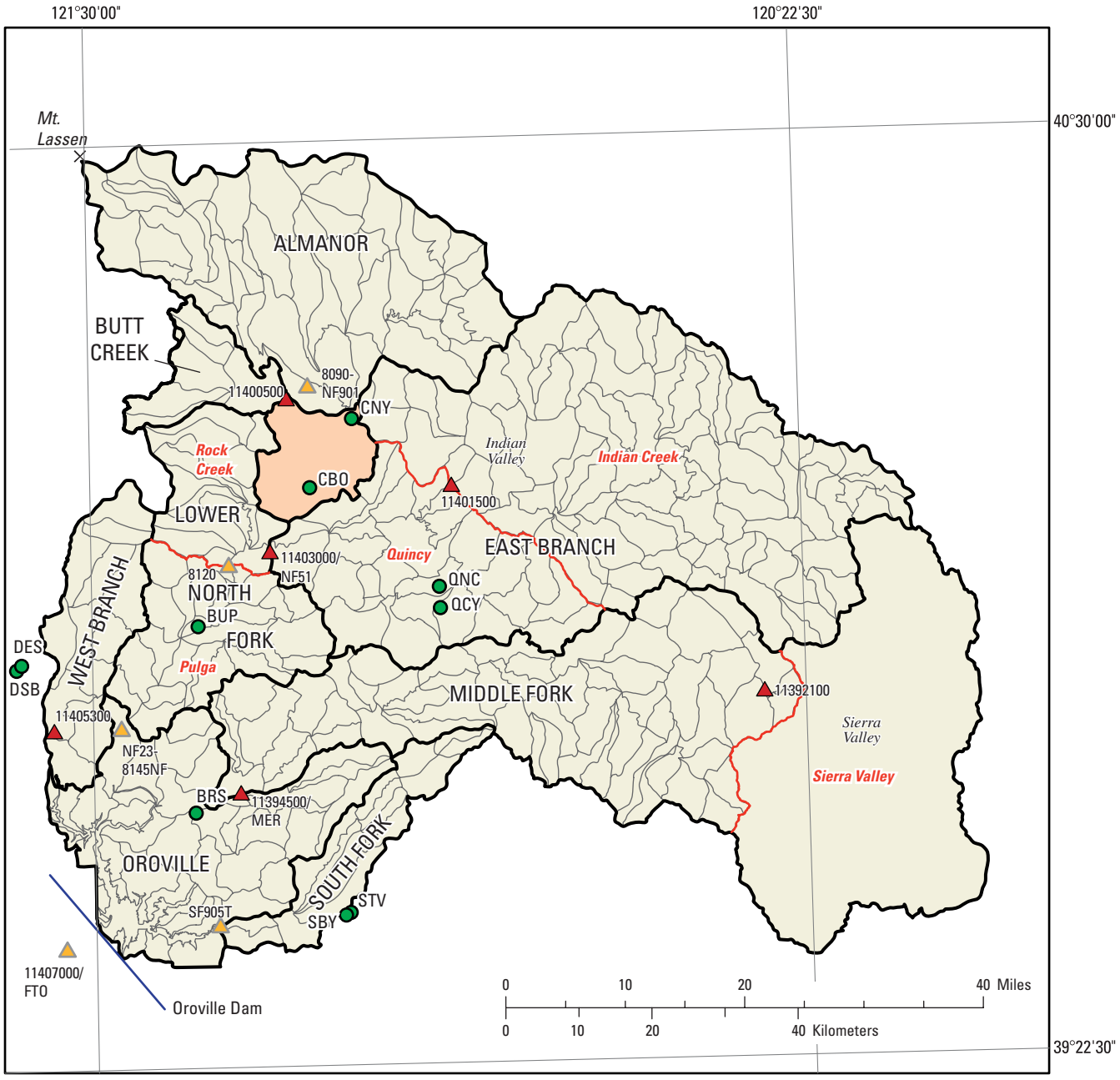

Modified from the California State Water Resources Control Board Basin Plain Maps, The California Watershed Map CALWATER version 2.0, 1:500,000, subbasins, catchments, and planning watershed area units.

EXPLANATION

- Not modeled area
- Model boundary
- Subdrainage model boundary
- Hydrologic Response Unit (HRU)
- Streamflow station (see table 2 for identification)
  - 11392100 Measured data
  - SF905T Reconstructed data
- STV Climate station (see table 1 for identification)

Figure 14. Hydrologic response units (HRUs) and model areas delineated for the Feather River Basin Precipitation-Runoff Modeling System (PRMS), California.

Precipitation Estimates for Hydrologic Response Units (HRUs)

In PRMS (Leavesley and others, 1983), as in most snowmelt models (World Meteorological Organization, 1986), the established method for assigning daily precipitation rates to models was to define lapse rates for the change in precipitation between lower and higher altitude climate stations. This method was not applicable for the Feather River Basin. The precipitation stations used in the present models were located only in the lower altitudes. Further, a portion of the basin was in the rain shadow of the Sierra Nevada, and precipitation stations in the rain shadow could not be correlated with stations outside the rain shadow. Winter storms funnel up the Lower North Fork (Gary Freeman, unpub. data, Pacific Gas & Electric Company, 1999), releasing most of their moisture before reaching Lake Almanor (fig. 8). Finally, because the Feather River Basin spans about 1 degree of latitude and longitude (fig. 1), on a given day, weather can differ considerably across the basin. A review of precipitation measurements showed that, in a single day, part of the basin can receive a downpour while another part is dry. Over the course of many days, storm movements could be tracked as precipitation totals rose and fell across the basin's climate stations.

For the present study, a technique was developed to combine measured daily precipitation variations with long-term mean precipitation estimates from the PRISM method (Daly and others, 1994). The PRISM surfaces offer full coverage of the basin area and account for topographic changes, including rain shadow. This new procedure is called the "draper" method because the monthly averaged PRISM precipitation surface was adjusted to account for daily precipitation patterns by mathematically "draping" the PRISM averages over the measurements at reporting precipitation stations (fig. 15).

The draper method requires the following input data: (1) precipitation measurements located by latitude and longitude, (2) location of the HRU centroids by latitude and longitude, and (3) mean-monthly HRU-averaged precipitation totals, in inches, from mean-monthly PRISM surfaces (http://www.ocs.orst.edu/prism/state_products/ca_maps.html, accessed May 1, 2001) for each month of the year.

Each day, precipitation measurements were converted to percentages of the long-term daily normal for the corresponding climate station and month of year. If three or more measurements were available for a given day, a plane was fitted, by linear regression between the day's precipitation percentage and the latitude and longitude of the observations (fig. 15*A*). The resulting "percent of normal" plane was then used to tilt the appropriate monthly PRISM surface (fig.15*B*) which represented "normal" precipitation rates. This created a tilted PRISM surface for each day simulated (fig. 15*C*). The tilted PRISM surface was then sampled at HRU centroids to obtain HRU-scale precipitation values for each day.

On days with only one or two observations of precipitation, the PRISM surface was not tilted, because three points are required to define a plane. Rather, average precipitation was computed by uniformly scaling up or down the monthly PRISM surface, according to the average "percent of normal" plane for that day's observations. Then, HRU precipitation was estimated by sampling that scaled map by HRU centroids.

For days with no precipitation data, the HRU precipitation was estimated to be the normalized daily PRISM precipitation for the given month. The normalized daily PRISM precipitation is the measurement obtained at the HRU centroid from the PRISM surfaces as noted above.

Model Calibration and Error Analysis

The most pressing use of the Feather River PRMS models may be to simulate (and eventually, forecast) year-to-year variations of inflows to Lake Oroville during the critical April–July snowmelt season. Therefore, calibration focused primarily on simulating flows during the April–July snowmelt season, secondly on monthly simulations, and finally on daily flow characteristics. The calibration period, chosen on the basis of available streamflow records, was generally wetter than the long-term average; thus the calibration may be better suited for wet rather than dry, climatic conditions. Of the eight models built, seven were calibrated to reconstructed or measured data (table 2). Parameter values for the Oroville model were based on those of the other seven. The calibration period is 1971–97, except for the West Branch model, which was calibrated to streamflow from 1971–86. Because calibration included the entire period of record, no separate verification period exists. The models were calibrated individually and the results were summed. This sum was compared to the monthly Lake Oroville FTO reconstructed streamflow. The comparison was not used in model calibration.

Some of the model sensitivities to parameter values can be understood from previous modeling studies in the Sierra Nevada (Jeton and others, 1996; Jeton, 1999a,b). Sensitivity analyses of the East Fork Carson River model (an eastern north-central Sierra Nevada watershed) have shown that streamflow simulations are most sensitive to (1) the snow-threshold temperature that determines precipitation form (tmax_allsnow; table 12); (2) the precipitation-correction factor for snow (similar to a precipitation lapse rate); (3) the monthly evapotranspiration coefficients for the Jensen-Haise potential-evapotranspiration computations (Jensen and Haise, 1963); (4) the coefficient for transmission of solar radiation through winter plant canopies to snow surfaces; and (5) the monthly temperature lapse rates. The models are sensitive to lapse rates for both maximum and minimum temperatures.

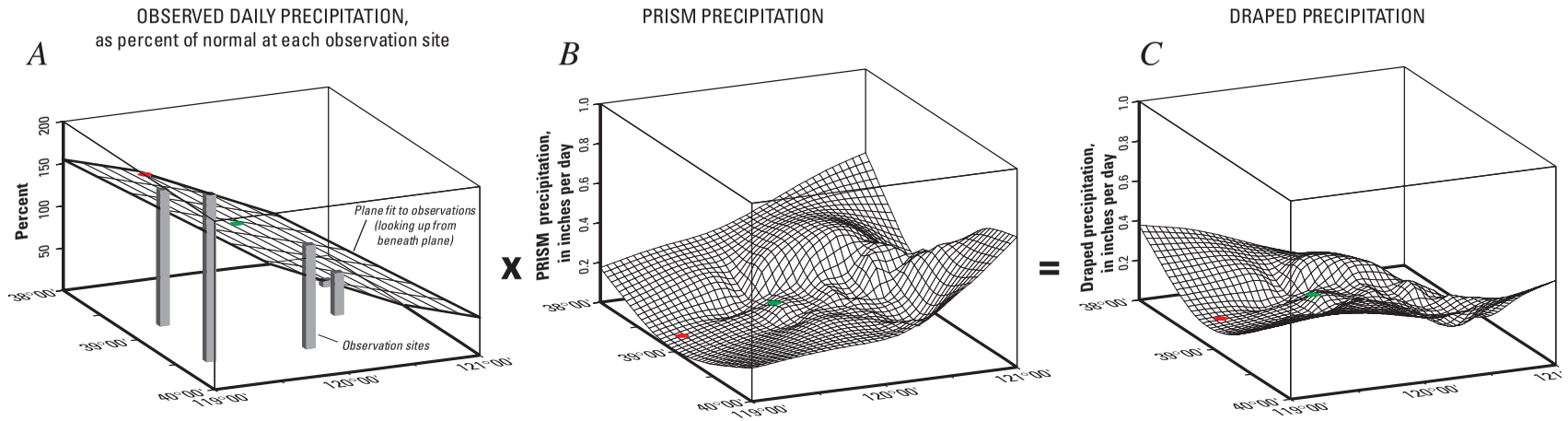

The red and green dots represent centers of hydrologic response units (HRU). Block ***A*** shows a computed plane of daily percent-of-normal measurements fit to actual daily precipitation measurements which are represented as bars. The normal measurements are considered to be the mean-monthly PRISM estimates for the month of interest. Block ***B*** shows an example of an unaltered mean-monthly PRISM surface. Block ***C*** shows the result of the mean-monthly PRISM surface corrected to fit the daily percent-of-normal plane shown in Block ***A***. An estimate of daily precipitation is then sampled at the red and green dots in Block ***C***, which represent daily precipitation at the HRU centroid.

Figure 15. Draper method to estimate daily precipitation from Parameter-Elevation Regressions on Independent Slopes Model (PRISM) surfaces, including (*A*) observed daily precipitation as a percent of normal at each observation site, (*B*) an example of a mean-monthly PRISM precipitation surface, and (*C*) resulting draped precipitation estimates.

Calibration of the Feather River PRMS models revealed other sensitivities. The models were found to be highly sensitive to the temperature threshold above which all precipitation falls as rain (tmax_allrain, table 12). The models also are sensitive to the flow-routing coefficients for subsurface and ground-water reservoirs, which control rates of flow from these reservoirs to the stream channel (affecting the timing of streamflow). Parameters that determined flows to and from the ground-water reservoirs were adjusted to fit observed shapes of seasonal recessions of streamflow.

No single calibration of the PRMS model will simulate all flow regimes with equal accuracy. Ideally, the Feather River PRMS simulations should have (1) little to no bias (table 14), (2) small simulation errors of volume and timing, and (3) realistic parameter values reflecting the conditions being modeled (Leavesley and others, 1983). In watershed modeling, common measures of simulation error are the sum of errors or bias, the sum of the absolute values of the errors, and the sum of the square of the errors. Absolute errors and errors squared tend to be dominated by a few large events (Troutman 1985; Haan and others, 1982), unless normalized by the reconstructed or measured flows to form "relative error" (table 14). The unnormalized root-mean-square error (RMSE) provides a common measure of the magnitude of simulation errors (table 14) that complements the relative measures provided by the bias and relative errors reported in table 14.

Calibration of PRMS models is an iterative process where, after each adjustment of model parameters, simulated flows are compared with measured or reconstructed flows visually and statistically. After initial parameters are set (table 12), the models are run and the simulated hydrograph is compared with measured or reconstructed flows, with special attention paid to matching flow volume and the timing of peak discharge. For the Feather River PRMS models, 19 parameters (marked as "calibrated" in table 12) were adjusted one at a time during calibration. When a good visual match was achieved, supporting statistics were computed for different time scales. Parameter adjustments were made as necessary and the fit of the hydrographs was compared again. The goal of this process was to maintain a good visual fit between the hydrographs and to keep biases and relative errors below 10 percent (established as an acceptable fit in previous work; Jeton,1999a,b).

Statistics at each time scale were computed from the difference between mean simulated and observed (measured or reconstructed) flows. Periods with missing data from the Lower North Fork, Middle Fork, and West Branch were not included in the statistics. The Lower North Fork model was further evaluated by excluding water year 1994, because reconstructed flows in that year are suspect. Finally, the sum of simulated flows from the eight models (including the Oroville Model) were compared with FTO reconstructions.

Model-calibration biases, relative errors, and RMSEs for the seven calibrated models are given in table 14 for three time increments: seasonal, monthly, and annual (water year) streamflows. On all three time scales, the overall biases, relative errors, and RMSEs are suitably low, especially for April–July snowmelt season totals, indicating acceptable simulations during the 1971–97 period. Poorer fit with large bias and relative error (especially in the East Branch) was obtained for August–September flows. Slightly larger errors in the East Branch model can be explained by reservoir storage and irrigation practices. The August–September season contributed only about 4 percent of the total annual inflow to Lake Oroville (table 9).

In the Almanor and Butt Creek models, bias and relative error are relatively large and indicate systematic under-simulation of October–December streamflow. These drainages are presumed to be more heavily influenced by underlying volcanic formations than are the other drainages. These influences may produce deeper ground-water reservoirs than the ones represented in PRMS and thus may limit how well simulations match the measured and reconstructed flows. However, these errors are from a season with low streamflows and thus are not of great practical concern.

During the season of most interest to water managers, the April–July snowmelt season, a very good fit was achieved (table 14). Relative errors are highest in the West Branch model, probably owing to the measured flows used in the calibration. The flows measured at the West Branch gaging station could not be corrected for human interventions upstream, including small reservoirs and diversions for irrigation. PRMS, which simulates natural flows, therefore would be expected to have large relative errors in that season.

Simulated and measured or reconstructed daily hydrographs are shown for each model in figure 16. The daily statistics (fig. 16 insets) show that—with the exception of the West Branch model, which has a high relative error—simulations are similar to measured and reconstructed flows. No measured or reconstructed daily streamflow data exist for the Oroville model, and only simulations are shown in that hydrograph.

The mean-monthly percentages of annual streamflows are accurately simulated in most months (fig. 17). Some models tend to simulate higher than measured or reconstructed streamflows in April and under-simulate by May. The Lower North Fork model simulates higher streamflows later in the season. However, in all of the models, the overall volume closely simulates measured or reconstructed streamflow data, with RMSEs ranging from 0.7–1.6 percent.

The mean-monthly percentage of simulated inflow to Lake Oroville for water-years 1971–97 was compared with DWR's FTO reconstructions (fig. 18). Figure 18 illustrates the contribution of each individual model to total Lake Oroville inflow. The combined simulated inflows from the eight models satisfactorily match the monthly graphed distribution of the FTO reconstructions, with a RMSE of 0.84 percent.

Table 14. Calibration statistics, Feather River Basin, California, water years 1971–97.

[RMSE, root-mean-square error; ft^3/s, cubic feet per second; FTO, California Department of Water Resources (DWR) streamflow reconstruction site: Feather River at Oroville, California]

Model	Seasonal												Monthly			Annual		
	Oct.–Dec.			Jan.–Mar.			Apr.–July			Aug.–Sept.								
	Bias[1] (percent)	Relative error[2] (percent)	RMSE[3] (ft^3/s), except for FTO (acre-feet)	Bias (percent)	Relative error (percent)	RMSE (ft^3/s) except for FTO (acre-feet)	Bias (percent)	Relative error (percent)	RMSE (ft^3/s) except for FTO (acre-feet)	Bias (percent)	Relative error (percent)	RMSE (ft^3/s) except for FTO (acre-feet)	Bias (percent)	Relative error (percent)	RMSE (ft^3/s) except for FTO (acre-feet)	Bias (percent)	Relative error (percent)	RMSE (ft^3/s) except for FTO (acre-feet)
Almanor	–4.1	–16.3	376	7.6	0.7	463	1.2	3.7	241	–8.7	–4.5	118	1.5	–3.9	494	1.5	–0.6	154
Butt Creek	–10.9	–22.7	33	–1.0	–5.8	36	0.5	–0.6	27	–15.5	–16.6	12	–3.1	–11.7	41	–3.2	–6.0	15
East Branch	6.1	–14.0	240	–1.2	0.4	604	3.4	10.0	351	52.4	49.8	94	2.8	10.7	591	2.7	1.6	204
Lower North Fork[4]	7.7	1.7	192	–10.5	–5.8	443	0.7	4.2	234	14.6	7.8	230	–1.6	4.6	515	–1.4	–1.6	123
Middle Fork	–0.2	–9.0	389	–3.4	5.1	837	–5.8	–6.8	503	–24.7	17.2	143	1.7	2.1	884	1.9	3.9	220
South Fork	4.2	19.5	63	7.4	18.5	140	6.7	11.6	125	35.1	21.7	16	7.5	18.7	164	7.3	7.9	57
West Branch[5]	–9.0	–13.6	72	–10.2	11.2	193	–6.6	26.4	86	16.3	48.5	5	–8.3	47.9	160	–8.2	11.1	68
FTO[6]	10.0	0.2	267,666	–4.9	–1.4	410,633	–3.7	–3.3	285,259	–16.4	–21.4	57,279	–3.2	–9.1	133,871	–3.2	–3.6	465,328

[1]Equation used for bias calculation: $\frac{\Sigma(s-o)}{\Sigma o} x100$.

[2]Equation used for relative error calculation: $\frac{\Sigma\left[\frac{(s-o)}{o}\right]}{N} x100$.

[3]Equation used for root-mean-square error (RMSE): $\sqrt{\frac{\Sigma(s-o)^2}{N}}$.

For all equations:

s is simulated mean streamflow, in cubic feet per second,

o is observed (measured or reconstructed) mean streamflow, in cubic feet per second, and

N is number of measured or reconstructed values greater than 0 cubic feet per second.

[4]Lower North Fork reconstructed data for 1994 was suspect, and this year was excluded from the analyses.

[5]West Branch calculations for 1971–86 only, corresponding to available measured data.

[6]FTO reconstructed inflow to Lake Oroville was provided by DWR, (http://cdec.water.ca.gov/ accessed March 12, 2002), and compared with combined simulated inflow for water years 1971–97. RMSE is in acre-feet.

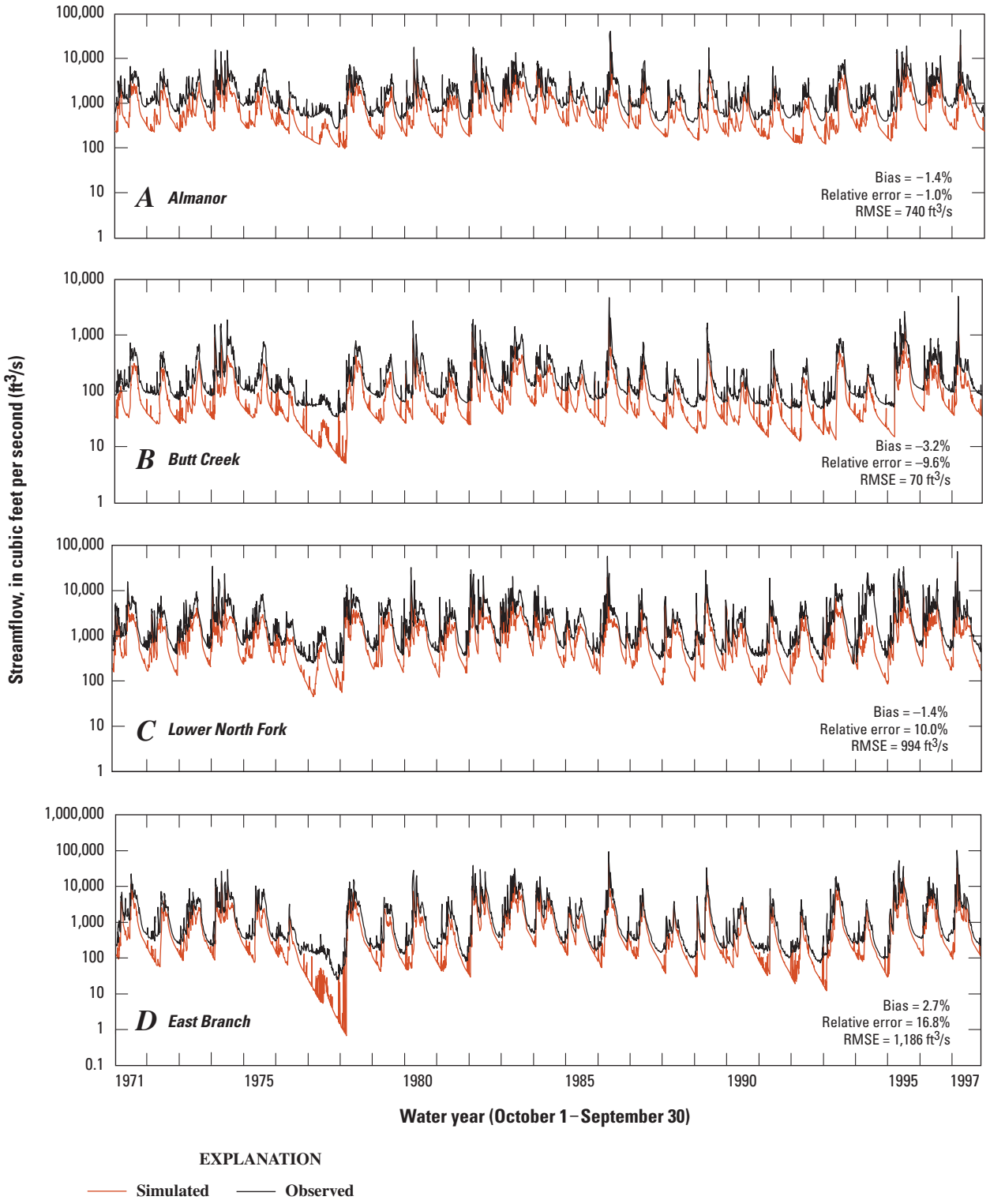

Figure 16. Daily streamflow hydrographs showing model simulations and observed (measured or reconstructed) streamflow, water years 1971–97, including (*A*) Almanor, (*B*) Butt Creek, (*C*) Lower North Fork, (*D*) East Branch, (*E*) Middle Fork, (*F*) West Branch, (*G*) South Fork, and (*H*) Oroville. Y-axes vary. RMSE, root-mean-square error.

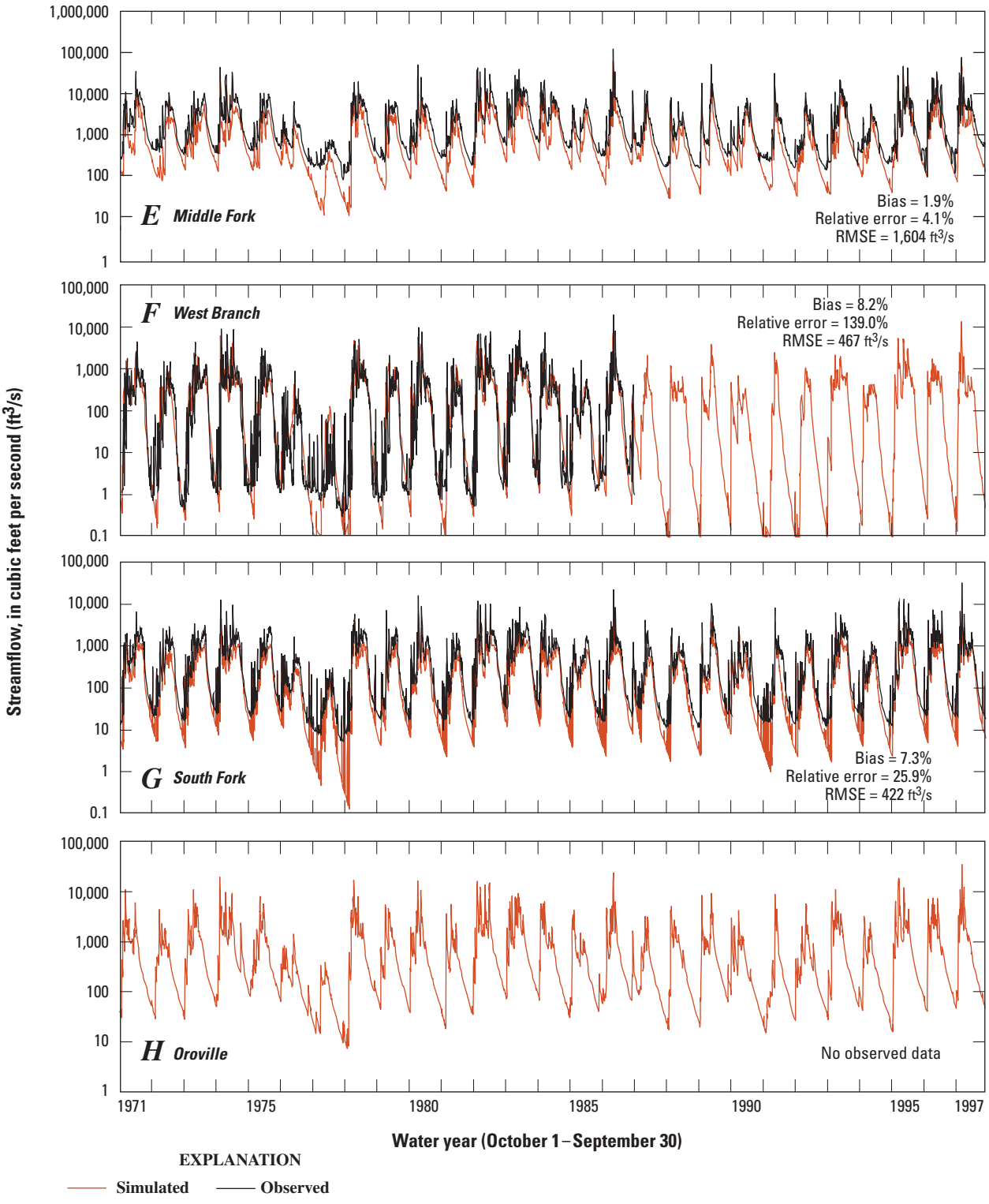

Figure 16.—Continued.

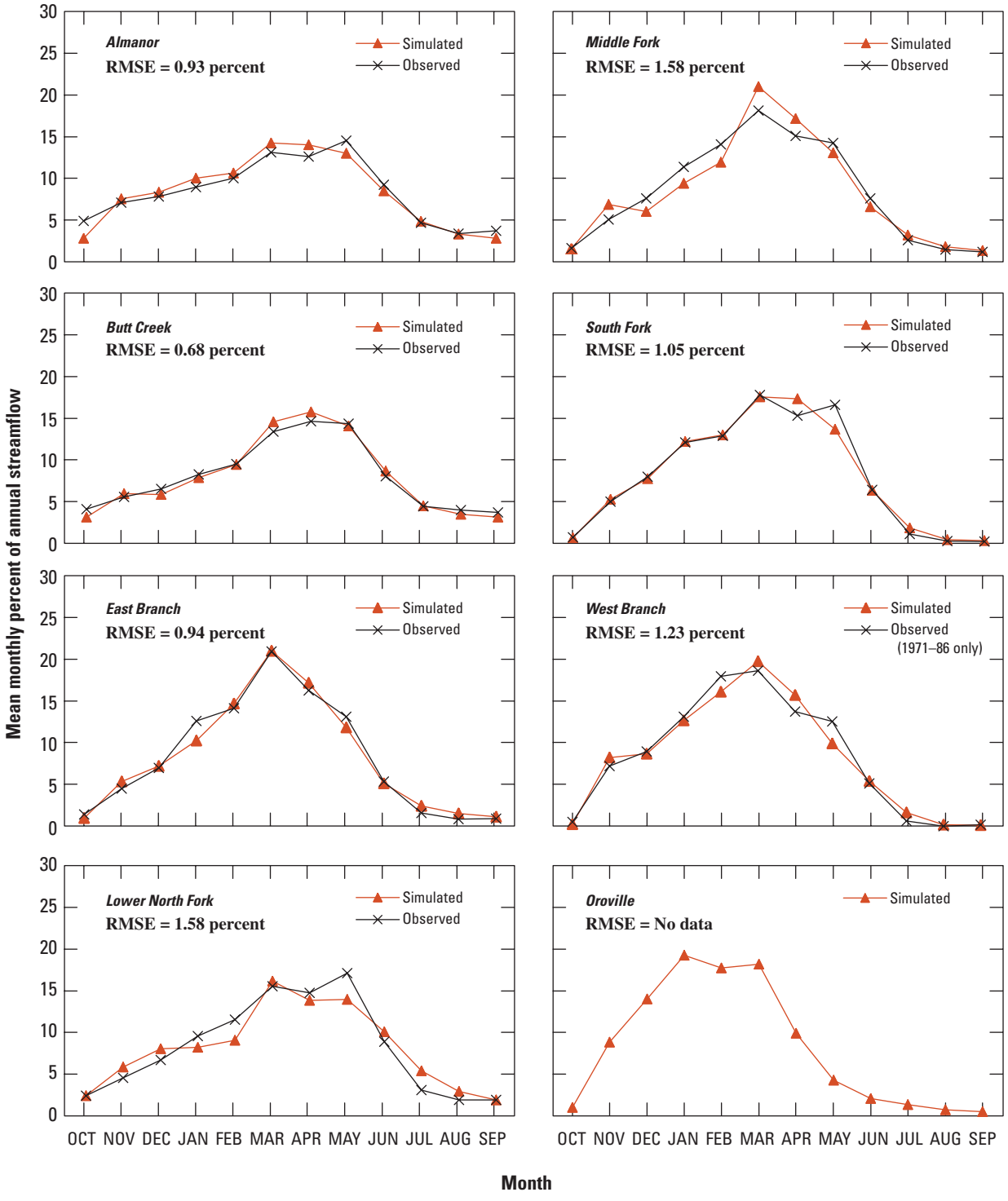

Figure 17. Mean-monthly percentages of annual streamflow for individual models, water years 1971–97. Observed streamflow is measured or reconstructed flow.

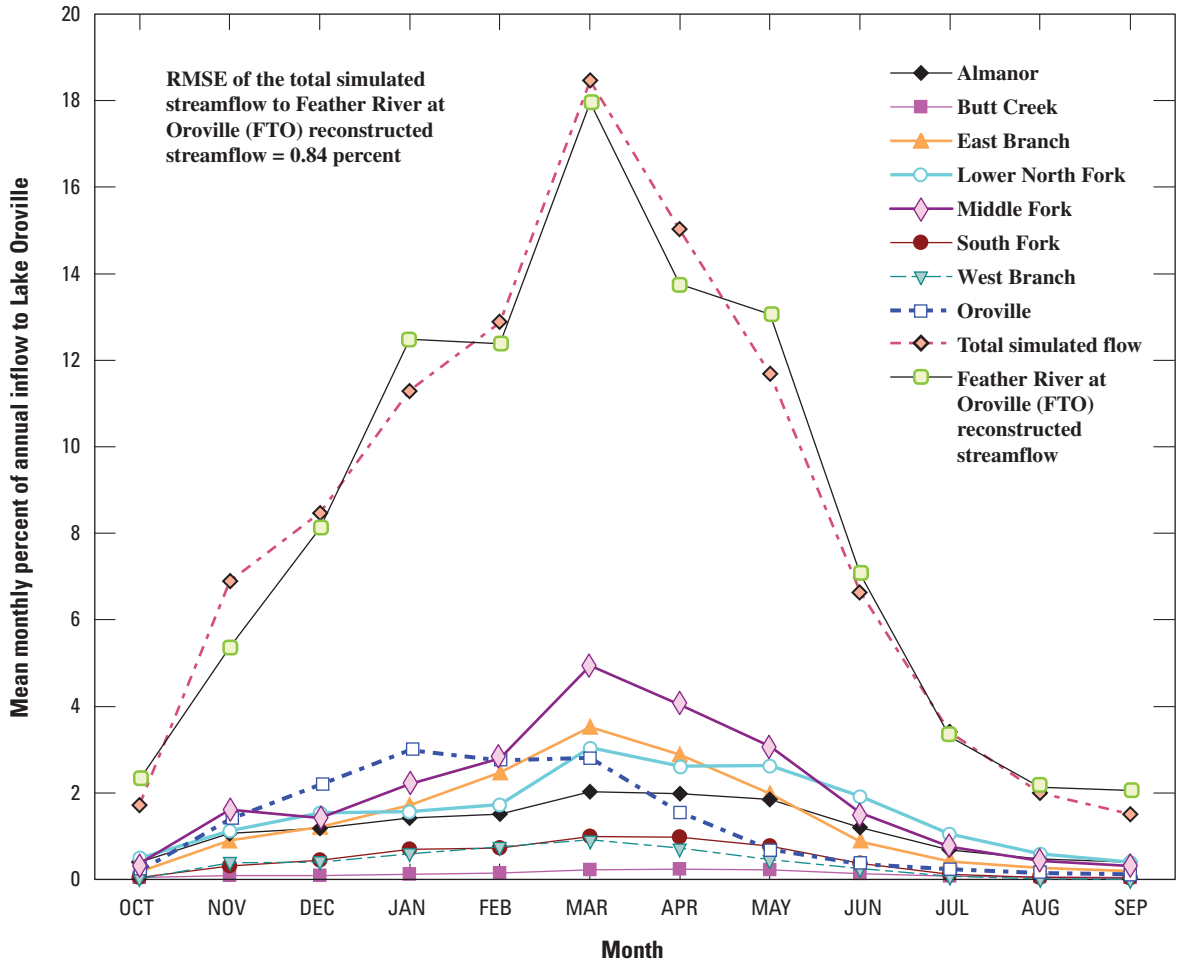

Figure 18. Mean-monthly percentages of simulated inflows to Lake Oroville and the Feather River at Oroville (FTO) reconstructed streamflow, water years 1971–97. RMSE, root-mean-square error.

Model simulations of seasonal volumes of flow into Lake Oroville were also compared with DWR's FTO reconstructions for selected seasons (January–March and April–July; fig. 19). A comparison of the January–March model simulations to FTO reconstruction volumes yields a RMSE of 410,852 acre-feet with flow volumes ranging from about 200,000 to 4,800,000 acre-feet (fig. 19). A comparison of April–July model simulations to FTO reconstruction volumes yields a RMSE of 289,963 acre-feet with flow volumes ranging from about 300,000 to 4,300,000 acre-feet (fig. 19). Based on the RMSEs and a visual comparison of the graphed data, model simulation totals reasonably match the FTO reconstruction volumes on this time scale.

The graph of total annual simulated inflow volumes closely tracks the phase and volume of FTO reconstructions for water years 1971–97, resulting in a RMSE of 465,328 with flow volumes ranging from about 200,000 to 9,400,000 acre-feet (table 14, fig. 20). A small bias and relative error of less than –4 percent were calculated for this annual comparison (table 14).

Three additional years of simulation (1998–2000), beyond the calibration period, were later compared to FTO annual reconstruction volumes (fig. 20). Overall, the timing of simulated streamflow is in phase with the FTO reconstructions. However, the modeled streamflow volumes after 1997 are too low when compared to FTO reconstruction volumes, with a higher RMSE of 633,544 acre-feet, higher relative error of –9.3 percent and a higher bias of –11.1 percent as compared to calibration statistics for 1974–1997 (table 14; fig. 20). This departure could be explained by the influence of the PDO on the Feather River Basin. The PDO entered a cool phase beginning about 1998, cooling basin temperatures. Cooler basin temperatures would shift peak streamflow to April–May. The models were calibrated mostly to conditions during the warmer phase PDO (1977–98), during which peak streamflow occurs by March (Koczot and Dettinger, 2003).

As mentioned, a double-mass analysis of old and new Quincy climate station temperatures revealed a change in the record in about November 1998. The Quincy temperatures are important inputs to the East Branch and Middle Fork models, which provide 40 percent of the inflow to Lake Oroville. Thus, the changes at the Quincy climate station could partially explain the recent systematic simulation errors for the years 1998–2000.

Simulated and Remotely Sensed Snow Cover Comparison

Snow cover simulated in PRMS on the Lower North Fork was compared, at the HRU level, with remotely sensed snow cover from the National Operational Hydrologic Remote Sensing Center (NOHRSC; http://www.nohrsc.nws.gov, accessed on Jan. 10, 1999; fig. 21). Comparisons such as these may be used in PRMS calibrations to determine how well snowpack accumulation and melt are being simulated. The comparison used a GIS tool—the Snow Cover Comparison Tool (SCCT; Koczot and Dettinger, 1999)—developed for this purpose.

A comparison of a NOHRSC snow cover map and simulated Lower North Fork snow-water content is shown for March 15, 1996, in figure 21. The NOHRSC imagery has a resolution of 0.68 mi (1,100 m), whereas the Lower North Fork simulation has an effective resolution of 0.02 mi (30 m).

Figure 21 shows areas where the PRMS simulations and NOHRSC remotely-sensed indications of snow are in agreement (the "both snow" and "both no snow" categories), and in disagreement (the "snow simulated only" or "snow remotely sensed only" categories). Despite the different resolutions of the imagery and model, the PRMS simulations and NOHRSC snow cover in this example agree in 80 percent of the study area. Examples where there is not an agreement include HRUs 14 and 23, where NOHRSC simulated snowcover and PRMS did not. Such disagreements can provide the starting point for identifying model errors that could not be recognized in a calibration based on only a single streamflow gage at the outflow from the model area.

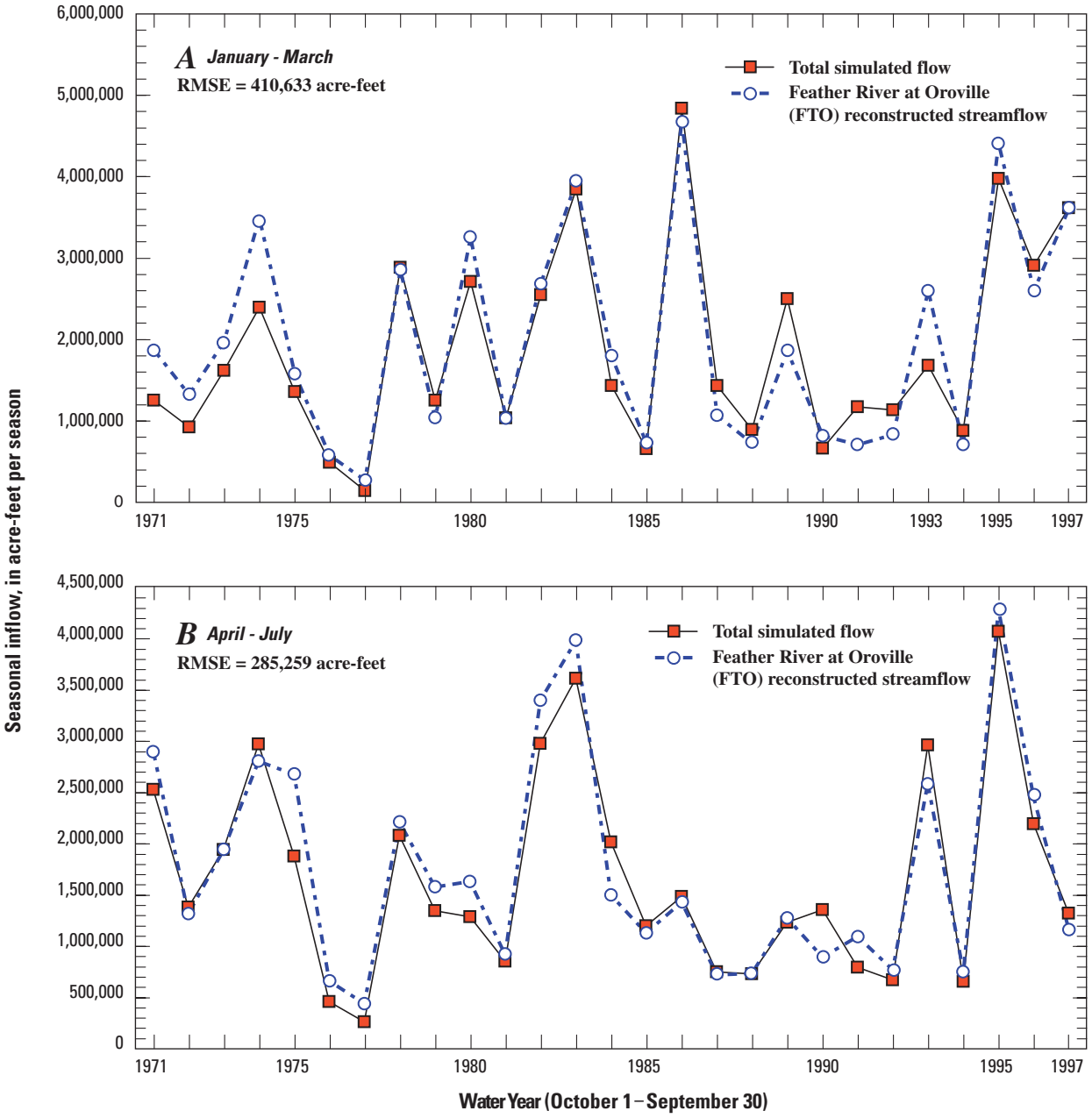

Figure 19. Seasonal streamflow into Lake Oroville in water years 1971–97, including (A) January–March, and (B) April–July. Y-axes vary. RMSE, root-mean-square error.

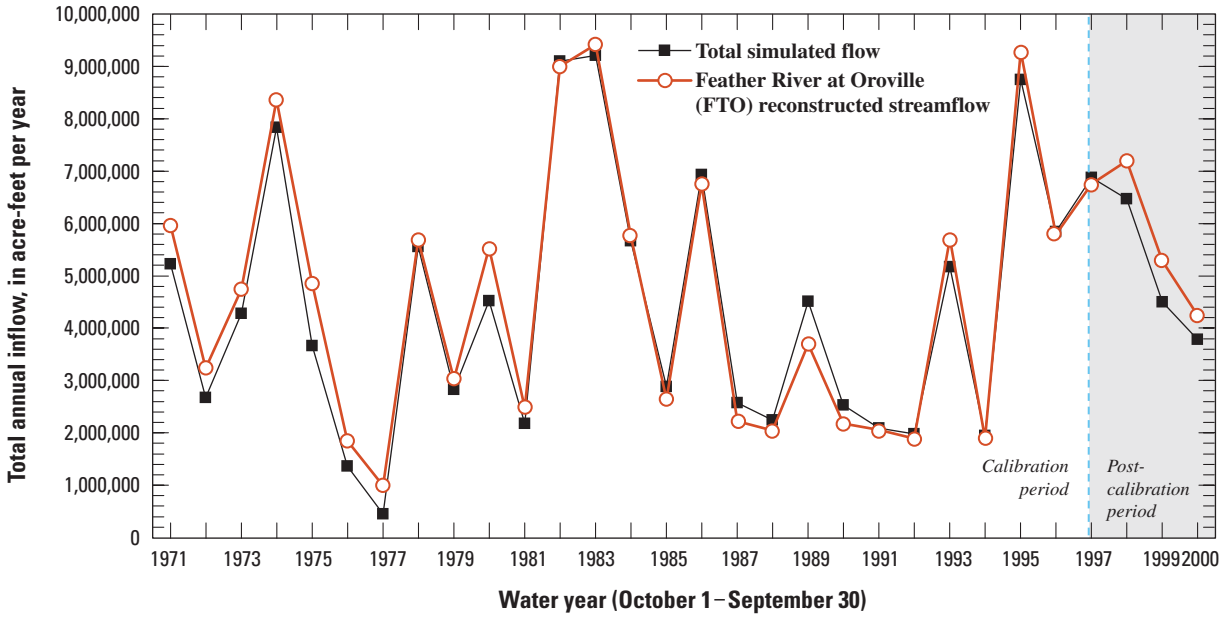

Figure 20. Total annual inflow to Lake Oroville, water years 1971–2000.

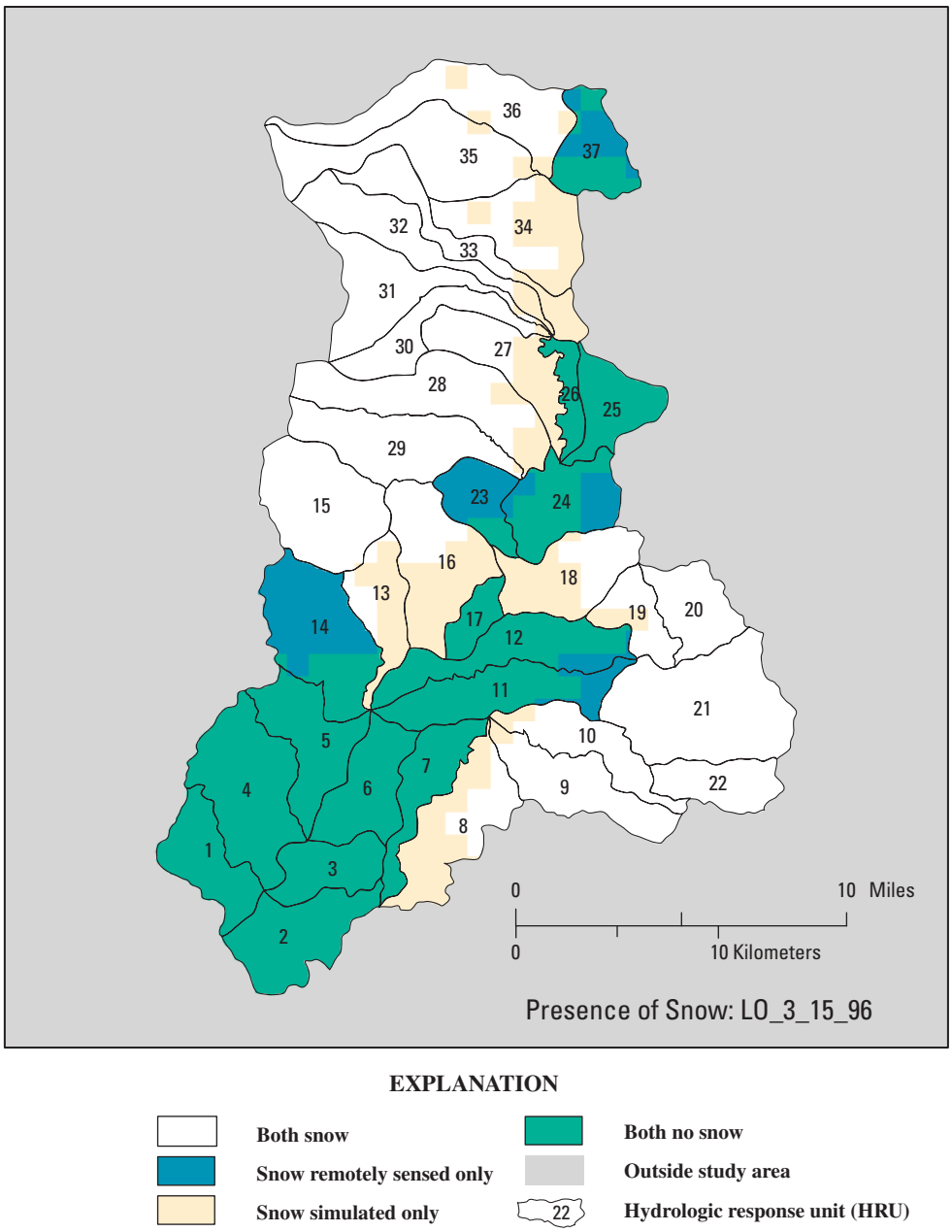

Figure 21. Simulated and remotely sensed snow cover for the Lower North Fork Model, March 15, 1996.

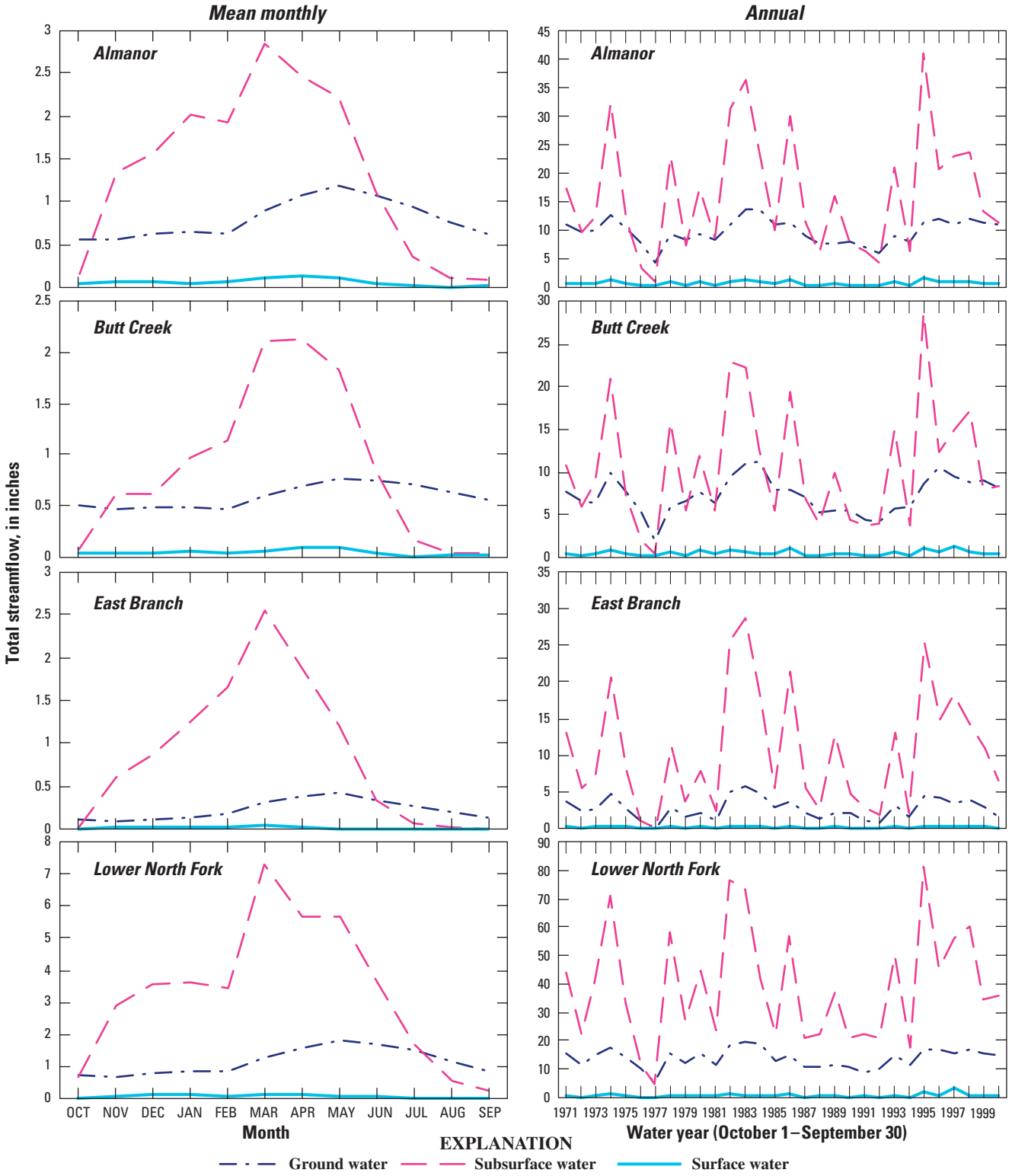

Figure 22. Components of streamflow: mean-monthly flow during water years 1971–97 (left panels) and annual flows during 1971–2000 (right panels).Y-axes vary.

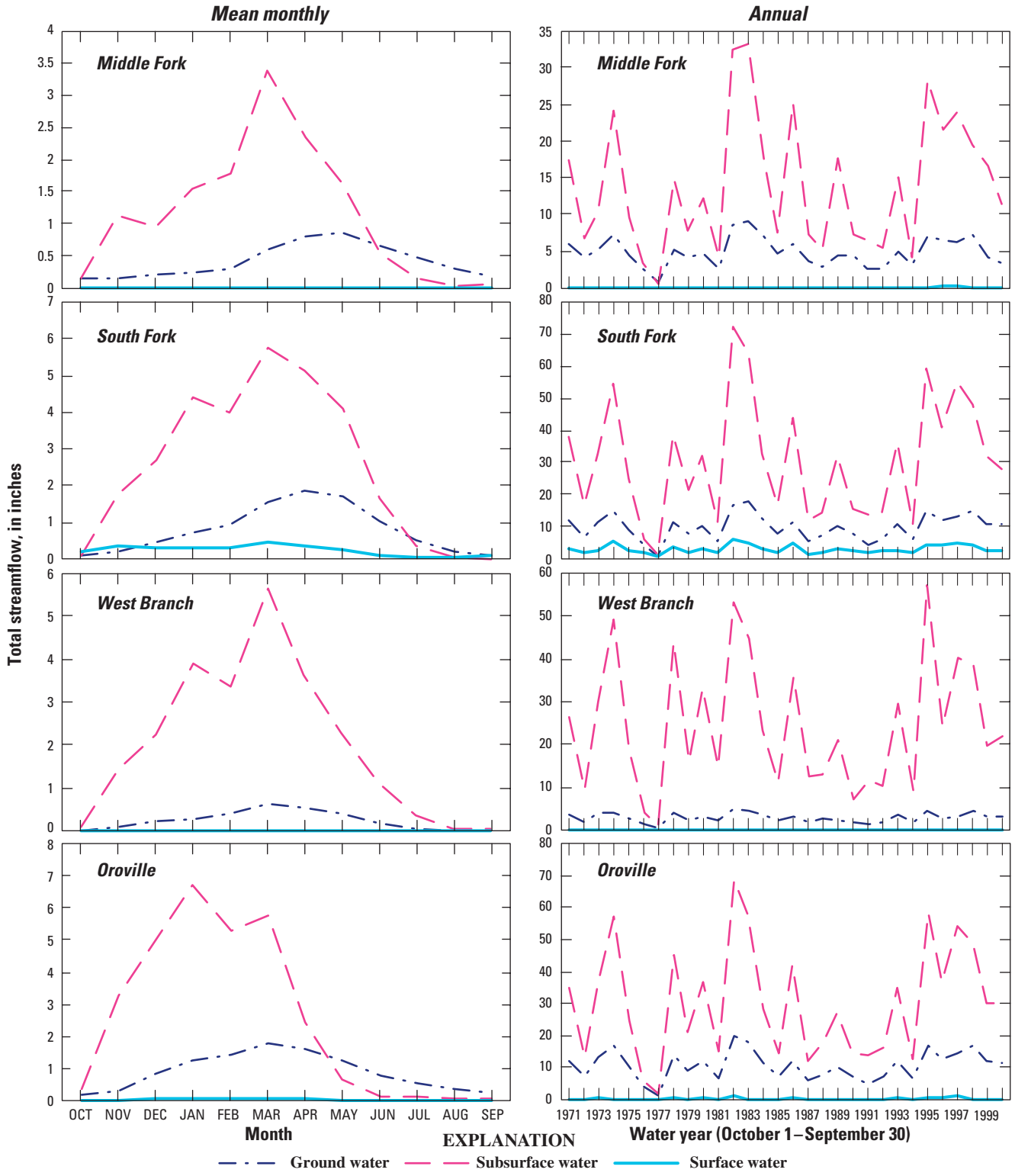

Figure 22.—Continued.

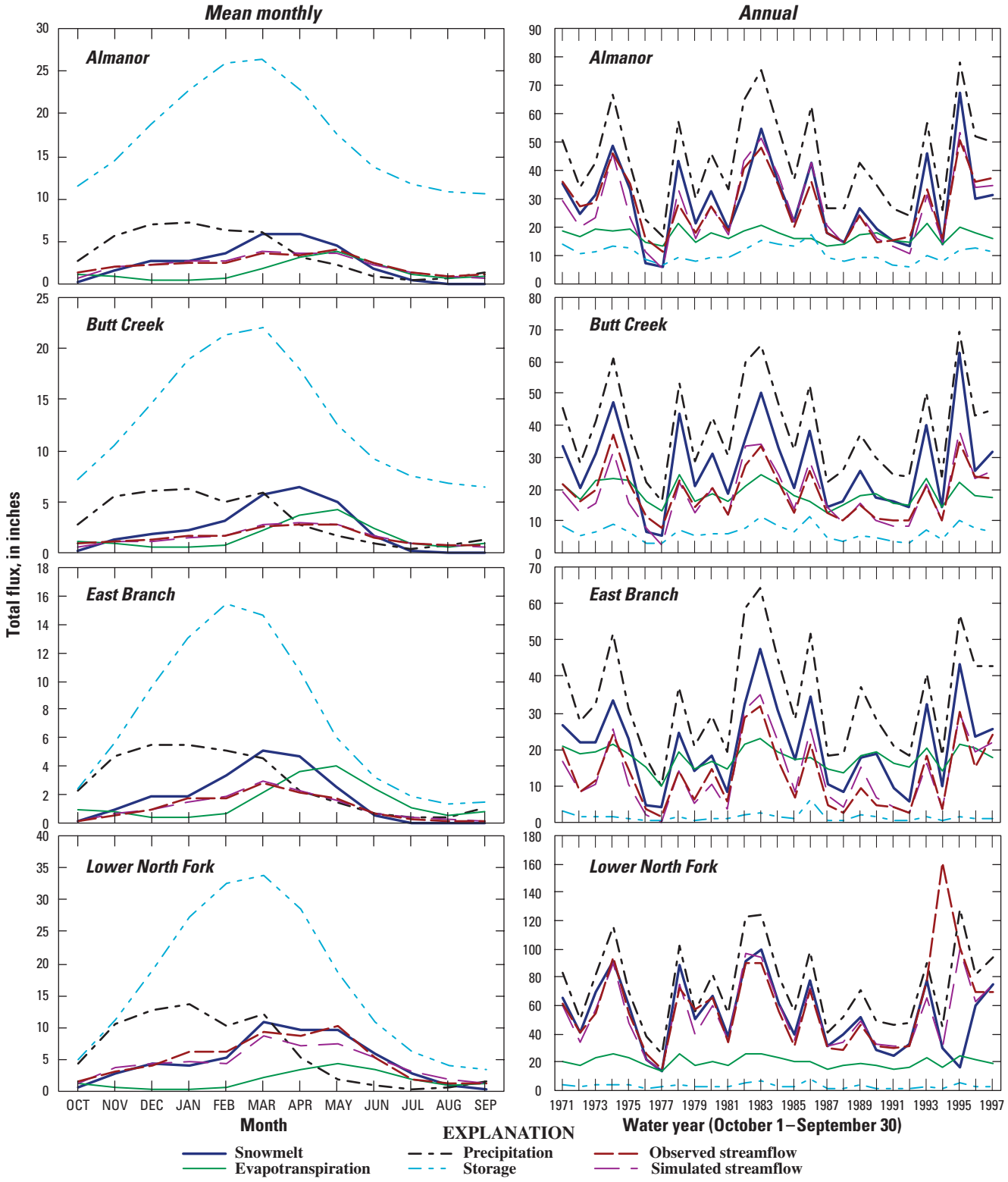

Figure 23. Water-budget components: mean-monthly (left panels) and annual (right panels) values, water years 1971–97. Storage values plotted are not fluxes, but rather are averages of the storage at the end of each month, in inches; other components reported as inches/year or inches/month. Y-axes vary. Observed streamflow is measured or reconstructed flow.

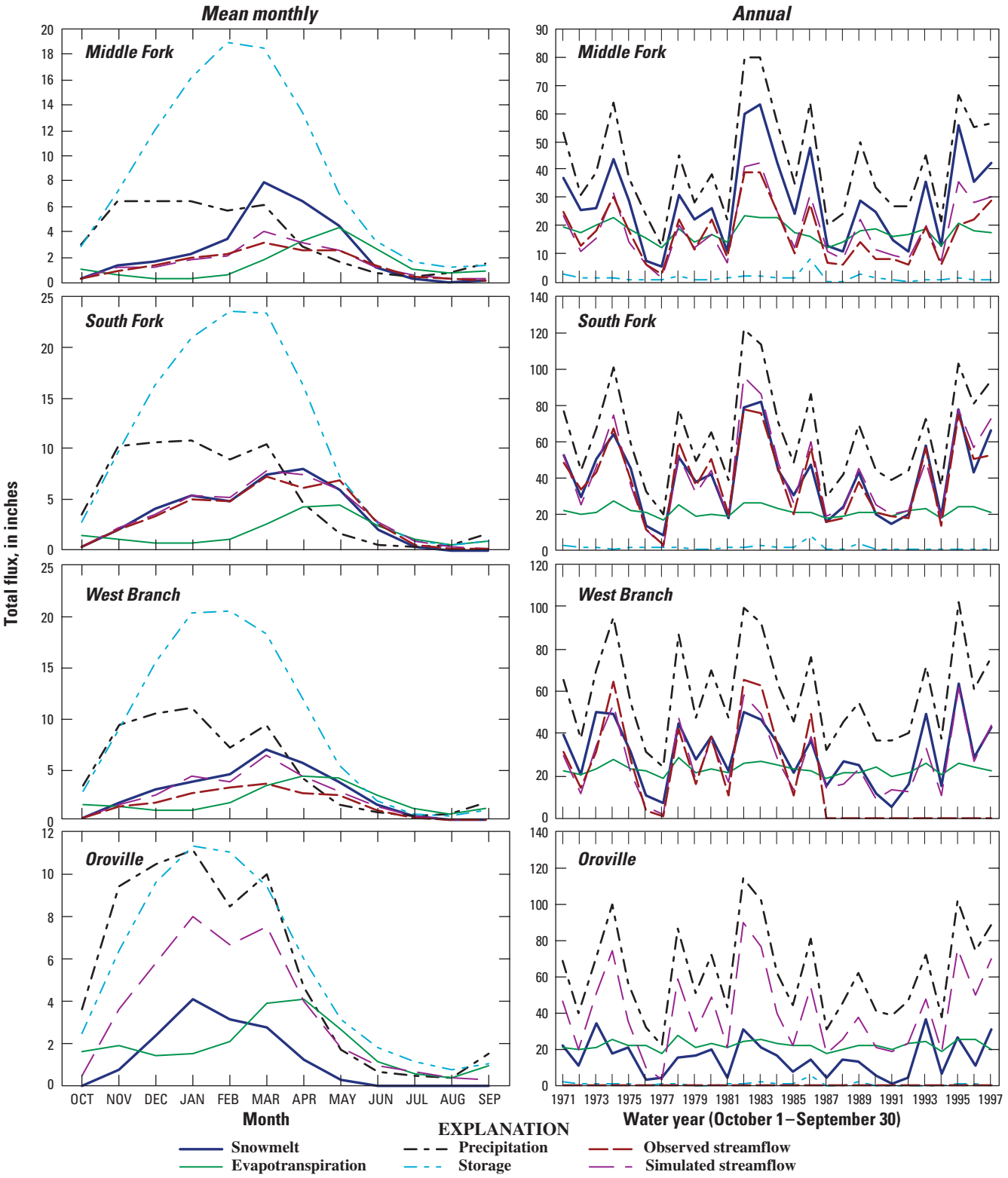

Figure 23.—Continued.

Applications of the Models

Water-Balance Assessment

In PRMS, the basin water budget consists of storage in snowpack, soil moisture, and ground water; inputs from precipitation and snowmelt; losses to evapotranspiration and recharge to the deeper aquifer system; and outflows to streams from surface, subsurface, and shallow ground-water reservoirs. About 60 percent of the water that enters the basin as precipitation leaves as streamflow to Lake Oroville. Nearly all the rest (except for small deep ground-water outflows from Sierra Valley) leaves the basin as evapotranspiration.

The major contributors of streamflow to Lake Oroville are the Lower North Fork and the Middle Fork (table 15, fig. 7). The simulated streamflow to Lake Oroville is primarily (72.4 percent) from subsurface flow with little surface runoff (overland flow; 2.3 percent). Ground-water flow contributes about 25.3 percent (table 16, fig. 22). Ground water makes the largest contribution to streamflow (relative to the models' overall area and flows) in the Almanor and Butt Creek models, because of ground-water-rich volcanic formations present in these basins (fig. 6*A*).

Mean-monthly and annual components of the water budget are shown in figure 23. Precipitation quickly increases from the summer lows to the highs of November through March. Evapotranspiration increases and decreases throughout the year governed by the availability of soil moisture and the vegetative life cycle (phenology). Evapotranspiration peaks by April–May in response to spring warming and vegetative growth. During the warmest months, evapotranspiration is limited by a decline in precipitation and soil moisture. Storage in soil, subsurface, and ground-water reservoirs is greatest during January through March.

In most of the Feather River PRMS models, the maximum streamflow occurs in March–May (fig. 17) and is overwhelmingly from subsurface flow fig. 22). However, in the lower altitude models of Oroville and West Branch (table 11), maximum streamflow occurs in January–March (fig. 17), corresponding with the rainy season. Generally, subsurface flow (fig. 22) is greatest in February–May (deriving from melting snow and rainfall) and declines from June through July, owing to low rainfall and little or no snowmelt. Therefore, in June–July, streams flow at much lower rates. In late June–September, when subsurface flow is at its lowest, the major contributor to streamflow is ground water.

Table 15. Percentages of annual inflow to Lake Oroville from modeled areas: simulated, and measured or reconstructed.

[PRMS; Precipitation-Runoff Modeling System; DWR, California Department of Water Resource; —, no data]

Model area	Percent of inflow to Lake Oroville, measured or reconstructed data[1]	Percent of simulated inflow into Lake Oroville[2]	Percent of inflow to Lake Oroville, DWR[3]
Almanor	15	14.9	18.0
Butt Creek	2	1.5	—
East Branch	16	16.5	—
Lower North Fork	20	18.1	—
North Fork[4]	53	51	56.0
Middle Fork	22	23.3	—
South Fork	5	5.5	6.0
West Branch	5	4.9	—
Oroville	[5]15	15.3	—

[1]Computed from annual measured or reconstructed streamflow data, as compared to FTO reconstructed data, water years 1971–97.
[2]Computed from PRMS annual output, water years 1971–97, excluding Lakes Almanor, Mt. Meadows, Oroville, and the area "not modeled."
[3] From DWR Bulletin 120-2-00 (California Department of Water Resources, 2000), computed from reconstructed streamflow data, water years 1941–90.
[4] Includes model areas Almanor, Butt Creek, East Branch, and the Lower North Fork.
[5] No measured or reconstructed data. This is the remainder of flow not accounted for from the other models.

Table 16. Average-annual simulated components of streamflow in the Feather River Basin, water years 1971–97, as inches/year (equal to streamflow volumes divided by drainage areas).

Model	Ground-water flow (inches)	Subsurface flow (inches)	Surface runoff (inches)
Almanor	9.8 (36 percent of model flow)	17.4	0.9
Butt Creek	7.1 (39 percent of model flow)	10.6	0.5
East Branch	2.7	10.5	0.2
Lower North Fork	13.7	38.8	0.7
Middle Fork	4.8	13.7	0.0
South Fork	9.5	30.0	2.9
West Branch	2.8	24.1	0.0
Oroville	10.4	29.7	0.3
Average cumulative inflow to Lake Oroville	7.6 (25.3 percent of flow)	21.7 (72.4 percent of flow)	0.7 (2.3 percent of flow)

The simulated annual water budgets for drainages and for the basin as a whole, are summarized in table 17. Storage (fig. 23; table 17) is reported as an average of the last daily estimate in the month or year of interest; other budget items are reported as long-term averages. Ground-water and subsurface storage are highest in the Almanor and Butt Creek drainages, and substantially less in other parts of the basin.

Within the Feather River Basin, the areas receiving the highest precipitation are not necessarily those highest in altitude (table 17; figs. 3, 23). The wettest modeled areas are Lower North Fork, South Fork, West Branch, and Oroville. Evapotranspiration, closely tied to precipitation, is higher in lower altitude basins. Per unit area, the largest contributions of streamflow come from the Lower North Fork and South Fork, which benefit from deep snowpacks and large volumes of snowmelt, and the upper reaches of the Oroville drainage (table 15). These reaches receive a high amount of precipitation.

In PRMS, snowmelt is simulated as an indirect contribution to streamflow because it is a source to surface, subsurface, and ground-water reservoirs. In the Feather River Basin as a whole, maximum snowmelt is simulated to occur in March–May. However, in the lower altitude Oroville model, maximum snowmelt occurs as early as January (fig. 23).

Seasonal Forecast Modeling using Ensemble Streamflow Prediction (ESP)

A modified version of the National Weather Services ESP program (Day, 1985) has been coupled with PRMS to provide forecasting capabilities that include short-term and seasonal forecasting for floods and water supply (Leavesley and Stannard, 1995). The ESP procedure uses historical or synthesized climate data to forecast future streamflow, starting with simulated initial hydrologic conditions at the beginning of the forecast period. When historical climate data are used, all past climatic events from the historical record are treated as examples of possible future climatic events. Future climate conditions, not yet witnessed in the historical record, can be included by adding in synthesized climate data series (Leavesley and Stannard, 1995).

Table 17. Average-annual simulated water-budget analysis in the Feather River Basin, water years 1971–97, with measured or reconstructed streamflow

Model	Snowmelt[1] (inches)	Precipitation (inches)	Evapo-transpiration (inches)	Storage[2], ground water and subsurface (inches)	Simulated streamflow (inches)	Measured or reconstructed streamflow (inches)
Almanor	30.9	45.7	17.5	10.9	28.1	27.7
Butt Creek	27.5	39.2	18.6	6.4	18.2	18.8
East Branch	21.0	33.8	17.8	1.4	13.4	13.0
Lower North Fork	53.4	73.5	20.2	3.3	53.9	58.8
Middle Fork	29.2	42.0	17.7	1.4	18.5	17.2
South Fork	40.8	63.9	21.6	1.0	42.3	39.4
West Branch	30.9	59.1	23.0	1.0	26.9	[3]18.7
Oroville	15.4	62.6	22.3	1.0	40.3	[4]N/A
Average for the Feather River Basin	31.1	52.5	19.8	3.3	30.2	[5]27.7

[1]Snowmelt contributes to other parts of the water budget, including evapotranspiration, storage and runoff. It is shown here to illustrate that it is a principle component of the hydrologic cycle.
[2]Average of last day-of-year storage estimate for each basin.
[3]West Branch measured streamflow data are for water years 1971–86 only, as available.
[4] No measured or reconstructed streamflow data are available for the Oroville model.
[5] Average of seven models as no observed runoff exists for Oroville model. Also, does not adjust for missing West Branch data.

The current implementation of ESP for the Feather River PRMS models is designed to predict streamflow for the April–July (snowmelt) season using historical data. Once initial conditions are established by simulating conditions up to the beginning of the forecast period, April–July streamflow is simulated using daily temperature and precipitation series from historical April–July periods. With each iteration, the model is re-initialized to use the initial conditions from the current March 31. Together, these simulations of the April–July streamflows compose an ensemble of streamflow predictions representing combinations of the current year's hydrologic conditions to date and observed examples of historical April–July weather. Maximum daily flows, seasonal volumes, and dates on which the flow decreases to user-specified thresholds can be extracted from each prediction hydrograph and used to produce probabilistic forecasts.

ESP results made from the Feather River PRMS were evaluated. Figure 24 shows the results of an ESP run for April 1, 1997, to July 31, 1997, using the initial conditions for March 31, 1997, and the historical input series from 1971, 1978, 1986, 1988, 1993, and 1996. The ensemble of predicted flows was sorted in PRMS to estimate the chance that a quantity of interest will occur. The likelihood is expressed as an exceedence-probability value: the probability that a particular flow level will be exceeded by the actual (observed) flow in 1997 is estimated by:

$$P(exceedence) = i/(N+1) \times 100$$

where

i = historical-trial rank order, in descending seasonal volume, and

N = total number of historical trials.

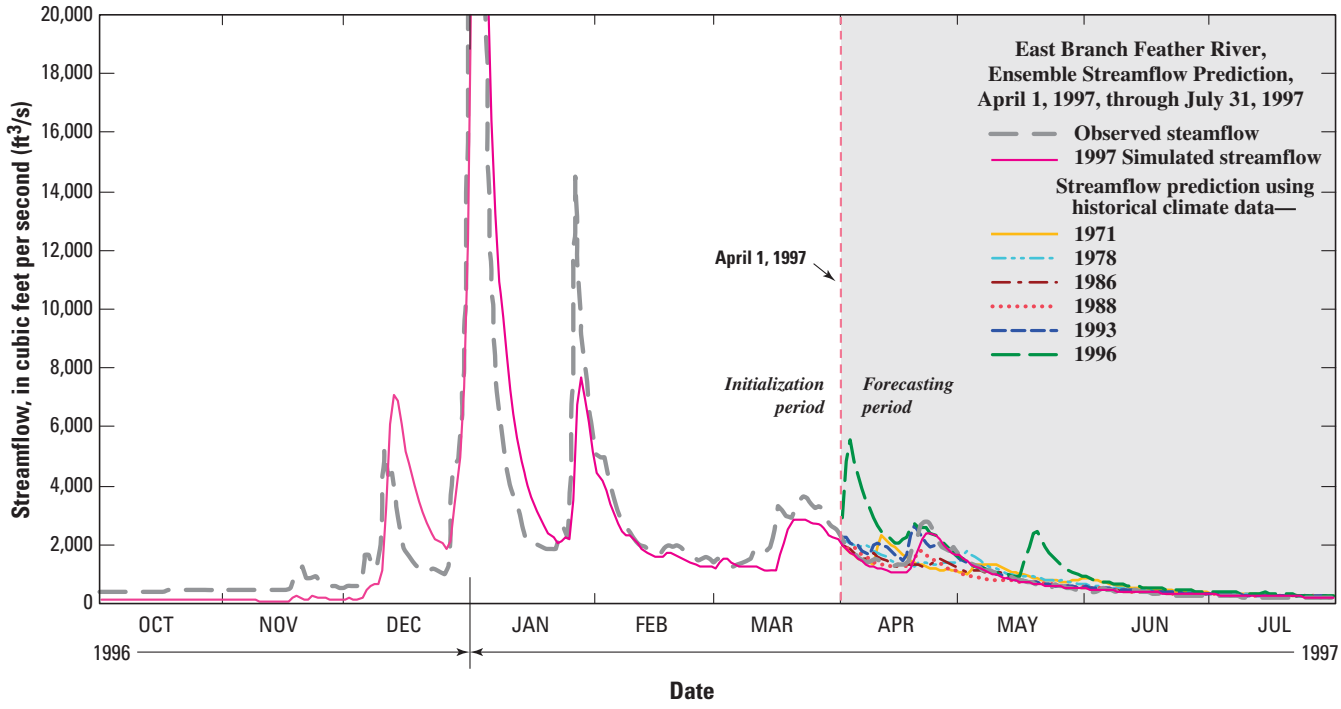

Figure 24. Ensemble Streamflow Prediction (ESP) runs. Observed streamflow is measured flow.

The ESP-exceedence probabilities thus computed tell only part of the story. A better understanding of the likelihood of a particular flow outcome can be obtained by evaluating the ESP-based probabilities from many past ensembles against the subsequent historical (observed) flows. To accomplish this, the ESP procedure was run for the eight models for each water year from 1971 to 2000, using initial conditions (March 31) of the year being forecasted in combination with climatic data from all the others. The simulated volumes are totaled to form ensembles of predictions of April–July inflow to Lake Oroville and are compared with the FTO reconstructions. Seasonal volumes for each "predicted" year (1971–2000) are ranked in descending order, along with the observed flow in the predicted year. The number of times in the 30 years that the observed flows exceeded the ESP flows at each ESP exceedence probability level is counted. These counts, transformed into frequencies and plotted against the ESP exceedence probabilities, provide a basis for correcting the model's ESP exceedence probabilities to reflect the historically accurate exceedence probabilities.

The results of the ESP evaluation for the PRMS models of April–July inflow to Lake Oroville are plotted in figure 25. Among the lowest exceedence probabilities (corresponding to the largest flow volumes), observed flows were larger than the 0 to 10 percent ESP flows in about 0 to 10 percent of the past 30 years. Thus, ESP exceedence probabilities for the largest ESP flows each year would have accurately reflected the exceedence probabilities of the observed flows under the conditions of the past 30 years. Observed flows were larger than the ESP flows at a wide range of (ESP) exceedence probabilities around the median. Thus, historically, the median flow value in a year's ESP ensemble would have been exceeded, by the real river, about 60 percent of the time rather than 50 percent of the time, and a reservoir operator would do well to interpret the median ESP projection in a given year as the 60th percentile exceedence level. Finally, among the highest exceedence probabilities (lowest flow volumes), the ESP exceedence percentiles are exceeded by observed flows somewhat less often than indicated by the ensembles, and an operator would do well to interpret the 90th-percentile flow prediction in a given year's ESP ensemble as a prediction of a flow at roughly the 80th percentile instead.

The graph shown in figure 25, then, can be used as a tool for adjusting the exceedence probabilities suggested by the ESP ensemble in a given year to more accurately reflect historical (observed) exceedence probabilities. When the reliability of the ESP ensembles have been corrected this way, the operator can use the current ESP predictions with more confidence.

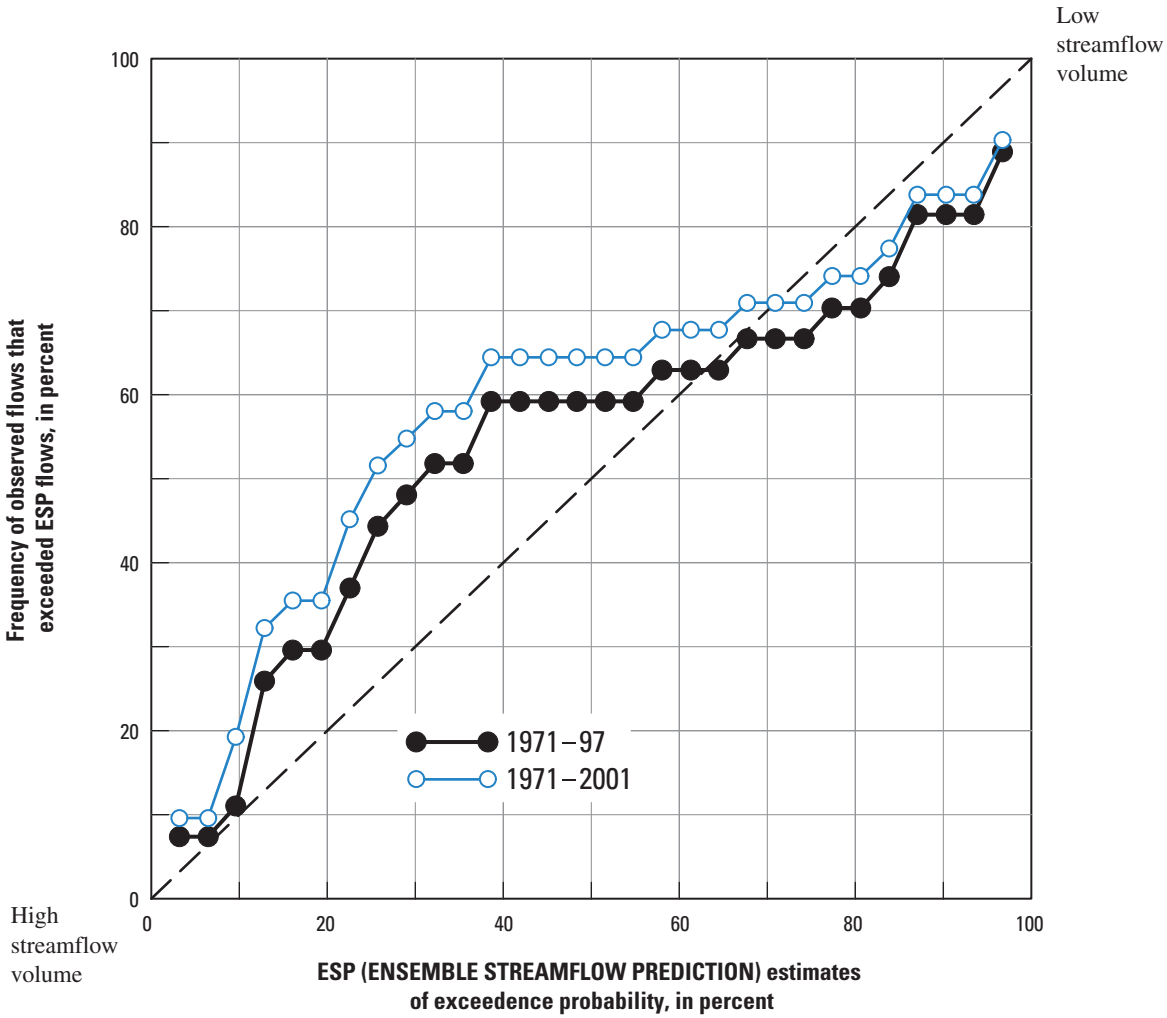

Figure 25. Probabilities of historical inflow to Lake Oroville for April–July forecasts.

Model Limitations

The Feather River PRMS models provide reasonable simulations of the long-term inflow contributions to Lake Oroville, as well as inflow at seven sites within the basin. The models, however, are limited by their spatial resolution (especially of altitude and temperature differences), by the focus of the calibration on seasonal totals of flow, by the lack of true unimpaired streamflow series for the river and its tributaries, and by the small number of real-time climate stations with long-term records available for use as model inputs. A significant limitation is the relatively short period of streamflow records, which prohibits calibration for a greater variety of climatic events (both wetter and dryer)

The large areas of Oroville, Almanor, and Mt. Meadows Lakes were not included in the models (fig. 1). Currently, PRMS is not designed to simulate an open-water body. A comparison of measured precipitation and estimates of pan evaporation showed that the input (precipitation) and output (evaporation) of these areas almost balance. Evaporation from Lake Oroville slightly exceeds precipitation on the lake surface.

Because much of the Feather River Basin is near the average snowline altitude of 5,500 ft, with 55 percent of the basin between 2,000 and 5,500 ft (fig. 3), slight variations in HRU temperature could make significant differences in simulating precipitation form, snow accumulation, and snowmelt. The altitudes encompassed by HRUs typically range over as much as 2,000 to 3,000 ft, with the average HRU altitude assigned as a parameter value (table 12). This may be too coarse to address temperature and other topographically mediated sensitivities well in the Feather River Basin. A comparison of the models developed in this study with models based on a more precise HRU altitude definition could help determine how much the altitudinal lumping limits the current models.

The models were calibrated primarily to the April–July snowmelt season, with secondary attention to monthly variation and then daily flow characteristics. These seasonal flows, and the available monthly FTO reconstructed inflow that was used for comparison with the summed simulations from the eight models, provide less temporal detail for calibration than would an application that focused on daily fluctuations. The models were not calibrated to extreme daily high and low streamflow events. Although the models performed well statistically on a daily and monthly basis (table 14, fig. 16), the models as calibrated can be used most confidently for simulating the April–July snowmelt season.

Half of the Feather River PRMS models were calibrated to reconstructed flows, and the total cumulative streamflow into Lake Oroville was compared with FTO reconstructions. While some error is present in the measured streamflow, errors in the reconstructed values may be larger or more systematic. Thus, in large part, simulations of the present models were compared to other reconstruction-algorithm models. Although the comparisons match well, it is not always clear which series (simulated or reconstructed) to believe.

The measured (gaged) streamflows used in calibration were not always representative of natural conditions. Extraneous factors altered natural flow. For example, in the West Branch model, hydrologic effects of irrigation diversions and reservoirs upstream from the gaging station could not be eliminated from the streamflow data used. The same is true for the East Branch and Middle Fork models. The Butt Creek gage measurements were influenced by a conduit from Lake Almanor that caused sharp streamflow peaks and by leakage from an abandoned tunnel upstream.

In order to provide options for real-time uses of the models, real-time climate stations were chosen as inputs. Available stations were clustered in the southwestern lower-to-intermediate altitude parts of the basin (fig. 3; fig. 7). This distribution made it difficult to make accurate estimates of temperature and precipitation on the eastern and northern sides, and in the parts of the basin at higher altitudes. However, given the encouraging calibration results (table 14), the current models and climate inputs appear to reasonably represent processes and climatic forces within the Feather River Basin. Improvements would be possible if new, accurate and reliable real-time stations were available in areas lacking stations.

Summary and Conclusions

The Feather River Basin and Lake Oroville form a large and crucial part of California's water-supply system. The basin is a major contributor of water to the California State Water Project and plays an important role in flood management, hydroelectric power production, water quality, and the health of fisheries downstream (as far as the Sacramento/San Joaquin River Delta). The basin has a mediterranean climate, and 55 percent of the basin is between 2,000 ft and the average snow line of 5,500 ft. Therefore, slight temperature changes affect the form of precipitation and the timing of snowmelt. The California Department of Water Resources (DWR) manages Lake Oroville for winter floods and summer streamflows during the April 1–July 31 snowmelt season, which is when about 40 percent of the average annual streamflow occurs. Existing statistical and physical models simulate streamflow, but cannot describe the effects of physical changes within the basin as well as the Precipitation-Runoff Modeling System (PRMS) models.

The objectives of this study were (1) to develop a new spatially detailed precipitation-runoff model of the basin that offers simulation capabilities at a higher spatial resolution than was available previously, and (2) to characterize and simulate the Feather River Basin in terms of daily rainfall, snowpack evolution, runoff, and water and energy balances that predict streamflow rates from, and within, the part of the basin above Lake Oroville.

The Feather River PRMS model simulates basin hydrologic response at two spatial scales: (1) as eight models within which hydrologic characteristics are represented in terms of 324 hydrologic-response units; and (2) as the sum of the eight models to represent overall inflow to Lake Oroville. The Feather River PRMS models were run on a daily time step and were calibrated primarily to simulate year-to-year variation of the April–July snowmelt-season flow totals, secondly for monthly variation, and thirdly to simulate daily flow characteristics. The modeling system does not capture all extreme high and low historical streamflow events.

The Feather River PRMS models were especially sensitive to parameters describing transmission of water to (and from) the subsurface and ground-water reservoirs. The models were also sensitive to small changes in temperature and precipitation. Climate data used in this study may have been biased: the real-time climate stations that were used are located at lower-to-intermediate altitudes and are concentrated in the southwestern part of the basin. Daily winter temperatures are frequently above freezing, which affects the mix of rain and snow during many storms, the formation of snow pack, and the relative amounts of winter and summer streamflow. Precipitation records for the basin were used to modify an existing long-term average precipitation map, to account for observed daily variations of east-west and north-south precipitation gradients across the basin. The use of these daily precipitation estimates improved the streamflow simulations.

Signatures of North Pacific decadal climate variations have been observed in the Feather River Basin as a shift in the month of maximum streamflow [from April during the cooler Pacific Decadal Oscillation (PDO) phase to March during the warmer decadal phase]. The calibration period was dominated by the warmer climatic (1977–98) phase, and the most recent simulations, shown in figure 20, were dominated by the newly re-established cool decadal phase since 1998. The response of the models to this subtle climatic fluctuation requires more evaluation.

Model calibrations focused on average to wet years (1971–97), with special attention to monthly and seasonal flows during the April–July snowmelt season (of most interest to water managers). Model simulations were calibrated against measured or reconstructed flow and, in sum, were compared with the DWR Feather River at Lake Oroville (FTO) reconstructions. Calibration biases, relative errors, and root-mean-square errors for daily, mean-monthly, seasonal, and mean-annual streamflows were computed. Periods with missing data and suspect data (Lower North Fork, Middle Fork, and West Branch) were removed in computing these statistics.

Overall, the calibration statistics indicated acceptable simulations during the 1971–97 period with low bias, relative error, and RMSE (table 14; figs. 16, 17, 18, and 19), with some explainable exceptions. Larger biases and relative errors of 50 percent in the August–September season, especially in the East Branch and West Branch models, likely were caused by reservoir storage and irrigation practices altering natural streamflow measurements but not accounted for in model simulations of natural streamflow. Statistics for October–December streamflow simulations were within acceptable ranges for a model focusing on calibration of the April–July snowmelt season. The Almador and Butt Creek models produced the largest relative errors (about −16 and −22 percent respectively), and Butt Creek produced the largest bias (about −11 percent) in this season. These models were influenced by underlying volcanic formations and may involve deeper ground-water reservoirs than were represented in PRMS. The daily statistics (fig. 16) indicated that the simulations closely mimicked measured and reconstructed flows, with the exception of a high relative error for the West Branch model that likely was due to unmodeled diversions.

The timing and quantity of simulated streamflows closely matched DWR FTO reconstructions when compared on a daily, monthly, seasonal, and annual basis. Monthly comparisons (averaged across the calibration period 1971–97), for individual models resulted in RMSEs under 2 percent. A good fit was achieved for the April–July snowmelt season, where the RMSE between model simulations and FTO reconstructions was computed as 285,259 acre-feet with flow volumes ranging from about 300,000 to 4,300,000 acre-feet (fig. 19). January–March seasonal inflow volumes into Lake Oroville closely simulated FTO reconstruction volumes with a RMSE of 410,633 acre-feet and flow volumes ranging from about 200,000 to 4,800,000 acre-feet. As mean-monthly percentages, the combined simulated inflow graphed closely to FTO reconstructions, with a RMSE of 0.84 percent. For water years 1971–97, the annual total simulated inflows also fit FTO reconstructions, resulting in a bias and relative error below −4 percent and a RMSE of 465,328 with inflow volumes ranging from about 200,000 to 9,400,000 acre-feet. However, after 1997 (post calibration period), a departure was seen that may reflect the Feather River Basin's sensitivity to PDO (and a change to a cool phase). Simulated volumes were less than FTO reconstructions.

Modeled contributions of inflow to Lake Oroville from surface runoff, and subsurface and ground-water flow were quantified. The major contributors of inflow according to the models are the Lower North Fork and the Middle Fork. Simulated streamflow is from subsurface flow (72.4 percent), ground-water flow (25.3 percent), and surface runoff (2.3 percent). In higher altitude models, the maximum streamflow (from subsurface flow) occurs in March–May. However, in the lower altitude models of Oroville and West Branch, maximum streamflow occurs in November–March corresponding with the rainy season. Storage is greatest in the Feather River Basin in January–March. Evapotranspiration peaks by April/May in response to spring warming and vegetative growth, and sharply declines in warm summertime months as soil-moisture storage empties and limits evapotranspiration. By June, owing to low rainfall and little to no snowmelt, the subsurface flow decreases rapidly and streams flow at much lower rates. In late June through September, when subsurface flow is at its lowest, the major contributor to streamflow is ground water.

Streamflow forecasts for the April–July snowmelt season can be estimated from predictions made with the Feather River PRMS models and a standard "ensemble streamflow prediction" (ESP) methodology. The April–July daily climate records from previous years are used to drive the model through a plausible range of April–July outcomes for the current year. Results are ranked by ESP as percentiles of exceedence of flow. Retrospective "predictions" by this method for each year from 1971 to 2000 were compared with the actual flows each year to evaluate the reliability of the ESP exceedence percentiles. The resulting comparisons of the simulated likelihoods of various flow totals to the number of times those simulated rates were exceeded suggests the model-predicted exceedence percentiles are most precise for the largest flows. The percentiles tend to underestimate the likelihoods of exceedence of most mid-range flow rates, and overestimate those of the lowest flows. Presumably, these comparisons can provide a guide for adjusting the confidence levels for any given ESP predictions in the future.

The current form of the Feather River Basin PRMS models provides an acceptable historical simulation of monthly and longer term flow within, and from, the basin. The models could be improved for a real-time application by a partial recalibration with focus on years (such as the present) that are from cool-PDO climate regimes. Further, a more comprehensive distribution of real-time climate stations would improve the representation of precipitation and temperature in the models. The current models assume a constant land-surface and plant canopy throughout the simulations. More detailed attention to historical (or projected) land-use changes and fire scars could provide improved simulations while also helping to quantify the hydrologic effects of such changes. More basically, greater control of temperature inputs to the models would be possible if the model HRUs were re-delineated on the basis of 1,000-foot altitude bands and on the 5,500-foot-altitude snowline. Each of these changes is feasible and would improve not only the models, but our understanding of, and ability to predict, Feather River Basin streamflows.

References Cited

Anderson, E.A., 1968, Development and testing of snowpack energy balance equations: Water Resources Research, v. 4, n. 1, p. 19–38.

Anderson, E.A., 1973, National Weather Service River Forecast System—Snow accumulation and ablation model: U.S. Department of Commerce, NOAA Technical Memorandum NWS-Hydro-17, March 1973.

Battaglin, W.A., Hay, L.E., Parker, R.S., and Leavesley, G.H., 1993, Applications of GIS for modeling the sensitivity of water resources to alterations in climate in the Gunnison River basin, Colorado: Water Resources Bulletin, v. 25, no. 6, p. 1021–1028.

Beven, K.J., 2001, Rainfall-runoff modeling—The primer: New York, John Wiley & Sons, 360 p.

Black, P.E., 1996, Watershed hydrology: Chelsea, Michigan, Ann Arbor Press, Inc., 449 p.

Bonner, L.J., Elliott, P.E., Etchemendy, L.P., and Swartwood, J.R., 1998, Water resources data, Nevada, water year 1997: U.S. Geological Survey Water-Data Report NV-97-1, 636 p.

Bostic, R.E., Kane, R.L., Kipfer, K.M., and Johnson, A.W., 1997, Water resources data, Nevada, water year 1996: U.S. Geological Survey Water-Data Report NV-96-1, 611 p.

Bower, 1985, D.E., Evaluation of the Precipitation-Runoff Modeling System, Beaver Creek, Kentucky: U.S. Geological Survey Water-Resources Investigations Report 84-4316, 39 p.

Brendecke, C.M., and Sweeten, J.G., 1985, A simulation model of Boulder's alpine water supply, *in* Proceedings of 53rd Annual Meeting of the Western Snow Conference: Boulder, Colorado, p. 63–71.

Buer, Stein, 1988, Program Manual—Headwater forecasting using HED71, Sept. 1988: California Department of Water Resources, Division of Flood Management.

Burnash, R.J.C., Ferral, R.L., and McQuire, R.A., 1973, A generalized streamflow simulation system, Conceptual Modeling for Digital Computers: U.S. Department of Commerce National Weather Service and California Department of Water Resources, 204 p.

California Department of Water Resources, 1979, Evaporation from water surfaces in California: Bulletin 73-79, November 1979, 163 p.

California Department of Water Resources, 1998, The California Water Plan update: Department of Water Resources, Bulletin 160-98.

California Department of Water Resources, 2000, Water conditions in California: California Cooperative Snow Surveys, Division of Flood Management, Bulletin 120-2-00, 16 p.

Cary, L.E., 1984, Application of the U.S. Geological Survey's Precipitation-Runoff Modeling System to the Prairie Dog Creek basin, Southeastern Montana: U.S. Geological Survey Water-Resources Investigations Report 84-4178, 98 p.

Cary, L. E., 1991, Techniques for estimating selected parameters of the U.S. Geological Survey's Precipitation-Runoff Modeling System in eastern Montana and northeastern Wyoming: U.S. Geological Survey Water-Resources Investigations Report 91-4068, 39 p.

Cayan, D.R., Kammerdiener, S.A., Dettinger, M.D., Caprio, J.M., and Peterson, D.H., 2001, Changes in the onset of spring in the western United States: Bulletin of the American Meteorological Society, v. 82, no. 3, March 2001, p. 399–415.

Daly, C., Neilson, R.P., and Phillips, D.L., 1994, A statistical-topographic model for mapping climatological precipitation over mountainous terrain: Journal of Applied Meteorology, v. 33, p. 140–158.

Day, G.N., 1985, Extended streamflow forecasting using NWSRFS: American Society of Civil Engineers, Journal of Water Resources Planning and Management, v. 111, no. 2, p. 157–170.

Dettinger, M.D., Battisti, D.S., Garreaud, R.D., McCabe, G.J., and Bitz, C.M., 2001, Interhemispheric effects of interannual and decadal ENSO-like climate variations on the Americas, *in* V. Markgraf (ed.), Interhemispheric climate linkages—Present and past climates in the Americas and their societal effects: Academic Press, p. 1-16.

Dettinger, M.D., and Cayan, D.R., 1995, Large-scale atmospheric forcing of recent trends toward early snowmelt in California: Journal of Climate, v. 8, p. 606–623.

Dettinger, M.D., Cayan, D.R., Meyer, M.K., and Jeton, A.E., 2004, Simulated hydrologic responses to climate variations and change in the Merced, Carson, and American River basins, Sierra Nevada, California, 1900–2099: Climatic Change, v. 62, p. 283-317.

Durrell, C., 1987, Geologic history of the Feather River country, California: University of California Press, Berkeley and Los Angeles, California, 337 p.

Emerson, D.G., 1991, Documentation of a heat and water transfer model for seasonally frozen soils with application to a precipitation-runoff model: U.S. Geological Survey Open-File Report 91-462, 97 p.

Environmental Systems Research Institute, Inc. (ESRI), 1992, Understanding GIS—The ARC/INFO method: Environmental Systems Research Institute Inc., Redlands, Calif., 1 v., variously paged.

Frank, E. C., and Lee, R., 1966, Potential solar beam irradiation on slopes: U. S. Department of Agriculture, Forest Service Research Paper RM-18, 116 p.

Frankoski, L., 1994, Effect of spatial resolution on hydrologic model results: Masters thesis, University of Colorado, 1994, 104 p.

Freeze, R.A., and Cherry, J.A., 1979, Groundwater: Englewood Cliffs, N.J., Prentice-Hall, 604 p.

Haan, C.T., Johnson, H.P., and Brankensiek, D.L, 1982, Hydrologic modeling of small watersheds: American Society of Agricultural Engineers Monograph 5, 533 p.

Hay, L.E., Battaglin, W.A., Parker, R.S., and Leavesley, G.H., 1993, Modeling the effects of climate change on water resources in the Gunnison River basin, Colorado, *in* Goodchild, M.F., Parks, B.O., and Steyaert, L.T., eds., Environmental modeling with GIS: Oxford University Press, p. 173–181.

Hejl, H.R., 1989, Application of the Precipitation-Runoff Modeling System to the Ah-Shi-Sle-Pah Wash watershed, San Juan County, New Mexico: U.S. Geological Survey Water-Resources Investigations Report 88-4140, 36 p.

Jennings, C.W., Strand, R.G, and Rogers, T.H., 1977, Geological map of California: scale 1:750,000, California Division of Mines and Geology, Sacramento.

Jensen, M.E., and Haise, H.R., 1963, Estimating evapotranspiration from solar radiation: Proceedings of the American Society of Civil Engineers, Journal of Irrigation and Drainage, v. 89, no. IR4, p. 15–41.

Jeton, A.E., 1999a, Precipitation-runoff simulations for the Lake Tahoe Basin, California and Nevada: U.S. Geological Survey Water-Resources Investigations Report 99-4110, 61 p.

Jeton, A.E., 1999b, Precipitation-runoff simulations for the upper part of the Truckee River Basin, California and Nevada: U.S. Geological Survey Water-Resources Investigations Report 99-4282, 41 p.

Jeton, A.E., Dettinger, M.D., and Smith, J.L., 1996, Potential effects of climate change on streamflow, eastern and western slopes of the Sierra Nevada, California and Nevada: U.S. Geological Survey Water-Resources Investigations Report 95-4260, 44 p.

Jeton, A.E., and Smith, J.L., 1993, The development of watershed models for two Sierra Nevada basins using a geographical information system: Water Resources Bulletin, v. 29, no. 6, p. 923–932.

Koczot, K.M., and Dettinger, M.D., 1999, Comparisons of simulated, in-situ, and remotely-sensed snow-cover observations in the Sierra Nevada, *in* Troendle, C., and Elder, K., eds., 67th annual meeting Western Snow Conference, April 19–22, 1999, Lake Tahoe, California: Colorado State University, Fort Collins, Colorado, p. 149–152.

Koczot, K.M., and Dettinger, M.D., 2003, Climate effects of Pacific decadal oscillation on streamflow of the Feather River, California, *in* Elder, K., and McGurk, B., eds., 71st annual meeting Western Snow Conference, April 22–25, 2003, Scottsdale, Arizona: Omnipress, www.omnipress.com, p.139–142.

Kuhn, G., 1989, Application of the U.S. Geological Survey's Precipitation–Runoff Modeling System to Williams Draw and Bush Draw basins, Jackson County, Colorado: U.S. Geological Survey Water-Resources Investigations Report 88-4013, 38 p.

Leavesley, G.H., 1989, Problems in snowmelt runoff modeling for a variety of physiographic and climatic conditions: Hydrological Sciences, v. 34, no. 6, p. 617–634.

Leavesley, G.H., Lichty, R.W., Troutman, B.M., and Saindon, L.G., 1983, Precipitation-runoff modeling system—User's manual: U.S. Geological Survey Water-Resources Investigations Report 83-4238, 207 p.

Leavesley, G.H., Markstrom, S.L., Restrepo, P.J., and Viger, R.J., 2002, A modular approach to addressing model design, scale, and parameter estimation issues in distributed hydrological modelling: Hydrological Processes, v. 16, p. 173–187.

Leavesley, G.H., Restrepo, P.J., Markstrom, S.L., Dixon, M., and Stannard, L.G., 1996, The modular modeling system (MMS)—User's manual: U.S. Geological Survey Open-File Report 96-151, 142 p.

Leavesley, G.H., and Stannard, L.G., 1995, The precipitation-runoff modeling system—PRMS, *in* Singh, V.P. (ed.), Computer models of watershed hydrology: Water Resource Publications, Highlands Ranch, Colorado, p. 281–310.

Linsley, R.K. Jr., Kohler, M.A., and Paulhus, J.L.H., 1975, Hydrology for engineers: New York, McGraw-Hill Inc., p. 81–82.

Mantua, N.J., Hare, S.R., Zhand, Y., Wallace, J.M., and Francis, R.C., 1997, A Pacific interdecadal climate oscillation with impacts on salmon production: Bulletin of the American Meteorological Society, v. 78, p. 1069–1079.

Markham, K.L., Anderson, S.W., Rockwell, G.L., and Friebel, M.F., 1996, Water resources data, California, water year 1995: U.S. Geological Survey Water-Data Report CA-95-4, v. 4, 407 p.

McCabe, G.J., and Dettinger, M.D., 2002, Primary models and predictability of year-to-year snowpack variations in the western United States from teleconnections with Pacific Ocean climate: Journal of Hydrometeorology, v. 3, p. 13–25.

Miller, N.L., Bashford, K.E, and Strem, E., 2001, Climate change sensitivity study of California hydrology, A report to the California Energy Commission: Lawrence Berkeley National Laboratory Technical Report no. 49110, November 2001, 30 p.

Mullen, J.R., Shelton, W.F., Simpson, R.G., and Grillo, D.A., 1987, Water resources data, California, water year 1985: U.S. Geological Survey Water-Data Report CA-85-4, v. 4, 289 p.

Norris, J.M., 1986, Application of the Precipitation-Runoff Modeling System to small basins in the Parachute Creek basin, Colorado: U.S. Geological Survey Water-Resources Investigations Report 86-4115, 38 p.

Norris, J.M., and Parker, R.S., 1985, Calibration procedure for a daily flow model of small watersheds with snowmelt runoff in the Green River coal region of Colorado: U.S. Geological Survey Water-Resources Investigations Report 83-4263, 32 p.

Obled, C., and Rosse, B.B., 1977, Mathematical models of a melting snowpack at an index plot: Journal of Hydrology, no. 32, p. 139–163.

Parker, R.S., and Norris, J.M., 1989, Simulation of streamflow in small drainage basins in the southern Yampa River Basin, Colorado: U.S. Geological Survey Water-Resources Investigation Report 88-4071, 47 p.

Puente, C., and Atkins, J.T., 1989, Simulation of rainfall-runoff response in mined and unmined watersheds in coal areas of West Virginia: U.S. Geological Survey Water-Supply Paper 2298, 48 p.

Risley, J.C., 1994, Use of a precipitation-runoff model for simulating effects of forest management on stream flow in 11 small drainage basins, Oregon Coast Range: U.S. Geological Survey Water-Resources Investigations Report 93-4181, 61 p.

Rockwell, G.L., Friebel, M.F., Webster, M.D., and Anderson, S.W., 1997, Water resources data, California, water year 1997: U.S. Geological Survey Water-Data Report CA-97-4, fig. 30.

Rockwell, G.L., Smithson, J.R., Friebel, M.F., and Webster, M.D., 2001, Water resources data, California, water year 2001: U.S. Geological Survey Water-Data Report CA-01-4, fig. 29.

Ryan, T., 1996, Development and application of a physically based distributed parameter rainfall runoff model in the Gunnison River basin: U.S. Bureau of Reclamation, Climate Change Response Program, 64 p.

Sabet, H., and Creel, C.L., 1991, Network flow modeling of Oroville Complex: Journal of Water Resources Planning and Management, v. 117, no. 3, May/June 1991, p. 301–320.

Schmidt, K.M., and Webb, R.H, 2001, Researchers consider U.S southwest's response to warmer, drier conditions: EOS, Transactions, American Geophysical Union, v. 82, no. 41, October 9, 2001, p. 475–478.

Swift, L.W., Jr., 1976, Algorithm for solar radiation on mountain slopes: Water Resources Research, v. 12, no. 1, p. 108–112.

Troutman, B.M., 1985, Errors and parameter estimation in precipitation-runoff modeling: Water Resources Research, v. 21, no. 8, p. 1214–1222.

U.S. Department of Agriculture Forest Service, 1988, Soil resource inventory, Plumas National Forest: in cooperation with U.S. Department of Agriculture Soil Conservation Service, 70 plates, approx. 400 p.

U.S. Department of Agriculture Forest Service, 1993, Soil survey of Lassen National Forest Area, California: Pacific Southwest Region, in cooperation with U.S. Department of Agriculture Soil Conservation Service and Regents of University of California. Soils surveyed by 1982, soil names and maps approved 1984. 90 plates, 283 p.

U.S. Department of Agriculture Forest Service, 1994, Soil survey, Tahoe National Forest Area, California: Pacific Southwest Region, in cooperation with U.S. Department of Agriculture Soil Conservation Service and Regents of University of California, October 1994, 60 plates, 377 p.

U.S. Environmental Protection Agency, 1998, State Soil Geographic (STATSGO) database for CONUS, Alaska, and Hawaii in BASINS: U.S. Environmental Protection Agency, Washington, D.C. http//www.epa.gov/OST/BASINS/, accessed on Feb. 5, 1999.

U.S. Geological Survey, 1965, Water resources data for California: U.S. Geological Survey annual Water-Data Report, 943 p.

U.S. Geological Survey, 1965-2001, Water resources data, California, volume 4, Northern central valley basins and the Great Basin from Honey Lake Basin to Oregon state line: U.S. Geological Survey Water-Data Reports.

Viger, R.J., Markstrom, S.M., and Leavesley, G.H., 1996, The GIS Weasel—An interface for the development of parameter inputs for watershed modeling, *in* Shank, K.L., ed., Programs and Abstracts, U.S. Geological Survey National Computer Technology Meeting: Rancho Mirage, California, May 19–23, 1996, p. 58.

Viger, R.J., Markstrom, S.L., and Leavesley, G.H., 1998, The GIS Weasel—An Interface for the treatment of spatial information used in watershed modeling and water resource management, in Proceedings of the First Federal Interagency Hydrologic Modeling Conference, April 19–23, 1998, Las Vegas, Nevada, v. II, p. 73–80.

Wilby, R.L., and Dettinger, M.D., 2000, Streamflow changes in the Sierra Nevada, California, simulated using statistically downscaled general circulation model output, *in* McClaren, S., and Kniveton, D., eds., Linking climate change to land surface change: Advances in Global Change Research, 6, Kluwer Academic Publishers, p. 99–121.

World Meteorological Organization, 1986, Intercomparison of models on snowmelt runoff: Geneva, World Meteorological Organization, Operational Hydrology Report 23, Publication 646, 430 p.

Zahner, R., 1967, Refinement in empirical functions for realistic soil-moisture regimes under forest cover, *in* Sopper, W.E., and Lull, H.W., eds., International Symposium of Forest Hydrology: New York, Pergamon Press, p. 261–274.

Appendixes

Appendix A. Components of reconstructed natural streamflow of the Feather River at Oroville, California (FTO), computed as acre-feet per month.

Monthly reconstructed streamflow for the Feather River at Oroville (FTO) is currently computed by DWR as the sum of:

(1) + Measured streamflow at USGS 11407000.
(2) + Thermalito Afterbay releases to the Feather River, through the Thermalito Afterbay River Outlet (fig. 2)
(3) + Diversions at the Thermalito Complex (from the Afterbay to Western Canal, Richvale Canal, PG&E lateral, and Sutter-Butte Canal; fig. 2)
(4) + Thermalito Irrigation District and Butte County diversions (California Water Service) from the Thermalito Power Canal Diversion (less than 2 acre-feet per year; fig. 2)
(5) + Gain in storage of Thermalito Complex (Diversion Pool, Forebay and Afterbay)
(6) + Evaporation at Thermalito Afterbay, Thermalito Forebay, and Diversion Pool
(7) + Lake Oroville gain in storage
(8) + Lake Oroville evaporation loss only. Zero when raining
(9) + Palermo diversion (from Lake Oroville) and Bangor Canal diversion (from South Fork; fig. 4)
(10) + Oroville-Wyandotte Canal, also known as Forbestown Ditch (from South Fork), and Hendricks and Miocene Canals (from West Branch)
(11) + Storage gain at Lake Almanor, Mt. Meadows, Butt Valley, Bucks Lake, Frenchman, Antelope, Lake Davis, Little Grass Valley, and Sly Creek reservoirs
(12) + Estimated evaporation for reservoirs listed in item 11, computed as 1.4 times the Lake Almanor evaporation, based on a monthly capacity. The evaporation table is from the Great Western Power Company (PG&E predecessor)
(13) − Slate Creek Tunnel import from the Yuba River basin, which flows into the South Fork at the Sly Creek Reservoir
(14) − Little Truckee River import into Sierra Valley
(15) + Depletion for upstream irrigation and consumptive use

Notes: Monthly reconstructed streamflow (FTO) in the Feather River is estimated for the flow below Lake Oroville at USGS gaging station 11407000 (figs. 1, 2). Since construction of the Oroville Complex in 1967, the gaging station 11407000, in the channel below the Thermalito Diversion Dam, does not measure streamflow through the Oroville Complex (fig. 2). Therefore, diversions out of Feather River basin from Thermalito Afterbay and Forebay, and releases from the Thermalito Afterbay flowing to the Feather River through the Thermalito Afterbay River Outlet, are added to the total flow at station 11407000 (fig. 2; J. Pierre Stephens, DWR Resources Hydrology Branch, unpub. data, 2001). The monthly streamflow reconstructions are reported on the California Data Exchange Center website, in acre-feet per month (http://cdec.water.ca.gov/cgi-progs/staMeta?station_id=FTO, accessed on June 6, 2002).

Appendix B. Programming for the draper method to estimate precipitation over Hydrologic Response Unit (HRU) surfaces from PRISM simulations, Feather River Basin, California.

The draper tool is compiled using a fortran77 compiler, either on a Unix or PC platform.

Input for #4 was computed using ARC/INFO by sampling 12 mean-monthly PRISM precipitation surfaces (http://www.ocs.orst.edu/prism/state_products/ca_maps.html, accessed on Jan. 1, 2000) at the HRU centroids.

Input files required are:

(1) Location of climate stations by latitude and longitude (example file: wsit.locs.update).

(2) Observed daily precipitation for these sites in inches (no data = –99)(example file: feather_ppt.txt)

(3) Location of the HRU centroid by latitude and longitude (example file: ac_centroids)

(4) Weighted-mean precipitation values, in inches, for each HRU sampled from each of the PRISM surfaces (for each of the 12 months) (example file: ac_ave_ppt)

Programming is attached. Draper is run by invoking the “draper” executable file at the command prompt.

Fortran program “draper.f” calls subroutine “trend.f” which in turn calls subroutine “inverse.f” to compute interpolated precipitation from the HRU coordinates on the trend-plane adjusted PRISM map.

wsit.locs.update

39.6920 121.3390 Brush Creek (DWR) - BRS
39.9170 121.3330 Bucks Creek Powerhouse - BUP
40.1670 121.0830 Canyon Dam - CNY
40.0830 121.1500 Caribou - CBO
39.8670 121.6170 Desabla (PG&E) - DSB
39.8720 121.6100 Desabla (DWR) - DES
39.9170 120.9500 Quincy (DWR) - QCY
39.9670 120.9500 Quincy RS (USFS) - QNC
39.5640 121.1060 Strawberry-DWR - SBY
39.5670 121.1000 Strawberry-NOAA - STV

feather_ppt.txt (4 lines required for header)

Real-time ppt stations, 1937/10/1 thru 1998/6/30 from Bruce McGurk. To present, updates from CDEC and PG&E.

Precipitation data for DRAPER program.

BRS BUP CNY CBO DSB DES QCY QNC SBY STV

year, month, day, Brush Creek (DWR), Bucks Creek PH, Canyon Dam, Caribou PH, DeSabla (PG&E), DeSabla (DWR), Quincy (DWR), Quincy RS (USFS), Strawberry-DWR, Strawberry-NOAA

1937 10 1 0.00 -99.00 0.16 -99.00 0.18 -99.00 -99.00 0.00 -99.00 -99.00
1937 10 2 0.09 -99.00 1.19 -99.00 2.34 -99.00 -99.00 1.30 -99.00 -99.00
1937 10 3 0.46 -99.00 0.36 -99.00 0.00 -99.00 -99.00 0.05 -99.00 -99.00
1937 10 4 0.00 -99.00 0.32 -99.00 0.00 -99.00 -99.00 0.90 -99.00 -99.00
1937 10 5 0.00 -99.00 0.00 -99.00 0.00 -99.00 -99.00 0.00 -99.00 -99.00
1937 10 6 0.00 -99.00 0.00 -99.00 0.00 -99.00 -99.00 0.00 -99.00 -99.00
1937 10 7 0.00 -99.00 0.00 -99.00 0.00 -99.00 -99.00 0.00 -99.00 -99.00
1937 10 8 0.00 -99.00 0.00 -99.00 0.00 -99.00 -99.00 0.00 -99.00 -99.00
1937 10 9 0.00 -99.00 0.00 -99.00 0.00 -99.00 -99.00 0.00 -99.00 -99.00
1937 10 10 0.00 -99.00 0.00 -99.00 0.00 -99.00 -99.00 0.00 -99.00 -99.00
1937 10 11 0.00 -99.00 0.00 -99.00 0.00 -99.00 -99.00 0.00 -99.00 -99.00
1937 10 12 0.00 -99.00 0.00 -99.00 0.00 -99.00 -99.00 0.00 -99.00 -99.00
1937 10 13 0.00 -99.00 0.05 -99.00 0.14 -99.00 -99.00 0.20 -99.00 -99.00
1937 10 14 0.22 -99.00 0.88 -99.00 1.12 -99.00 -99.00 1.16 -99.00 -99.00
1937 10 15 0.30 -99.00 0.10 -99.00 0.25 -99.00 -99.00 0.10 -99.00 -99.00
1937 10 16 0.00 -99.00 0.00 -99.00 0.00 -99.00 -99.00 0.00 -99.00 -99.00
1937 10 17 0.00 -99.00 0.00 -99.00 0.00 -99.00 -99.00 0.00 -99.00 -99.00
1937 10 18 0.00 -99.00 0.04 -99.00 0.00 -99.00 -99.00 0.00 -99.00 -99.00
1937 10 19 0.00 -99.00 0.00 -99.00 0.00 -99.00 -99.00 0.00 -99.00 -99.00
1937 10 20 0.00 -99.00 0.00 -99.00 0.00 -99.00 -99.00 0.00 -99.00 -99.00
1937 10 21 0.00 -99.00 0.00 -99.00 0.00 -99.00 -99.00 0.00 -99.00 -99.00
1937 10 22 0.00 -99.00 0.00 -99.00 0.00 -99.00 -99.00 0.00 -99.00 -99.00
1937 10 23 0.00 -99.00 0.00 -99.00 0.00 -99.00 -99.00 0.00 -99.00 -99.00
1937 10 24 0.00 -99.00 0.00 -99.00 0.00 -99.00 -99.00 0.00 -99.00 -99.00
1937 10 25 0.00 -99.00 0.00 -99.00 0.00 -99.00 -99.00 0.00 -99.00 -99.00
1937 10 26 0.00 -99.00 0.00 -99.00 0.00 -99.00 -99.00 0.00 -99.00 -99.00
1937 10 27 0.00 -99.00 0.00 -99.00 0.00 -99.00 -99.00 0.00 -99.00 -99.00
1937 10 28 0.00 -99.00 0.00 -99.00 0.00 -99.00 -99.00 0.00 -99.00 -99.00
1937 10 29 0.00 -99.00 0.00 -99.00 0.28 -99.00 -99.00 0.00 -99.00 -99.00
1937 10 30 0.00 -99.00 0.24 -99.00 0.21 -99.00 -99.00 0.00 -99.00 -99.00
1937 10 31 0.03 -99.00 0.10 -99.00 0.00 -99.00 -99.00 0.27 -99.00 -99.00
1937 11 1 0.00 -99.00 0.00 -99.00 0.00 -99.00 -99.00 0.00 -99.00 -99.00
1937 11 2 0.00 -99.00 0.00 -99.00 0.00 -99.00 -99.00 0.00 -99.00 -99.00
1937 11 3 0.00 -99.00 0.00 -99.00 0.00 -99.00 -99.00 0.00 -99.00 -99.00
1937 11 4 0.00 -99.00 0.00 -99.00 0.00 -99.00 -99.00 0.00 -99.00 -99.00

ac_centroids

45

1	40.23135761	121.06362980
2	40.19690874	121.15221148
3	40.28509346	121.27800123
4	40.29808895	121.24026264
5	40.32818344	121.15530849
6	40.29461548	121.12225809
7	40.30088775	121.04523185
8	40.23574141	120.96246325
9	40.23903817	120.88863060
10	40.27289577	120.91551104
11	40.28629538	120.86656202
12	40.29943799	120.95356983
13	40.31974464	120.99936432
14	40.32525125	120.94899070
15	40.31658227	120.91982407
16	40.34020507	120.88986997
17	40.37039442	120.97665194
18	40.36611801	120.90502175
19	40.38488658	120.94880292
20	40.41379822	121.02713467
21	40.36547001	121.04684081
22	40.34408043	121.09091515
23	40.40513833	121.10453834
24	40.44216094	121.08757837
25	40.46594559	121.13003944
26	40.39605854	121.14512527
27	40.44009010	121.20020590
28	40.36639548	121.20930922
29	40.36447779	121.24049525
30	40.34976334	121.24918170
31	40.32700297	121.25956581
32	40.34477335	121.28695431
33	40.31583661	121.32320989
34	40.39119704	121.31053348
35	40.38586009	121.34453696
36	40.34665519	121.37535086
37	40.37664432	121.37887845
38	40.38336765	121.44731197
39	40.44377225	121.47195906
40	40.43186465	121.40332002
41	40.44609134	121.41162315
42	40.46472382	121.42098658
43	40.45293705	121.32635921
44	40.40741915	121.29593903
45	40.42621291	121.26546864

ac_ave_ppt

'ac_avg_ppt'

'HRU	jan_ppt	feb_ppt	mar_ppt	apr_ppt	may_ppt	jun_ppt	jul_ppt	aug_ppt	sep_ppt	oct_ppt	nov_ppt	dec_ppt'
1	6.8189	5.9305	3.8906	2.5438	1.5397	0.7651	0.2500	0.2500	0.7500	1.9805	4.1450	5.9444
2	6.6878	5.4930	5.1271	2.3724	1.2676	0.7500	0.2500	0.2937	0.7500	2.3795	5.2869	5.7002
3	6.2254	5.3616	4.8991	2.2518	1.3321	0.7500	0.2500	0.5685	0.7986	2.4548	5.1828	5.2934
4	5.9483	4.8237	4.3496	2.2275	1.2500	0.7500	0.2500	0.2500	0.7500	2.2500	4.7500	5.1574
5	6.5454	5.7132	4.9849	2.5098	1.5469	0.7500	0.2500	0.5283	0.9260	2.5272	5.3372	5.6906
6	6.3912	5.3538	4.2826	2.2993	1.3224	0.7500	0.2500	0.2673	0.7500	2.1894	4.5603	5.5480
7	6.7783	5.8707	3.5097	2.6839	1.6976	0.7792	0.2500	0.2500	0.7500	1.8256	3.7654	5.8663
8	7.1301	6.3362	4.2028	2.7842	1.7924	0.7968	0.2500	0.2500	0.7504	2.2794	4.5064	6.2655
9	6.9910	6.1917	4.2242	2.7500	1.7500	0.7500	0.2500	0.2500	0.7500	2.2384	4.6055	5.9746
10	6.8915	6.1794	3.7571	2.7500	1.7500	0.7500	0.2500	0.2500	0.7500	2.2500	4.2500	6.1377
11	6.7651	6.3039	3.7261	2.7500	1.8639	0.7525	0.2500	0.2500	0.7500	2.2363	4.1865	5.9568
12	7.1855	6.1004	3.8658	2.7500	1.7500	0.7521	0.2500	0.2500	0.7500	2.2500	4.2933	6.2500
13	6.9304	5.9116	3.7463	2.7500	1.7500	0.7500	0.2500	0.2500	0.7500	2.1483	4.1177	6.1043
14	7.2500	6.2500	4.2500	2.7500	1.7500	0.9872	0.2500	0.2500	0.7500	2.2523	4.7368	6.3188
15	7.0190	6.2500	3.7995	2.7500	1.7500	0.8498	0.2500	0.2500	0.7500	2.2500	4.2504	6.2500
16	6.6180	6.1805	3.6809	2.7415	1.7500	0.7887	0.2500	0.2500	0.7500	2.1764	4.1052	5.9351
17	6.6156	5.8937	3.8159	2.6288	1.7500	0.7827	0.2500	0.2500	0.7500	2.2161	4.2407	5.9330
18	6.5518	5.8075	3.4724	2.7399	1.7500	0.7516	0.2500	0.2500	0.7500	2.1192	3.8633	5.8498
19	6.4261	5.8117	3.4569	2.6898	1.7500	0.7500	0.2500	0.2500	0.7500	2.0807	3.8492	5.7773
20	6.5703	5.9657	4.1976	2.7408	1.7500	0.7500	0.2500	0.2500	0.7500	2.2500	4.5059	5.7520
21	6.7438	5.8848	4.0720	2.7333	1.7500	0.7500	0.2500	0.2500	0.7500	2.2292	4.3391	5.7500
22	6.7497	5.8863	4.3179	2.5748	1.6167	0.7500	0.2500	0.2547	0.7500	2.2357	4.6206	5.7673
23	6.8830	6.5043	5.3065	2.8917	2.0597	0.8440	0.2500	0.5309	0.9946	2.7205	5.6801	6.2513
24	6.8494	6.4469	5.1232	2.8259	1.9867	0.7954	0.2500	0.4395	0.9066	2.6886	5.5085	6.1522
25	7.0974	6.5568	5.4684	3.0565	2.1502	1.0372	0.2500	0.6469	1.1186	2.8539	5.7125	6.4266
26	6.9443	6.4974	5.5666	2.8770	2.0220	0.8219	0.2500	0.7457	1.1573	2.7709	5.9680	6.2150
27	7.5269	7.0445	6.1026	3.3795	2.3300	1.1998	0.2500	0.7500	1.2500	2.8326	6.3970	6.8549
28	6.7687	6.1010	5.4206	2.7246	1.7525	0.8519	0.2500	0.6957	1.0781	2.6483	5.8010	5.9872
29	6.4256	5.7712	5.1555	2.4468	1.5672	0.7502	0.2500	0.7298	0.9750	2.6269	5.5169	5.7383
30	6.2445	5.4240	4.7927	2.3079	1.4247	0.7500	0.2500	0.5542	0.8624	2.4680	5.1732	5.4728
31	6.2237	5.2388	4.6160	2.2500	1.2500	0.7500	0.2500	0.3728	0.7500	2.2590	4.8494	5.2615
32	6.3000	5.4805	4.9665	2.3072	1.3913	0.7500	0.2500	0.6923	0.8245	2.5028	5.3359	5.4984
33	6.4424	5.7331	5.3394	2.5277	1.6490	0.8030	0.2500	0.7499	1.0701	2.7315	5.7389	5.7658
34	6.8689	6.0694	5.4897	2.7781	1.7403	0.9632	0.2500	0.7500	1.1102	2.7153	5.8690	6.1850
35	7.7673	6.5274	6.0135	3.2023	1.9961	1.0334	0.2500	0.8248	1.2475	3.1611	6.4386	6.9849
36	7.2675	6.1343	5.8995	3.0256	1.7500	1.1540	0.2500	0.7500	1.2500	3.0006	6.3102	6.4885
37	7.9567	6.5279	6.2274	3.3466	1.9475	1.2002	0.2500	0.7885	1.2706	3.2450	6.6335	7.1150
38	10.3069	7.9948	8.0436	4.8397	2.6232	1.5365	0.2500	1.0246	1.5060	4.5082	8.8179	9.5401
39	17.2589	12.4426	12.3425	9.0173	4.3823	2.4601	0.2500	1.9517	1.8975	7.1152	14.5467	16.3912
40	12.2512	9.1200	8.5404	5.7586	3.2479	1.8044	0.2500	1.3069	1.5960	4.7741	9.2527	11.0308
41	12.4581	9.0967	8.4933	5.8964	3.4115	1.8885	0.2500	1.3724	1.6295	4.7856	9.2015	11.0641
42	12.4248	8.9668	8.3190	5.8672	3.5789	2.0035	0.2500	1.4257	1.6800	4.6930	9.0206	10.8943
43	9.2283	6.9149	6.0889	4.1779	2.7868	1.4984	0.2500	0.9763	1.3440	3.3190	6.5890	7.8860
44	7.4229	6.7102	5.9285	3.2259	2.0746	1.1129	0.2500	0.7500	1.2500	2.7066	6.3426	6.7274
45	7.8850	7.1650	6.1539	3.6252	2.3837	1.1887	0.2500	0.7500	1.2500	2.7959	6.6073	7.2189

draper.f

```
      parameter (nsit=10,ndays=36500,nhru=200)
      parameter (smooth=0.5,nmax=8,lwrk=1000)

      dimension sitlat(nsit),sitlon(nsit)
      dimension sitppt(ndays,nsit),w(nsit)
      dimension hrulat(nhru),hrulon(nhru)
      dimension hruppt(nhru),ppt(nsit)
      dimension pptlat(nsit),pptlon(nsit)
      dimension prism_hru(12,nhru)
      dimension nmon(12),mon(ndays),iy(ndays),id(ndays)
      dimension sit_mean(12,nsit),ncount(12,nsit)
      dimension tx(nmax),ty(nmax)

      character file*2,ap*8,cd*15,filnm*60

      data nmon/31,28,31,30,31,30,31,31,30,31,30,31/
      ap='ave_ppt/'
      cd='centroids_mike/'
      pi=4.*atan(1.)
      eps=1.e-20

      print *,'Enter name of file with',
     &   ' weather station lat longs'
      read(5,'(a60)') filnm
      open(14,file=filnm,status='old',readonly)

      print *,'Enter name of file with observed',
     &    ' daily precipitation for these sites'
      read(5,'(a60)') filnm
      open(16,file=filnm,status='old',readonly)
      read(16,*)
      read(16,*)
      read(16,*)
      read(16,*)

      print *,'Enter two-letter basin designator'
      read(5,'(a2)') file
      open(15,file=cd//file//'_centroids_mike',
     &     status='old',readonly)
      read (15,*) nru

      open(13,file=ap//file//'_ave_ppt',
     &    status='old',readonly)
      read (13,*)
      read (13,*)

      print *,'Enter output-file name'
      read(5,'(a60)') filnm
      open(17,file=filnm,status='unknown')
```

```
      do j=1,nsit
        w(j)=1.
      enddo

      do k=1,nru
        read(13,*) kk,(prism_hru(i,k),i=1,12)
        do i=1,12
          prism_hru(i,k)=prism_hru(i,k)/nmon(i)
        enddo
      enddo

      do k=1,nru
       read(15,*) ihru,hrulat(k),hrulon(k)
       hrulat(k)=hrulat(k)*pi/180.
       hrulon(k)=hrulon(k)*pi/180.
      enddo

      do j=1,nsit
       read(14,*) sitlat(j),sitlon(j)
       sitlat(j)=sitlat(j)*pi/180.
       sitlon(j)=sitlon(j)*pi/180.
      enddo

      do i=1,ndays
        read(16,*,end=99) iy(i),mon(i),id(i),
     &      (sitppt(i,j),j=1,nsit)
        im=mon(i)
        do j=1,nsit
         if(sitppt(i,j).ge.0.) then
          sit_mean(im,j)=sit_mean(im,j)+sitppt(i,j)
          ncount(im,j)=ncount(im,j)+1
         endif
        enddo
      enddo
 99   nday=i-1
      do i=1,12
        do j=1,nsit
          if(ncount(i,j).gt.0) then
           sit_mean(i,j)=sit_mean(i,j)/ncount(i,j)
          else
           sit_mean(i,j)=-99.
          endif
        enddo
      enddo

      print *,'Data read and averages calculated'

      iopt=0
      none=1
      do i=1,nday
        if(mod(i,30).eq.0)
```

```
&     print *,'Interpolating on day ',iy(i),mon(i),id(i)
      n=0
      do j=1,nsit
       if(sitppt(i,j).ge.0..and.
&         sit_mean(mon(i),j).gt.0.)then
         n=n+1
         ppt(n)=sitppt(i,j)/sit_mean(mon(i),j)
         pptlat(n)=sitlat(j)
         pptlon(n)=sitlon(j)
       endif
      enddo
      if(n.ge.3) then
       call trend(n,pptlon,pptlat,ppt,a,b,c)
       do k=1,nru
         xx=hrulon(k)
         yy=hrulat(k)
         call interpol(xx,yy,a,b,c,zz)
         hruppt(k)=zz*prism_hru(mon(i),k)
         if(hruppt(k).le.0.) hruppt(k)=0.
       enddo
      elseif(n.lt.3.and.n.gt.0) then
       avep=0
       do k=1,n
         avep=avep+ppt(k)/n
       enddo
       do k=1,nru
         hruppt(k)=avep*prism_hru(mon(i),k)
         if(hruppt(k).le.0.) hruppt(k)=0.
       enddo
      elseif (n.le.0) then
       do k=1,nru
        hruppt(k)=prism_hru(mon(i),k)
        if(hruppt(k).le.0.) hruppt(k)=0.
       enddo
      endif
     if(nru.ge.200) then
      nh=200
     else
      nh=nru
     endif
     write(17,10)iy(i),mon(i),id(i),(hruppt(k),k=1,nh)
     if(nru.gt.200) then
       write(17,11) (hruppt(k),k=201,nru)
     endif

10   format(i5,2i3,200(1x,f6.1))
11   format(10(t12,200(1x,f6.1)))
    enddo

    stop
    end
```

trend.f

```
      subroutine trend(n,x,y,p,a,b,c)
          parameter (nsit=10)
          dimension x(1),y(1),p(1)
          dimension beta(3),xm(nsit,3)
          dimension xx(3,3),xy(3)

          do i=1,n
           xm(i,1)=1.
           xm(i,2)=x(i)
           xm(i,3)=y(i)
          enddo

          do j=1,3
            xy(j)=0
           do i=1,n
             xy(j)=xy(j)+xm(i,j)*p(i)
           enddo
          enddo

          do i=1,3
           do j=1,3
             xx(i,j)=0
             do k=1,n
               xx(i,j)=xx(i,j)+xm(k,i)*xm(k,j)
             enddo
           enddo
          enddo

          ithree=3
          call inverse(ithree,xx,xy,beta)

          a=beta(1)
          b=beta(2)
          c=beta(3)

      return
          end
```

inverse.f

```
      subroutine inverse(n,x,y,b)
      dimension x(3,3),y(1),b(1)
      dimension indx(3)

      do i=1,n
        b(i)=y(i)
      enddo

      call ludcmp(x,3,indx,d)
      call lubksb(x,3,indx,b)

      return
      end

      subroutine ludcmp(a,n,indx,d)
      dimension indx(1),a(3,3),vv(3)
      tiny=1.0e-20

      d=1.
      do 12 i=1,n
        aamax=0
        do 11 j=1,n
          if(abs(a(i,j)).gt.aamax) aamax=abs(a(i,j))
11      continue
        if (aamax.eq.0.) print *,'Singular matrix'
        if (aamax.eq.0.) stop
        vv(i)=1/aamax
12    continue
      do 19 j=1,n
        do 14 i=1,j-1
          sum=a(i,j)
          do 13 k=1,i-1
            sum=sum-a(i,k)*a(k,j)
13        continue
          a(i,j)=sum
14      continue
        aamax=0.
        do 16 i=j,n
          sum=a(i,j)
          do 15 k=1,j-1
            sum=sum-a(i,k)*a(k,j)
15        continue
          a(i,j)=sum
          dum=vv(i)*abs(sum)
          if(dum.ge.aamax) then
            imax=i
            aamax=dum
          endif
```

```
16     continue
       if(j.ne.imax) then
         do 17 k=1,n
           dum=a(imax,k)
           a(imax,k)=a(j,k)
           a(j,k)=dum
17       continue
         d=-d
         vv(imax)=vv(j)
       endif
       indx(j)=imax
       if(a(j,j).eq.0.) a(j,j)=tiny
       if (j.ne.n) then
         dum=1./a(j,j)
         do 18 i=j+1,n
           a(i,j)=a(i,j)*dum
18       continue
       endif
19   continue
     return
     end

     subroutine lubksb (a,n,indx,b)
     dimension a(3,3),indx(1),b(1)

     ii=0
     do 12 i=1,n
       ll=indx(i)
       sum=b(ll)
       b(ll)=b(i)
       if(ii.ne.0) then
         do 11 j=ii,i-1
           sum=sum-a(i,j)*b(j)
11       continue
       elseif (sum.ne.0.) then
         ii=i
       endif
       b(i)=sum
12   continue
     do 14 i=n,1,-1
       sum=b(i)
       do 13 j=i+1,n
         sum=sum-a(i,j)*b(j)
13     continue
       b(i)=sum/a(i,i)
14   continue
     return
     end
```

Appendix C. Name, size, and description of data and parameter files used for the Feather River PRMS models.

File	Size (bytes)	Description
AC_draper_climateQ.data	1717823	Daily precipitation adjusted for each HRU, temperature, and observed streamflow—Almanor model input.
BC_draper_climateQ.data	537119	Daily precipitation adjusted for each HRU, temperature, and observed streamflow—Butt Creek model input.
EB_draper_climateQ.data	5368088	Daily precipitation adjusted for each HRU, temperature, and observed streamflow—East Branch model input.
LO_draper_climateQ.data	1446364	Daily precipitation adjusted for each HRU, temperature, and observed streamflow—Lower North Fork model input.
MF_draper_climateQ.data	3150909	Daily precipitation adjusted for each HRU, temperature, and observed streamflow—Middle Fork model input.
SF_draper_climateQ.data	803329	Daily precipitation adjusted for each HRU, temperature, and observed streamflow—South Fork model input.
WB_draper_climateQ.data	1019154	Daily precipitation adjusted for each HRU, temperature, and observed streamflow—West Branch model input
OR_draper_climateQ.data	1461010	Daily precipitation adjusted for each HRU, temperature, and observed streamflow—Oroville model input.
AC_feather.param	75127	PRMS parameter input file for Almanor model.
BC_feather.param	15485	PRMS parameter input file for Butt Creek model.
EB_feather.param	174248	PRMS parameter input file for East Branch model.
LO_feather.param	62969	PRMS parameter input file for Lower North Fork model.
MF_feather.param	94706	PRMS parameter input file for Middle Fork model.
SF_feather.param	29798	PRMS parameter input file for South Fork model.
WB_feather.param	24096	PRMS parameter input file for West Branch model.
OR_feather.param	69068	PRMS parameter input file for Oroville model.